



Final Report

Recovery Processes for Schrader Bluff, Alaska

Joint Project between U.S. DOE and BP Exploration Inc.

by
Arden Strycker and Shawn Wang
TRW Petroleum Technologies

December 2000

Work Performed Under Contract No.
DE-AD26-99FT00874 (GS-23LF-8079H)

Prepared for BP Amoco p.l.c. &
U.S. Department of Energy
National Petroleum Technology Office

Final Report

Recovery Processes for Schrader Bluff, Alaska

Joint Project between U.S. DOE and BP Exploration Inc.

by

Arden Strycker and Shawn Wang
TRW Petroleum Technologies

Work Performed Under Contract No.
DE-AD26-99FT00874 (GS-23LF-8079H)

Prepared for BP Amoco p.l.c. &
U.S. Department of Energy
National Petroleum Technology Office

DISCLAIMER

This report was prepared as an account of work sponsored by an agency of the United States Government. Neither the United States Government nor any agency thereof, nor any of their employees, makes any warranty, expressed or implied, or assumes any legal liability or responsibility of the accuracy, completeness, or usefulness of any information, apparatus, product, or process disclosed, or represents that its use would not infringe privately owned rights. Reference herein to any specific commercial product, process, or service by trade name, trademark, manufacturer, or otherwise does not necessarily constitute or imply its endorsement, recommendation, or favoring by the United States Government or any agency thereof. The views and opinions of authors expressed herein do not necessarily state or reflect those of the United States Government or any agency thereof.

TRW Petroleum Technologies
P.O. Box 2543
Bartlesville, OK

Table of Contents

1. Introduction.....	1
2. Reservoir Rock and Fluid Properties	3
2.1 Schrader Bluff Reservoir Rock Properties.....	3
2.2 Schrader Bluff Reservoir Fluid Properties.....	3
3. Recovery Process Screening	5
3.1 Background.....	5
3.2 Screening Criteria	6
3.3 Predictive Models	8
3.4 Analogous Reservoirs.....	11
3.4.1 Polymer Flood	13
3.4.2 In Situ Combustion.....	14
3.4.3 Gas Flooding	14
3.4.4 Steam Injection.....	14
3.4.5 Alkaline Processes.....	14
3.4.6 Micellar/Polymer Floods.....	15
3.5 Recommendations.....	15
4. Recovery by In-Situ Combustion.....	17
4.1 Background.....	17
4.2 Tube Run Tests	18
4.2.1 In-situ Combustion Tube Run Number 1	18
4.2.2 In-situ Combustion Tube Run Number 2	19
4.3 Simulation Sensitivity Studies	20
4.3.1 Model Description and Data Input.....	20
4.3.2 Sensitivity Studies and Results	27
4.4 Extinction Radius Calculations	36
4.5 Summary	38
5. Recovery by Gas Injection	40
5.1 Background.....	40
5.1.1 Miscible vs. Immiscible Recovery at Schrader Bluff	40
5.1.2 EOR and CO ₂ Sequestration	40
5.1.3 Phase Behavior at Schrader Bluff (3-Hydrocarbon Phases).....	40
5.1.4 Evaluation of Gas Injection.....	41
5.2 Recovery Estimates (Simulation/Simulation Screening).....	42
5.2.1 UTCOMP.....	42
5.2.2 1D Simulation (UTCOMP).....	42
5.2.3 2D Simulations	51

5.3 Multi-phase CO ₂ Fluid Flow (Compositional Simulation).....	53
5.3.1 Simulation: Slim Tube History Match Study.....	54
5.3.2 Four-phase Relative Permeability (Sensitivity Study).....	57
5.3.3 Effects of Temperature and Pressure (Sensitivity Study).....	58
5.3.4 Mechanism of Displacement.....	60
5.3.5 Conclusions	61
5.4 Summary	62
6. Asphaltene Precipitation Potential	63
6.1 Background.....	63
6.1.1 Chemical nature of asphaltenes	63
6.1.2 Solubility Characterization Methods	64
6.1.3 Solubility prediction methods.....	68
6.1.4 Summary of activities done on this project	70
6.2 Comparison of Schrader Bluff with other Fields.....	70
6.3 PVT Studies of Schrader Bluff Oil	73
6.4 Model Predictions Asphaltene Behavior for Schrader Bluff Oil	74
6.4.1 Introduction	74
6.4.2 Describe model and basis of input.....	75
6.4.3 West Sak	76
6.4.4 Schrader Bluff (PVT).....	78
6.4.5 Summary.....	80
6.5 Summary	80
7. Conclusions.....	81
8. Bibliography	81
8.1 General	81
8.2 In-situ Combustion	85
9. Appendices.....	87

Tables

	Page
Table 1. - Summary of reservoir parameters for Schrader Bluff Milne Point, Alaska	4
Table 2. - Modified EOR screening criteria	6
Table 3. - Reservoir properties of selected sands in Schrader Bluff	9
Table 4. - Screening parameter ranges for analogous reservoirs	12
Table 5. - Number of analogous reservoirs by process and status	13
Table 6. - Summary of favorable and unfavorable risk factors for in-situ combustion	18
Table 7. - Summary of results for Run 1	19
Table 8. - Summary of results for Run 2	20
Table 9. - Properties of heavy and light fractions	20
Table 10. - Four chemical reactions	21
Table 11. - Schrader Bluff reservoir 36-layer model description	21
Table 12. - Schrader Bluff reservoir 14-layer model description	23
Table 13 (a). - Liquid-gas and water-oil relative permeabilities for layers 1, 8 and 9	23
Table 14. - Two sets of K values	35
Table 15. - Composition of Schrader Bluff oil	43
Table 16. - Defined compositions of twelve-component oil and solvent (mole%)	43
Table 17. - Fluid component description parameters	44
Table 18. - Average saturation for pure CO ₂ injection at high and low pressures	45
Table 19. - Mixture model design, high pressure case (1984 psi)	48
Table 20. - Mixture design, low pressure case (820 psi)	49
Table 21. - Relative permeability input parameters from Stone II model	51
Table 22. - Input parameters for linear approximation of asphaltene solubility	68
Table 23. - SARA of phases in MI swelling study for Schrader Bluff	74
Table 24. - Composition of West Sak for asphaltene modeling study	76
Table 25. - Composition of Schrader Bluff for asphaltene modeling study	78

Line

Figures

Page

Figure 1. - Comparison of EOR methods from DOE predictive model study	10
Figure 2. - Position of combustion front for various injection rates.....	28
Figure 3. - Effect of injection rates on cumulative oil production, oil recovery and AOR	29
Figure 4. - Comparison of cumulative oil recovery-14-layer vs. 8-layer (10 MMscf/D air inj.)	30
Figure 5. - Effect of enriched oxygen on daily oil production and oil recovery	31
Figure 6. - Effect of kinetics of cracking reaction (10 MMscf/D air injection).....	32
Figure 7. - Oil recovery in wet combustion is superior to the corresponding dry combustion	32
Figure 8. - Comparison of producing AOR for wet and dry combustion.....	33
Figure 9. - Effect of the amount of water injected on oil recovery (5 MMscf/D air injection).....	33
Figure 10. - Effect of wet combustion on temperature distribution (5 MMscf/D air injection).....	34
Figure 11. - Effect of wet combustion on oil saturation (5 MMscf/D air injection).....	34
Figure 12. - Effect of phase equilibrium K-values on oil recovery (10 MMscf/D air injection)	36
Figure 13. - Well spacing sensitivity study (10 MMscf/D air injection).....	36
Figure 14. - Extinction radius at various injection rates	38
Figure 15. - CO ₂ Injection, simulated 1D Flow at various pressures	45
Figure 16. - NGL injection, simulated 1D flow at various pressures.....	46
Figure 17. - Lean gas injection, simulated 1D at various pressures	46
Figure 18. - Comparison of two CO ₂ injection methods (reservoir pressure = 1984 psi)	47
Figure 19. - Injection time comparison between two CO ₂ injection methods (P=1984 psi).....	48
Figure 20. - Contour map of recovery as a function of solvent composition, 1984 psi.....	50
Figure 21. - Contour map of recovery as a function of solvent composition, 820 psi.....	51
Figure 22. - Oil recovery prediction by UTCOMP and GEM.....	52
Figure 23. - Effect of CO ₂ rich second liquid phase on oil recovery	53
Figure 24. - Oil recovery for 1:1 WAG process.....	53
Figure 25. - History match of E-20 slim tube test.....	54
Figure 26. - Slim tube average saturation vs. injection pore volume	55
Figure 27. - Distribution of CO ₂ rich second liquid phase saturation	56
Figure 28. - Effect of CO ₂ rich phase on oil recovery	56
Figure 29. - Effect of relative permeability models on oil recovery	58
Figure 30. - Oil recovery at various reservoir temperature (0.26 PV/day)	59
Figure 31. - CO ₂ /oil phase equilibrium at 92° F	60

Figure 32. - Oil recovery at various reservoir pressures (0.26 PV/day).....	60
Figure 33. - density profile for the CO ₂ rich and oil phases	61
Figure 34. - Comparison of Hildebrand's solubility parameter and wt% soluble asphaltenes of Athabasca bitumen for a range of solvents	66
Figure 35. - Comparison of solvent density and wt% soluble asphaltenes of Athabasca bitumen for a range of solvents	67

Abstract

Acknowledgements

Executive Summary

1. Introduction

The purpose of the overall project was to develop one or more methods for economic recovery of viscous oil from the Schrader Bluff formation at Milne Point, Alaska. The work described here was conducted for the U.S. Dept. of Energy (DOE) in support of this purpose by identifying those advanced oil recovery processes most likely to be successful and by estimating the incremental benefit possible with each process.

This project was conducted jointly with BP Amoco, p.l.c. under a Cooperative Research and Development Agreement (CRADA). The CRADA is an agreement vehicle that enables businesses to utilize federal laboratory facilities with unique capabilities. Tasks under the CRADA were defined jointly between the DOE and BP Exploration (Alaska) to develop an economic method of recovering more viscous oil from Schrader Bluff. Each group funded their own share of the work on these tasks. Work funded by the DOE was conducted by TRW Petroleum Technologies (formerly BDM Petroleum Technologies at the National Institute for Petroleum and Energy Research, NIPER).

The CRADA was initially signed, January 25, 1996, and was to last 5 years. A major revision of the CRADA was signed, October 18, 1999, and is expected to be completed by March 17, 2001. This document represents the final report of this project, and summarizes the activities and results conducted under the CRADA. As it is currently written, virtually all of the work described in this report is based on work conducted by TRW Petroleum Technologies for the DOE.

The first tasks of the CRADA focused on characterizing the Schrader Bluff reservoir and conducting an initial screening of the many recovery methods to determine which are more favorable for Schrader Bluff conditions. From the initial screening tasks, a recommendation was made to further investigate the more promising methods that were identified. Ultimately, the best approach identified in the previous tasks are up-scaled to a field-scale test. The field test could be a field pilot with the primary purpose of quantifying the field level parameters and project more accurately the economic potential. Alternatively, the field test could be a small-scale field project with expectations of commercial success and subsequent expansion. The latter for example, might be justified for a gas injection type project where prior field experience already exists in the arctic Alaska region.

As the project progressed, several potentially critical issues were identified worthy of further investigation. These include: evaluation of the potential impact on fluid flow of multiple hydrocarbon phases, on the potential of asphaltene precipitation from certain injected solvents, and on techniques to mitigate unfavorable mobility with certain injected solvents. The revised scope of the CRADA signed October 1999 included tasks that focused on these issues.

For example, the relatively low temperature gradient in the Arctic region results in the presence of 3 hydrocarbon phases for such solvents as CO₂ and CO₂/hydrocarbon mixtures. Commercial simulators are not designed to account for 3 hydrocarbon phases and laboratory studies of relative permeability and other fluid flow properties in the presence of 3 hydrocarbon phases are extremely difficult to conduct (time consuming, expensive, etc.). A reliable alternative approach was desired.

This report documents and discusses the work conducted by TRW Petroleum Technologies under the CRADA for Schrader Bluff reservoir. In order, each section focuses on a different task of the CRADA. First, the reservoir rock and fluid properties for Schrader Bluff is discussed and summarized. The enhanced oil recovery process screening tasks are next discussed and are based on these properties. Based on the screening tasks, 2 recovery processes were recommended for further study: in-situ combustion and gas injection. The evaluation of potential asphaltene precipitation is discussed next. The overall results are then summarized in the conclusion section of the report. The Appendices contain additional reports from other groups. Sub-tasks were often sub-contracted to groups outside of TRW Petroleum Technologies when appropriate.

2. Reservoir Rock and Fluid Properties

2.1 Schrader Bluff Reservoir Rock Properties

The Schrader Bluff consists of Late Cretaceous, near shore marine sand sequences, informally referred to as the "N" and "O" sands. The individual reservoir units are predominantly, very fine to fine grained, moderately sorted, unconsolidated quartz sands with varying amounts of accessory minerals, mainly rock fragments, mica and glauconite. The reservoir units are amalgamations of storm deposits redistributed, for the most part, below wave base. Bioturbation, and burrows are common in some intervals whereas, others display finely laminated bedding, suggesting more rapid sedimentation. Calcareous interbeds are locally common, often associated with concentrations of bivalve debris.

The upper "N" sands consist of multiple reservoir layers varying in thickness between 5 and 15 feet, with permeability's ranging between 5 millidarcies to 5 darcies. The lower "O" sands consist of two main sand bodies that although are finer grained than the "N" sands, are generally more massive and competent. These sands are more continuous and correlative across the North Slope than the thinner, more discontinuous "N" interval. The "O" sands thickness varies between 10 to 35 ft with permeabilities between 10 millidarcies and 1 darcy. The average porosity in all sand units varies between 25 to 28 percent.

The formation dips gently north-northeast at a rate of approximately 70 ft per mile. The resulting monocline is broken by numerous faults of variable displacement, most of which trend north-northeast and progressively downdrop the reservoir to the northeast. Depths range from 3500 feet to 4500 feet. Faults, with throws between 20 to 150 feet, compartmentalize the reservoir to some degree. This coupled with stratigraphic discontinuities, can hydraulically isolate individual reservoir units.

The fracture gradient is between 0.66-0.7 psi/ft with an overburden stress gradient of 0.85 psi/ft. The estimated net confining stress is between 1000 to 1300 psi.

2.2 Schrader Bluff Reservoir Fluid Properties

The Schrader Bluff Pool is undersaturated by about 500 psi and correspondingly has no gas cap. The initial average reservoir pressure is 1750 psig at 4000 ft true vertical depth subsea with an average reservoir temperature of 81° F. These pressures are only slightly higher than the local hydrostatic pressures. Currently, the average reservoir pressure is between 1400 to 1750 psi depending on producing fault block.

The hydrocarbon quality varies between the N and O sands, the deeper O sand containing a better-quality crude than the N sand. The N sand oil gravities range from 14° to 19° API with viscosities between 40 and 140 centipois (cP). The oil gravities and viscosities improve in the O sands, oil gravities typically falling between 18° to 21.5° API with viscosities from 30 to 45 cP.

In general, the PVT properties of the Schrader Bluff hydrocarbons bear a resemblance to conventional heavy oil systems, namely:

- 1 Low API gravities (14-22°)
- 2 Low gas oil ratio (GOR 100-200 scf/stb)
- 3 Low oil formation volume factor (about 1.04-1.08 bbl/stb)
- 4 High average viscosity (30 to 70 cP at original conditions)

The live oils of the Schrader Bluff are dominated by the C7+ fractions (67 mole percent on average). This corresponds to an exceedingly small amount of C2-C6 intermediate hydrocarbons and suggests high biodegradation. The hydrocarbons contain no hydrogen sulfide, and very little quantities of carbon dioxide or nitrogen. The gas composition is primarily methane. The formation water contains approximately 27,000 ppm total dissolved solids, with an average salinity of 20,000 ppm NaCl equivalent.

In common with fluid systems from shallow and soft sands, the Schrader Bluff hydrocarbon properties exhibit significant variations across sand bodies. This variance is seen vertically, from sand to sand, and laterally within one sand as it is traced down dip. The mapped variance is poorly understood at this time. A summary reservoir properties are provided in Table 1 below.

Table 1. - Summary of reservoir parameters for Schrader Bluff Milne Point, Alaska

Property	Value
OOIP (MMbbl)	1800 (Milne Point Unit)
Recoverable (MMbbl)	250
Produced (MMbbl)	3 (1996)
Areal Extent (Acres)	22,000 (MPU)
Depth (ft)	4300 (3700-4800)
Temperature (°F)	90 (85-100)
Gross Pay (ft)	270 (30-40, individual sands)
Net Pay (ft)	75 (15-20, individual sands)
Porosity (fraction)	0.25 (0.25-0.30)
Permeability (mD)	250-1250 (50-3000)
Swi (fraction PV)	0.35 (0.35-0.55)
FVF (bbl/STB)	1.06
Gravity (°API)	19 (14-21)
Viscosity (reservoir conditions, live oil, cP)	37 (30-600)
GOR (scf/stb)	200 (100-200)
Initial Pressure (psi)	1900 (1900-2000)

Summary of Fluid Characterization Studies

[continue]

3. Recovery Process Screening

3.1 Background

Typically, initial production of reservoirs results in only 5-15% recovery of the total petroleum resource. A number of methods have been developed for recovering a higher percentage of oil from the subsurface. The most commonly applied is waterflooding. However, for viscous and heavy oils, the mobility of water is much higher than that of oil and results in premature channeling of injected water through the reservoir. Sweep efficiencies and corresponding recovery efficiencies are poor.

A number of other methods are then considered, termed enhanced oil recovery (EOR). In order to quickly and inexpensively determine which processes are applicable to a particular reservoir, engineers apply empirically developed screening methods. Three approaches were taken to review the Schrader Bluff reservoir to determine which of the many EOR methods are most applicable. These include (1) classical screening criteria, (2) predictive models, and (3) analogous reservoirs.

Screening criteria are simply defined ranges of critical parameters found to be common to successful projects previously conducted. Such ranges are readily available in the literature for the different EOR process and are easy to apply. Unfortunately, application of a given process in reservoirs fitting all of the critical parameters is not guaranteed and successful projects have been documented where one or more parameters did not meet the criteria. Finally, economic environments change, technologies are advanced, etc., and screening criteria are not always updated to reflect these changes. Even so, applying screening criteria provides some indication of the relative risks involved for a given reservoir.

A number of predictive models have been developed where production performance may be predicted for a given process ^{with} given limited input data. The advantages include relatively short computational times, reduced need for detailed input data, more detailed information predicted, and the convenience of using relatively simple calculation tools. Unfortunately, these models are empirical and as with screening criteria are based on past results. The degree to which the reservoir being analyzed is similar to the fields on which the models are based will determine the degree of reliability in the results. The cooler temperature gradient among other things makes Schrader Bluff uniquely different. None-the-less, the additional information provided by predictive models were compared with the other screening methods to help provide a consistent picture concerning the oil recovery potential.

Finally, an extensive literature search was conducted to identify reservoirs similar in properties to Schrader Bluff and where one or more EOR processes had been applied. Ideally, one would find another reservoir exactly like Schrader Bluff, but in fact this did not occur. As with the previous 2 screening methods, the degree to which Schrader Bluff is uniquely different determined how meaningful the comparison to EOR results reported elsewhere.

Results from any one of these approaches were not considered by itself absolute in deciding which processes warrant further consideration. The next step in the evaluation of EOR processes would be to utilize more sophisticated simulators to refine estimates of field. However, some processes are clearly not going to be very effective, and the obvious poor choices are likely to appear so consistently with all three

screening methods. The goal of the effort described in this section is to identify those processes that clearly are poor choices for Schrader Bluff and discontinue more detailed evaluations of these processes.

3.2 Screening Criteria

A recent review summarizes nicely screening criteria for EOR processes (Taber et al., 1996). A number of criteria have been published over the years and each is a little different. These may be found in the references of Taber's paper. For the purposes of this study, the values from Taber et al., 1996, are used. The average reservoir properties in Table 1 are used for Schrader Bluff in this screening criteria comparison.

We have also put together an in-house version of the classical screening criteria. This version should be considered a draft, since it has not received any peer reviews from outside NIPER. However, it is based on published screening criteria with modifications from experts in the different areas of EOR residing at NIPER. This version is comprised of two values for each process: (1) acceptable range, and (2) possible range (given in parentheses in Table 2). Generally, the acceptable range is considered typical of projects economically successful, and the possible range is considered typical of projects technically challenged but still feasible. These are general definitions, but the intent was to differentiate between (1) good candidate, (2) possible candidate with creative engineering, and (3) not a good candidate. These criteria are provided in Table 2.

Table 2. - Modified EOR screening criteria

Parameter	Steamflood	Cyclic Steam	In Situ Combustion
API Gravity	8-35 (>4)	8-35	≥10
Oil Viscosity (cP)	10-10,000 (<100,000)	10-10,000 (<100,000)	6-2000 (≤100,000)
So (%)	45-80 (≥30)	50-80 (≥30)	>35
Net Pay (ft)	≥30 (≥15)	≥30 (≥20)	10-100 (≥5)
Depth (ft)	400-4000 (≤6000)	400-3000 (≤6000)	NA
Permeability (mD)	≥250 (≥50)	≥250 (≥50)	≥50
Porosity (%)	≥20 (≥15)	≥20 (≥15)	≥20 (≥10)
Transmissibility	≥50 (≥10)	≥50 (≥10)	≥10 (≥5)
So*Porosity	≥0.1 (≥0.07)	≥0.1 (≥0.07)	≥0.1 (≥0.09)

Parameter	Lean Gas, Miscible	Hydrocarbon, Miscible	Carbon Dioxide, Miscible
API Gravity	38-54 (NA)	24-54 (NA)	≥25 (≥13)
Oil Viscosity (cP)	0.07-0.3 (≤10)	0.04-2.3 (≤10)	≤12 (NA)
So (%)	60-80 (≥30)	≥30 (≥25)	≥30 (≥20)
Depth (ft)	7000-13,000 (≥5000)	4000-16,000 (≤2000)	≥1800 (≥1800)
Reservoir Pressure (psi)	≥4500 (≥3000)	NA*	≥1250* (≥800)

*MMP values can be estimated if additional information is known about crude oil

Parameter	Polymer Flood	Microbial Stimulation	Surfactant Polymer Flood
API Gravity	NA	≥15 (NA)	≥25 (NA)
Oil Viscosity (cP)	10-115 (≤200)	NA	≤40 (≤100)
So (%)	NA	NA	≥25 (≥15)
Depth (ft)	≤8000 (NA)	≤8000 (NA)	900-6500 (≤9000)
Permeability (mD)	10-2500 (≥5)	≥50 (≥25)	≥50 (≥40)
Porosity (%)	NA	NA	17-25 (NA)
Mobile oil saturation (%)	≥10 (≥5)	NA	NA
Temperature (°F)	≤150 (≤250)	≤175 (NA)	65-200 (≤250)
Salinity (ppm TDS)	≤140,000 (≤200,000)	≤150,000 (NA)	400-150,000 (≤250,000)

Parameter	Alkaline Surfactant Polymer Flood	Steam-Assisted Gravity Drainage
API Gravity	24-40 (≥12)	NA
Oil Viscosity (cP)	2-20 (≤90)	10-10,000 (NA)
Net Pay (ft)	NA	≥50 (≥15)
Depth (ft)	2500-6500 (≥500)	400-3000 (≤6000)
Permeability (mD)	150-1400 (≥20)	NA
Porosity (%)	23-30 (≥20)	≥20 (≥15)
Temperature (°F)	130-160 (≤200)	NA
Salinity (ppm TDS)	4000-46,000 (≤100,000)	NA
Transmissibility	NA	≥50 (≥10)

NA-no limiting parameters provided for specified property

Values in parentheses indicate extreme limit of technical feasibility

Based on the classic screening criteria the following EOR processes would be acceptable for average reservoir properties: polymer flooding (prefer higher oil saturation), immiscible gases, in situ combustion, and steam (would prefer higher net pay) (Taber et al., [continue] date). The group of micellar/polymer, alkaline surfactant polymer, and alkaline flooding are possible for the lightest oils (>20° API, <35 cP) of Schrader Bluff. Miscible gases (nitrogen, flue gas, carbon dioxide, hydrocarbon) are excluded because of viscosity. Nitrogen and flue gas are also excluded because Schrader Bluff is too shallow (difficult to achieve miscibility). Microbial stimulation was not considered (no criteria provided).

Based on the NIPER modified screening criteria, the following EOR processes would be acceptable for the average reservoir properties: polymer flooding, microbial stimulation, immiscible carbon dioxide flooding, and in situ combustion. Other possible candidate processes that test the limits of conditions include: cyclic steam stimulation, steamflood, surfactant/polymer flood, alkaline surfactant polymer flood, and steam assisted gravity drainage (SAGD) processes. Lean gas and hydrocarbon miscible

processes are rejected because of high fluid viscosity. Depth is also a problem for lean gas (difficult to achieve miscibility).

Sensitivity to the above processes was also tested for the range of reservoir parameters indicated in Table 1. For API gravity, the microbial stimulation process is challenged by the lower densities ($\leq 14^\circ$). Similarly, the higher viscosities (600 cP) eliminates polymer flood, surfactant/polymer flood, and alkaline surfactant polymer flood. These are values corresponding to the Ugnu sands of Schrader Bluff.

The lower values of net pay challenges the steam stimulation processes (steamflood, cyclic steam, and SAGD). If multiple sands are flooded simultaneously, heat efficiency would be improved reducing the adverse impact of thin sands. Similarly, depth strongly affects these processes. The shallowest (3700-3900 ft) depths reduce the heat losses from the wellbore and improves the chances of success. The impact of deep permafrost is not accounted for, however.

In summary, polymer flood, immiscible gas injection, microbial stimulation, and in-situ combustion appear to be the most promising EOR method for obtaining additional oil from Schrader Bluff. Steam injection appears possible for the shallower and thicker sands. Injection of surfactant systems (surfactant/polymer, alkaline surfactant polymer) are limited to the lower viscosity oils (excluding Ugnu). Injection of miscible gases (nitrogen, flue gas, carbon dioxide, hydrocarbon) are not recommended for Schrader Bluff because of the higher oil viscosity. Miscibility will be most easily achieved for enriched carbon dioxide and hydrocarbon systems.

It is recognized that evaluating reservoirs based on screening criteria does not consider all factors and that results may not be completely valid. Some of the factors not accounted for in this analysis include the impact of the permafrost on steam injection, availability of gases for gas injection, transportation costs of chemicals to the North Slope, size of injection pattern (i.e., 40 acres), and harsh surface environment for chemical injection processes (including polymer flood). However, additional studies are recommended for those processes identified as being potentially successful.

3.3 Predictive Models

The DOE has developed and makes available predictive models (they may be downloaded from <http://www.npto.doe.gov/Software/softindx.html>) for quickly estimating production of oil using certain EOR methods. Models available include steamflood, in situ combustion, polymer flood, chemical flood, carbon dioxide miscible flood, and basic waterflood models. These models were used for predicting the performance of EOR processes in Schrader Bluff. In addition to these processes, hot waterflood was predicted by using the steamflood model and setting the steam quality to near zero. Immiscible gas (carbon dioxide, hydrocarbon) floods were predicted by using the gas flood models and ensuring that the viscosities were high enough (creating an immiscible condition).

While quick and convenient, these methods of predicting production performance are of limited value. As with screening criteria, they are empirically based on previously conducted field projects. Provided the field being tested is similar to those used in developing the predictive models, the results are likely to be representative. However, these models are relatively simple, and this approach should be considered with caution. Some of the reservoir parameters are not modeled. In our study, we used

predictive model studies to compare with screening criteria and analogous reservoirs to develop a consensus of relative ranking for various EOR processes.



There are 2 main oil zones in Schrader Bluff, labeled “N” and “O” sands. The reservoir properties between these two zones are quite different. Within each of these major zones, ^{is} are a number of sands or sand lenses having relatively similar properties. For the purposes of this study, a better sand was selected for each zone and properties for these sands are given in Table 3. 

Table 3. - Reservoir properties of selected sands in Schrader Bluff

Property	NB Sand	OA Sand
Depth (ft)	4285	4410
Initial Pressure (psia)	1924	1981
Initial Temperature (°F)	89	93
Net Thickness (ft)	15.5	20
Gross Thickness (ft)	29	30
Permeability (mD)	1828	356
Porosity (fraction)	0.30	0.27
Initial Oil Sat. (fraction)	0.62	0.54
Initial Water Sat. (fraction)	0.38	0.46
Oil Gravity	16°	21°
Dead Oil Viscosity (cP)	500	40
Oil FVF (bbl/STB)	1.04	1.05
Total developed area (acres)	640	640
Total Producing Wells	16	16

 Each of the EOR methods ^{was} were evaluated and compared. Figure 1 shows production over a 10 year period. Clearly, the in situ combustion process did the best. The performance of the surfactant/polymer process was the worst. The others were intermediate between these two processes and similar to basic waterflooding. The large pattern spacing is likely to have contributed to the poor performance for steam, hot water, surfactant, and polymer floods. The heat loss rates (thin sands, deep reservoir, thick permafrost, etc.) also contributed to poorer performance for steam and hot water floods. Very little improvement was seen from hot waterflood over the normal waterflood process.

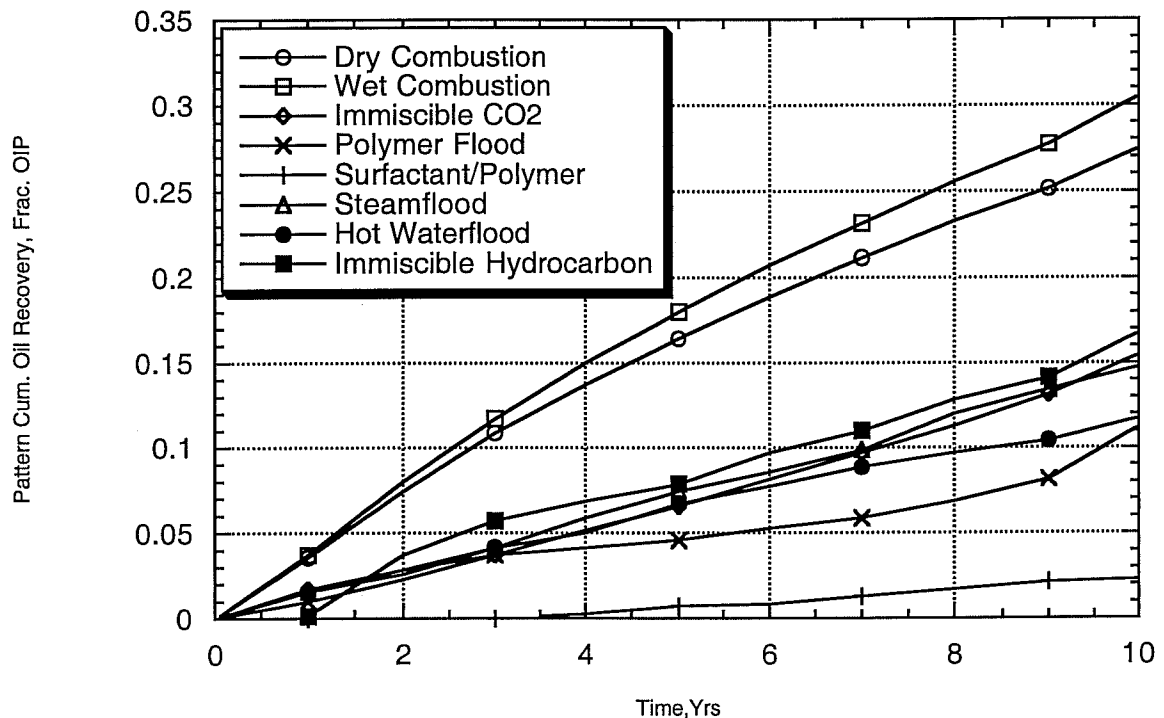


Figure 1. - Comparison of EOR methods from DOE predictive model study

As mentioned previously, the DOE predictive models are empirically based to enable quick determinations of performance. However, some simplifications are needed in developing these models. As a result, results may be misleading when these simplifications ignore factors relevant to Schrader Bluff and different from the average properties derived for the models.

One common simplification is reservoir heterogeneity. This predictive model study assumed a homogeneous reservoir with homogeneous oil properties as defined in Table 3. This is obviously not the case, and heterogeneities in the reservoir are certain to affect the ultimate sweep efficiencies, overall recoveries, etc. In situ combustion is particularly sensitive to this factor and the predictions may be overly optimistic. Reservoir engineers often have a difficult time predicting where in situ combustion fronts are likely to move and what the sweep efficiencies are likely to be.



Another issue is that a number of sands actually exists in Schrader Bluff with varying sand and oil properties. These variations are not accounted for in the predictive model study, as single layer systems were modeled.

In addition, these models were developed in the early 1980's. Consequently, the results on which the empirical correlations were based do not include anything conducted after about 1982 (1974 for in situ combustion). Since then, a number of developments were made and performance predictions improved. More up to date simulation models would be needed to incorporate relatively newer improvements in project design and process performance.

Permeability effects (relative permeability tables) are not incorporated in the steamflood model, although this property is incorporated in waterflood and polymer flood predictions. Adsorption in the chemical flood is not well modeled, either. The effects of salinity and temperature are not modeled, and of course, the adsorption isotherm itself was not determined for a specific surfactant. Typical literature values were used.

Gravity override and channeling effects are not incorporated in the steamflood model. Results are likely to be poorer than predicted. The gas injection models are based on first contact miscibility. This recovery mechanism rarely occurs in the field, but often is used to approximate the multiple contact miscibility that more commonly occurs.

Finally, as already mentioned the immiscible recovery process (carbon dioxide, hydrocarbon, etc.) and the hot waterflood process were approximated by controlling the input parameters. However, the miscible gas and steamflood models were not specifically designed for the immiscible and hot waterfloods, and the accuracy of these predictions are likely to be diminished.

Therefore, the predictive models are used to provide a quick and simple prediction of the EOR recovery processes in Schrader Bluff. These results should be compared with other screening processes before selecting the more promising methods for further study. These results should not be taken out of context nor accepted without further verification by other analytical and comparative studies.

In summary, the DOE predictive models showed that in situ combustion gave the highest recovery of the processes evaluated. Surfactant/polymer injection produced oil very poorly. The remaining processes (polymer, immiscible carbon dioxide, steamflood, and hot waterflood) were similar in performance giving intermediate results. These results should not be accepted in isolation, but compared with other studies to provide a more general assessment of EOR process potential in Schrader Bluff.

3.4 Analogous Reservoirs

⇒ The purpose for conducting a literature search of results published on similar projects is straightforward. In addition to identifying which processes are applicable to reservoirs similar to Schrader Bluff, one also has information on how those processes were best applied, and on what the expected production performance is likely to be. To the extent that the reservoirs are similar, results are likely to also be similar and one need not rely on inaccuracies of other predictive methods. Sophisticated simulators are very effective when all the input parameters are known. But this is never the case, and assumptions are always needed.

Unfortunately, 2 reservoirs are never exactly alike and comparison of analogous reservoirs is likewise an approximation. Furthermore, Schrader Bluff presents some very differentiating conditions. Due to the location in the Arctic circle, the temperature gradient is quite different from most reservoirs produced

outside of Alaska. Because of this fact, no analogous reservoir was found that conformed reasonably close to all relevant reservoir parameters, and where some EOR process was applied. As a result, analogous reservoirs were sought for different sets of reservoir parameters, depending on the EOR process and its relative importance to the reservoir temperature gradient.

The following primary sources were reviewed:

- 5 Oil & Gas Journal EOR reports (1986-1996)
- 6 NIPER Heavy Oil Database
- 7 DOE EOR Database
- 8 Literature Reviews on EOR Processes (technical publications, government reports)
- 9 Technical Papers (SPE, etc.)
- 10 SIMTECH Report to BP Exploration

Table 1 provides a summary of reservoir parameters encompassing most of Schrader Bluff and uses the basis of comparison. Two separate sets of Screening parameters (sets A and B) were selected for identifying analogous reservoirs. Set B excluded steam, hot water, and miscible gas processes because depth is a critical parameter for these processes. The screening parameters are summarized in Table 4. Reservoirs were considered analogous if complying with either Set A or Set B criteria. Any reservoir not complying with all of Screening Set A or Screening Set B as described, was excluded from the final list.

Table 4. - Screening parameter ranges for analogous reservoirs

Parameter	Screening Set A	Screening Set B
Depth (ft)	3800-5000	NA
API Gravity*	12°-23° (OR viscosity criteria)	12°-23° (OR viscosity criteria)
Viscosity * (cP, reservoir conditions)	15-1000 (OR density criteria)	15-1000 (OR density criteria)
Permeability (mD)	>50	>50
Temperature (°F)	NA	80-100
Net Pay (ft)**	10-30	10-30

*Reservoirs were considered to apply when either the viscosity or API Gravity criteria was satisfied. For example, a reservoir would be included if viscosity were 900 cP, even if API gravity was 10°.

**Not applied rigorously. Excluded reservoirs on this basis when information was available. When net pay was not available, reservoir was assumed to comply.

A number of analogous reservoirs were found that fit the criteria in Table 4, and a number of EOR processes were applied in these reservoirs. They include:

- 1 Polymer floods, 53 projects

- 2 In situ combustion, 11 projects
- 3 Carbon dioxide immiscible floods, 8 projects
- 4 Steamfloods, 8 projects
- 5 Alkaline floods including Alkaline Surfactant Polymer floods, 7 projects
- 6 Micellar/Polymer floods, 6 projects

Table 5 summarizes the number of projects considered economically successful and not successful, as stated in Oil & Gas Journal. As can be seen in the table, at least 1 project was successful and 1 project was not successful for each of these processes. Based on this cursory review, one cannot quickly dismiss any of these processes for Schrader Bluff.

Table 5. - Number of analogous reservoirs by process and status

EOR Process	Projects Successful	Projects Failed	Status Unknown	Total No. Projects
Polymer	22	7	24	53
In Situ Combustion	4	5	2	11
CO ₂ Immiscible	3	5	0	8
Alkaline	2	1	4	7
Micellar/Polymer	1	3	2	6

If the relative chance of success can be inferred by the number of projects tried, one would conclude that polymer floods are most likely to be successful. It was tried most often. Indeed, the proportion of successful to not successful projects are the greatest for this approach. However, the status for a number of projects were not known, and if inferred that the unknowns are more likely to be unsuccessful than successful (one is more likely to advertise a successful project than an unsuccessful one), the odds of success may not be any better for polymer floods.

The details of the reports associated with these projects were reviewed in a bit more detail. From this evaluation, the following conclusions were obtained.

3.4.1 Polymer Flood

Many projects were identified from the analogous reservoirs that were considered economically successful with polymer floods.

Polymer flooding improves the recovery rate by improving sweep efficiency and mobility ratio of waterflood—a particular problem for more viscous crude oils like that of Schrader Bluff.

Schrader Bluff reservoir conditions appear to present no major barriers for this method of enhancing production from a technical perspective. Unique factors associated with the Arctic environment are not emphasized in this analysis, however, and may present unique challenges. For example, preparing a

polymer solution at sub-zero temperatures would require additional equipment not typical of the examples found in the literature.

3.4.2 *In Situ Combustion*

Some economically successful projects were found among the analogous reservoirs.

Technically, Schrader Bluff reservoir parameters do not appear to present any major technical barriers. However, compartmentalization is particularly detrimental to poorly designed in situ combustion projects and was not included in the screening parameters. The issue of communication between the different sands is also a consideration that needs to be evaluated, but was not included in this cursory review. Therefore, the “lack” of major technical barriers needs to be more fully evaluated for in situ combustion.

Finally, operational risks not considered in this screening are likely causes of economic failure in other cases. This factor must be considered for all in situ combustion projects

3.4.3 *Gas Flooding*

Of the different types of gas injection, only carbon dioxide immiscible processes were found for analogous reservoirs to Schrader Bluff.

Improved recoveries result from viscosity reduction, fluid swelling, and pressure maintenance for immiscible gas injection processes.

Fluid swelling capacity is reduced in crude oils containing solution gas, which is the case for Schrader Bluff. More detailed simulation studies would be needed to estimate the recovery potential.

Availability of a cheap source of gas is critical to economic success. At this time a cheap source of carbon dioxide is not available on the North Slope.

3.4.4 *Steam Injection*

Some projects were found to be economically successful. These were all cyclic injection processes and did not include any steamflood (drive) across the pattern from injector to producer.

While not reported, it is suspected that the successful projects were in reservoirs with pay zones much thicker than those typical of Schrader Bluff.

Insulated tubing is generally required for reservoirs at depths exceeding 4000 ft. This is particularly so with Schrader Bluff because of the thick permafrost that exists. Insulated tubing adds additional cost to well completions.

Large pattern sizes typical of Schrader Bluff (>10 acres) are likely to present a major barrier to economic success for any non-cyclic process, including that of steamflooding.

3.4.5 *Alkaline Processes*

(Alkaline, Alkaline/Surfactant Polymer, etc.)

A few alkaline projects were found in Schrader Bluff analogous reservoirs. Two of these were considered economic successes.

Very little detail is available on these projects. Very little can be said about these projects in Schrader Bluff type reservoirs.

3.4.6 Micellar/Polymer Floods

A few micellar/polymer projects were found in Schrader Bluff analogous reservoirs. One of these was considered an economic success.

Anticipated difficulties with this process includes high chemical costs and increased risks with large pattern spacing (>10 acres).

Based on a review of analogous reservoirs,

1. The process having the greatest potential for success is polymer flooding. All of the processes listed have some chance of success demonstrated in each case by at least one successful project in Schrader Bluff analogous reservoirs.
2. Based on a review of analogous reservoirs, those processes least likely to succeed include: micellar/polymer floods, alkaline injection processes, and steamfloods. Note that unlike steamfloods, cyclic injection of steam has worked in some analogous reservoirs.
3. Some of the unique circumstances of Schrader Bluff were not considered. These could strongly influence the final decision. Severe surface operation conditions, high shipping costs, high well completion and maintenance costs, geological compartmentalization, etc., all adversely impact ultimate production costs and the chances of economic success for EOR processes.
4. Microbial injection was not identified in any of the analogous reservoirs. Use of indigenous species has not been ruled out as a possibility for Schrader Bluff. It is uncertain whether any of the classical approaches of microbial injection would be successful.

Although injection of enriched hydrocarbon processes were not identified for any of the Schrader Bluff analogous reservoirs, this process has some unique advantages on the North Slope. Production engineers are familiar with this process. NGL's are available on the North Slope with unique economic advantages, because of the constrained transportation of it to other parts of the world. Finally, its absence in analogous reservoir cases is more the result of being limited to unique circumstances throughout the world where it is successfully applied (including the north slope of Alaska) than to the reservoir conditions defined in this review. Further investigation is warranted for this process.

3.5 Recommendations

An initial screening process was conducted on Schrader Bluff to determine what EOR processes are obvious choices for further investigation. Other processes with modifications may be suitable, but would only be considered after more detailed studies suggest that the obvious first choices are unlikely to be economically successful.

Three approaches were taken in this initial screening evaluation of Schrader Bluff. Classic screening criteria were applied to Schrader Bluff reservoir properties. Simple DOE Predictive Models were used to compare the recovery potential of certain EOR processes. Finally, a search for reservoirs with properties

similar to Schrader Bluff was made, where one or more EOR processes were applied. While each of these screening methods provided different types of answers, the following generalizations are made.

1. No one process was considered best by all three process screening methods.
2. Screening criteria suggested that polymer flood, immiscible gas injection, microbial stimulation, and in situ combustion processes may be applicable for Schrader Bluff.
3. DOE Predictive models indicated that in situ combustion had the greatest recovery potential for Schrader Bluff. All other processes were marginal or not promising.
4. Search for analogous reservoirs did not find any reservoirs comparable to Schrader Bluff where an EOR process was applied. However, by selecting key parameters examples were found for most of the EOR processes being tried at least once. The most commonly tried process was polymer flooding, with many of these projects being economically successful. Those processes found least likely to succeed include: alkaline processes, micellar/polymer processes, and steamfloods (excluding cyclic steam).
5. Miscible gas injection was not identified as a viable process by these screening methods. This is primarily because miscible recovery for more viscous hydrocarbons is usually quite expensive, and the poor mobility ratios are likely to result in poor sweep efficiencies (low ultimate recoveries). However, the unique circumstances for Schrader Bluff on the Alaska North Slope are sufficient to warrant further study of this process.

Three processes were recommended for further study: polymer flooding, gas injection (miscible, immiscible), and in situ combustion. The results of the in situ combustion study are outlined in the remaining sections of this report.

4. Recovery by In-Situ Combustion

4.1 Background

In-situ combustion, or fireflooding, as it is sometimes called, is the oldest member of the thermal oil recovery family. It is basically a gas injection process with gas being air to supply oxygen. The air sustains combustion of a portion of the reservoir oil for the purpose of generating heat in-situ and subsequently reducing the viscosity of the remaining oil. The combined effects of reduced fluid viscosity, increased oil swelling from generated carbon dioxide, and increased volume expansion from generated flue gases including steam, contribute to the enhanced recovery of oil.

Advantages over other advanced recovery methods include improved heat efficiency over steamfloods (no heat lost in wellbore during injection), more effective than steam injection in thin reservoirs, not limited by reservoir pressure, more robust with respect to variations in reservoir permeability, injection fluid (air) not limited by source location, less limited by well spacing as compared to other processes, and in general when successful is the most efficient thermal recovery process available. In-situ combustion can be used to effectively recover a high percentage of oil in situations unsuitable for any other process.

Disadvantages include the requirement of expensive initial laboratory evaluation costs, increased economic uncertainties in prediction of field performance, sensitivity to more extensive field management practices, and in general all the disadvantages associated with implementation of a complex and sophisticated field project. The inability to reasonably predict field results for a given situation have led to many project failures. Subsequent analyses of these failures inevitably revealed that the implementation, design, or reservoir conditions were not appropriate for the in-situ combustion process attempted.

A number of past in-situ combustion field projects have been reviewed (Sarathi 1994; Sarathi 1995; Sarathi 1998). Nearly all of them were considered economically unsuccessful. The one successful project that was reviewed did not circumvent the planning steps discussed below and did carefully design for operator contingencies. In general, in-situ combustion may enhance oil production by substantial amounts, provided the reservoir conditions are suitable and just as importantly, provided the project design is fully evaluated, well planned, and carefully implemented.

In order to determine if in-situ combustion can be effectively applied in a particular field, one must follow a prescribed scaling path. Other recovery processes have become more standard practice and often can circumvent some of these steps, but they are still required to manage economic risks most effectively. Essentially, these steps in order are: (1) consider the favorable and unfavorable risk factors of the particular reservoir (reservoir screening), (2) conduct laboratory tube runs (laboratory scale burns), (3) evaluate the technical and economic sensitivities to project design factors, and (4) conduct a field pilot test. To progress along this path in order, choosing to stop when perceived risks exceed perceived benefits offers the best route to risk management.

Table 6 summarizes the favorable and unfavorable risk factors for in-situ combustion processes. This is the first step and can be used to determine relatively quickly if the process is suitable or not. Although

not definitive (individual factors are not exclusive to success or failure), it is the basis for deciding whether to continue or not with the expensive laboratory testing.

Table 6. - Summary of favorable and unfavorable risk factors for in-situ combustion

Favorable Risk Factors	Unfavorable Risk Factors
High reservoir temperature ($\geq 150^{\circ}\text{F}$)	Extensive reservoir fractures and faults
Low vertical permeability	Large gas caps
Good lateral continuity	Strong water drive
Thin sand layers ($\leq 50\text{ ft}$)	Highly heterogeneous reservoir
High oil saturation ($S_o \cdot \text{porosity} \geq 0.1$)	Low oil saturation
Good fluid transmissibility ($\text{permeability} \cdot \text{thickness} / \text{viscosity} \geq 20\text{ md-ft/cp}$)	High oil viscosity ($> 5000\text{ cp}$), low oil permeability in thin sands
Good overburden competence	
High dip	
Uniform permeability profile	

If conditions appear favorable, laboratory tube runs are conducted to determine the kinetic parameters of oil combustion at reservoir conditions. From this information minimum air requirements, ignition requirements, burn efficiency (air/fuel ratio), extinction radius, and overall favorability are further determined. These values can then be used in simulation studies to develop estimates of potential recovery and economic costs. Sensitivities to ranges in project design parameters can be evaluated using simulation tools. However, full scalability is not possible until a field pilot project is conducted. The impact of heterogeneity, discontinuity, etc., can only be measured in such a pilot project, and burn front performance cannot be properly scaled in the laboratory. Furthermore, simulation techniques for in-situ combustion is not as reliable as that of other more commonly applied processes such as gas flooding or steamflooding.

This section of the report focuses on the evaluation results for in-situ combustion in Schrader Bluff. Based on the overall screening of EOR processes, in-situ combustion was among the methods considered potentially favorable and was evaluated further. Laboratory scale tube runs were conducted followed by simulation sensitivity studies to determine if the kinetic parameters for the crude oil were favorable. Results of the sensitivity studies indicated which parameters warrant more careful attention. Described in the following subsections are the results of (1) experimental tube runs, and (2) simulation sensitivity studies as related to in-situ combustion in Schrader Bluff.

4.2 Tube Run Tests

4.2.1 In-situ Combustion Tube Run Number 1

The primary information of interest from laboratory tube runs for specified operational conditions include: general burning characteristics, fuel requirement, air requirement, air/fuel ratio, peak combustion temperature, and hydrocarbons recovered from swept zone. However, because many of the operational conditions of a laboratory experiment of this type is not scaled to field conditions, results should be

considered qualitative. Certain combustion characteristics of the oil tested in the laboratory can be considered representative of a field operation.

For Schrader Bluff, a stable burn was maintained as expected at the designed injection rate. The coreholder is divided into 12 zones (6 in long) with 12 thermocouples to monitor the front progression. When the front reached zone 8, the temperature never reached the optimal range and it appeared that the burn began to die out. At 14 hr into the experiment, it was evident that a stable burn could not be reestablished and the experiment was terminated.

Upon inspection of the system after the experiment was concluded, it was found that the high pressures involved in the experiment resulted in the crushing of the downstream portion of the tube, and combined with high heat losses resulted in the quenching of the fire front. Even so, some results were obtained and are summarized in the following table.

Table 7. - Summary of results for Run 1

Core Porosity	0.436	Pre-Heat Temp.	89° F
Core Permeability	4.3 Darcy	Peak Temperature	1146° F
Pressure	1800 psig	Displ. Front Velocity	0.61 ft/hr
Inj. (Air) Flux <i>a f</i>	100 scf/ft ² hr	Air Requirement, Stabilized	166 l(ST)/l
Water/Air Ratio	0	Oxygen Requirement, Stabilized	35.7 l(ST)/l
Oil Sat., Initial	0.588	Fuel Requirement, Stabilized	1.04 lbm/ft ³
Water Sat., Initial	0.412	Air/Fuel Ratio, Stabilized	160 scf/lb
Overall recovery	0.845*	Oxygen Utilization, Stabilized	0.983

*Not comparative with Run 2, since only 60% of the core was burned.

inconsistent with previous table 6 Capitalize?

4.2.2 In-situ Combustion Tube Run Number 2

The primary difference between this run and run 1 was the designed injection of water after a stable burn was established. The primary purpose of injecting water is to carry more of the heat forward from behind the front to the oil ahead of the front via steam generation. Air is very inefficient in heat transfer processes relative to water. Injection of brine was initiated 0.5 hr after the burn was initiated. The test was terminated at the normal time of 15 hr. The overall results with Schrader Bluff oil were very favorable for water injection.

Also, learning from the first run, care was taken to temporarily reduce injection rates (air, water) when system pressures reached high levels. For example, water injection was stopped for about 5 hr (starting about 0.5 hr. after water injection was started), but once resumed was continued for the

remainder of the run. The lower core permeability was also a factor leading to high system pressures. Results for run number 2 are given in Table 8.

Table 8. - Summary of results for Run 2

Core Porosity	0.426	Pre-Heat Temp.	89° F
Core Permeability	0.5 Darcy	Peak Temperature	1053° F
Pressure	1800 psig	Displ. Front Velocity	0.48 ft/hr
Inj. Air Flux	100 scf/ft ² hr	Air Requirement, Stabilized	210 l(ST)/l
Water/Air Ratio	0.98 kg/l	Oxygen Requirement, Stabilized	41.2 l(ST)/l
Oil Sat., Initial	0.582	Fuel Requirement, Stabilized	1.40 lbm/ft ³
Water Sat., Initial	0.418	Air/Fuel Ratio, Stabilized	151 scf/lb
Overall recovery	0.921	Oxygen Utilization, Stabilized	0.985

4.3 Simulation Sensitivity Studies

4.3.1 Model Description and Data Input

Oil was divided into two components, light (CO₂, C₁-C₁₆) and heavy fractions (C₁₇-C₃₆₊). The simulator modeled three phases: solid (coke), liquid (water, heavy oil, light oil) and gas (oxygen and inert gas) for a total of six components. Inert gas included all noncondensable gases other than oxygen. Its property was assumed to be that of nitrogen except molecular weight was assigned a value between that of nitrogen and carbon dioxide. The oil properties were molar average values derived from the individual component properties. The critical pressure, critical temperature, molecular weight, and component formula for light oil were 526 psi, 372° F, 82, and C_{5.7}H_{13.6}, respectively, while that for heavy oil were 158 psi, 1092° F, 409 and C_{29.1}H_{60.24}, respectively. Other properties, such as thermal expansion, fluid compressibility, and fluid heat capacity, were also reported in Table 9.

Table 9. - Properties of heavy and light fractions

	Heavy Fraction	Light Fraction
Molecular Weight, lbm/lbm mol	409	82
Critical Pressure, psi	158	526
Critical Temperature, °F	1092	372
Gas-Phase Heat Capacities, C _p =A+BT+CT ² +DT ³ , Btu/(lbm mol-°F)		
A	-8.14	-1.89
B	0.549	0.1275

C	-1.68e-4	-3.9e-5
D	1.98e-8	4.6e-9
Compressibilities, psi ⁻¹	5e-6	5e-6
Thermal Expansion Coefficient, °F ⁻¹	1.496e-4	2.839e-4

Four chemical reactions were included in the simulation. They were cracking of heavy oil and oxidation of heavy oil, light oil, and coke. The stoichiometries were derived for the hydrogen, carbon, and oxygen separately, as shown in Table 10.

Table 10. - Four chemical reactions

Reaction Type	Reaction Equation
Cracking	$C_{29.1}H_{60.24} \rightarrow 2.754 C_{5.7}H_{13.6} + 13.4 CH_{1.7} + 2.00 \times 10^4 \text{ Btu/lbmol}$
Heavy Oil Burning	$C_{29.1}H_{60.24} + 44.16 O_2 \rightarrow 30.12 H_2O + 29.1 CO_2 + 3.49 \times 10^6 \text{ Btu/lbmol}$
Light Oil Burning	$C_{5.7}H_{13.6} + 9.1 O_2 \rightarrow 6.8 H_2O + 5.7 CO_2 + 9.48 \times 10^5 \text{ Btu/lbmol}$
Coke Burning	$CH_{1.7} + 1.425 O_2 \rightarrow 0.85 H_2O + CO_2 + 2.25 \times 10^5 \text{ Btu/lbmol}$

Note: Reaction rate is proportional to $A \exp(-E/RT)$

For combustion of the light oil, heat of reaction was assumed to be 948,000 Btu/lb-mol of oil, while that for the heavy oil was assumed to be 3,490,000 Btu/lb-moll. For the coke, heat of reaction was assumed to be 225,000 Btu/lb-moll of coke. These are average values typically found in published literature.

The reservoir was modeled based on a 36-layer model developed by BPX-Alaska. In our study, 36 layers were lumped into 14 layers. Average values for initial water saturation, oil saturation, porosity, permeability, and compressibility were calculated based on the 36 layer model. In each layer properties are constant and pertinent data of the 36 and 14 layer properties, such as initial water and oil saturation, together with pay zone thickness, permeability, porosity, and compressibility are documented in Tables e and f.

Table 11. - Schrader Bluff reservoir 36-layer model description

36-layer Model								14-Layer Model
Zone	Layer	Dz, ft	netgrs	Por	Cr	Sw	Kx, md	Layer
NA	1	4	0.671	0.304	6.2E-5	0.5235	234	1
	2	4	0.762	0.319	5.6E-5	0.5235	445	

	3	4	0.963	0.306	4.6E-5	0.5235	343	
	4	4	0.42	0.235	3.8E-5	0.5235	23	
Silt	5	10.11	0.08	0.24	3.18E-4	1	0.7	2
NB	6	4.21	0.633	0.24	3.3E-5	0.4283	51	3
	7	4.21	0.76	0.3	5.0E-5	0.4283	261	
	8	4.21	0.76	0.324	5.2E-5	0.4283	501	
	9	4.21	0.76	0.316	3.8E-5	0.4283	409	4
	10	4.21	0.62	0.29	2.8E-5	0.4283	46	
	11	4.21	0.61	0.221	3.6E-5	0.4283	6	
Silt	12	11.24	0.08	0.23	1.96E-4	1	0.7	5
NC/ ND	13	1.07	0.923	0.304	4.6E-5	0.4	292	6
	14	1.07	0.624	0.328	6.7E-5	0.4	312	
	15	1.07	0.76	0.31	5.2E-5	0.4	358	
	16	1.07	0.868	0.231	2.6E-5	0.4	7	
Silt	17	9.43	0.08	0.24	2.04E-4	1	0.7	7
NE	18	48.01	0.549	0.262	2.04E-4	0.5511	20	8
NF	19	36.72	0.08	0.24	2.04E-4	0.5073	0.7	9
OA	20	3.75	0.687	0.238	5.5E-5	0.398	33	10

Dz = Layer Thickness

Netgrs = Net-to-Gross Multplier

Por = Porosity

Cr = Compressibility

Sw = Water Saturation

Kx = Permeability in the X Direction

Table 11. continued

Zone	Layer	Dz, ft	netgrs	Por	Cr	Sw	Kx, md	layer
	21	3.75	0.946	0.315	6.7E-5	0.398	417	
	22	3.75	0.505	0.183	3.3E-5	0.398	27	
	23	3.75	0.946	0.262	5.0E-5	0.398	111	
	24	3.75	0.964	0.306	5.6E-5	0.398	246	11
	25	3.75	0.837	0.279	5.0E-5	0.398	159	
	26	3.75	0.711	0.225	3.1E-5	0.398	63	
	27	3.75	0.883	0.244	3.3E-5	0.398	84	
Silt	28	31.83	0.07	0.22	3.5E-4	1	0.7	12
OB	29	3.84	0.882	0.262	4.6E-5	0.4571	75	13
	30	3.84	0.943	0.285	5.3E-5	0.4571	135	
	31	3.84	0.941	0.29	4.5E-5	0.4571	186	
	32	3.84	0.941	0.307	4.6E-5	0.4571	279	
	33	3.84	0.836	0.274	4.0E-5	0.4571	129	14
	34	3.84	0.08	0.217	3.7E-5	0.4571	7	

	35	3.84	0.08	0.228	3.5E-5	0.4571	10	
	36	3.84	0.941	0.257	4.3E-5	0.4571	75	

Table 12. - Schrader Bluff reservoir 14-layer model description

14-Layer Model							
Zone	Layer	Dz, ft	netgrs	Por	Cr	Sw	Kx, md
NA	1	16.00	0.704	0.298	5.133E-5	0.5235	296.90
Silt	2	10.11	0.080	0.240	3.180E-4	1.0000	0.70
NB	3	12.63	0.718	0.291	4.571E-5	0.4283	283.98
	4	12.63	0.663	0.279	3.427E-5	0.4283	172.37
Silt	5	11.24	0.080	0.230	1.960E-4	1.0000	0.70
NC/ND	6	4.28	0.794	0.290	4.610E-5	0.4000	233.81
Silt	7	9.43	0.080	0.240	2.040E-4	1.0000	0.70
NE	8	48.01	0.549	0.262	2.040E-4	0.5511	20.00
NF	9	36.72	0.080	0.240	2.040E-4	0.5073	0.70
OA	10	15.00	0.771	0.260	5.354E-5	0.3980	173.73
	11	15.00	0.849	0.266	4.330E-5	0.3980	144.09
Silt	12	31.83	0.070	0.220	3.500E-4	1.0000	0.70
OB	13	15.36	0.927	0.286	4.753E-5	0.4571	170.22
	14	15.36	0.484	0.261	4.113E-5	0.4571	92.81

Dz = Layer Thickness

Netgrs = Net-to-Gross Multiplier

Por = Porosity

Cr = Compressibility

Sw = Water Saturation

Kx = Permeability in the X Direction

Capillary pressure was neglected and initial pressure (1981 psi) and temperature (88°F) were kept the same as in the BPX-Alaska 36 layer model. Relative permeabilities vary with different types of rock. In this simulation, 14 layers are classified as six types of rock and their relative permeabilities for each layer are listed in Table 13.

Table 13 (a). - Liquid-gas and water-oil relative permeabilities for layers 1, 8 and 9

Liquid-Gas Relative Permeabilities			Water-Oil Relative Permeabilities		
Liquid Saturation, Sl	Krg	Krog	Water Saturation, Sw	Krw	Krow

0.00	1.0000	0.0000	0.00	0.0000	1.0000
0.05	0.8563	0.0013	0.05	0.0061	0.909
0.10	0.7342	0.0046	0.10	0.0122	0.818
0.15	0.6378	0.0107	0.15	0.0204	0.7271
0.20	0.5627	0.0199	0.20	0.0294	0.6301
0.25	0.4794	0.0332	0.25	0.0387	0.5167
0.30	0.4171	0.0510	0.30	0.0482	0.4116
0.35	0.361	0.0735	0.35	0.0587	0.305
0.40	0.3081	0.1020	0.40	0.0703	0.2136
0.45	0.2567	0.1362	0.45	0.0815	0.1475
0.50	0.2042	0.1767	0.50	0.094	0.1048
0.55	0.1559	0.2236	0.55	0.1101	0.0759
0.60	0.1201	0.2773	0.60	0.1322	0.0569
0.65	0.0863	0.3383	0.65	0.1566	0.0385
0.70	0.067	0.4072	0.70	0.1928	0.0243
0.75	0.0517	0.4843	0.75	0.2397	0.0186
0.80	0.0398	0.5698	0.80	0.3006	0.0125
0.85	0.0299	0.6639	0.85	0.3915	0.0094
0.90	0.0199	0.7667	0.90	0.5106	0.0062
0.95	0.01	0.8788	0.95	0.6948	0.0031
1.00	0.0000	1.0000	1.00	1.0000	0.0000

Table 13(b). - Liquid-gas and water-oil relative permeabilities for layers 3 and 4

Liquid-Gas Relative Permeabilities			Water-Oil Relative Permeabilities		
SI	Krg	Krog	Sw	Krw	Krow
0.00	1.0000	0.0000	0.00	0.0000	1.0000
0.05	0.8563	0.0013	0.05	0.0045	0.8466
0.10	0.7342	0.0046	0.10	0.009	0.7489
0.15	0.6378	0.0107	0.15	0.0136	0.6588
0.20	0.5627	0.0199	0.20	0.0181	0.5768
0.25	0.4794	0.0332	0.25	0.0226	0.5144
0.30	0.4171	0.0510	0.30	0.0286	0.4494
0.35	0.361	0.0735	0.35	0.0355	0.3871
0.40	0.3081	0.1020	0.40	0.0446	0.3333
0.45	0.2567	0.1362	0.45	0.0574	0.2831
0.50	0.2042	0.1767	0.50	0.0743	0.2192
0.55	0.1559	0.2236	0.55	0.0965	0.1696
0.60	0.1201	0.2773	0.60	0.1254	0.128
0.65	0.0863	0.3383	0.65	0.1622	0.0929

0.70	0.067	0.4072	0.70	0.2104	0.0654
0.75	0.0517	0.4843	0.75	0.2736	0.0469
0.80	0.0398	0.5698	0.80	0.3544	0.0314
0.85	0.0299	0.6639	0.85	0.4588	0.0208
0.90	0.0199	0.7667	0.90	0.5971	0.0122
0.95	0.01	0.8788	0.95	0.7741	0.0056
1.00	0.0000	1.0000	1.00	1.0000	0.0000

Table 13(c). - Liquid-gas and water-oil relative permeabilities for layer 6

Liquid-Gas Relative Permeabilities			Water-Oil Relative Permeabilities		
Sl	Krg	Krog	Sw	Krw	Krow
0.00	1.0000	0.0000	0.00	0.0000	1.0000
0.05	0.8563	0.0013	0.05	0.0038	0.8466
0.10	0.7342	0.0046	0.10	0.0075	0.7489
0.15	0.6378	0.0107	0.15	0.0113	0.6588
0.20	0.5627	0.0199	0.20	0.0151	0.5768
0.25	0.4794	0.0332	0.25	0.0189	0.5144
0.30	0.4171	0.0510	0.30	0.0243	0.4494
0.35	0.361	0.0735	0.35	0.0305	0.3871
0.40	0.3081	0.1020	0.40	0.0398	0.3333
0.45	0.2567	0.1362	0.45	0.0521	0.2831
0.50	0.2042	0.1767	0.50	0.0681	0.2192
0.55	0.1559	0.2236	0.55	0.0888	0.1696
0.60	0.1201	0.2773	0.60	0.1167	0.1280
0.65	0.0863	0.3383	0.65	0.153	0.0929
0.70	0.067	0.4072	0.70	0.2	0.0645
0.75	0.0517	0.4843	0.75	0.261	0.0469
0.80	0.0398	0.5698	0.80	0.3418	0.0314
0.85	0.0299	0.6639	0.85	0.4486	0.0208
0.90	0.0199	0.7667	0.90	0.5873	0.0122
0.95	0.01	0.8788	0.95	0.7672	0.0056
1.00	0.0000	1.0000	1.00	1.0000	0.0000

Table 13(d). - Liquid-gas and water-oil relative permeabilities for layers 10 and 11

Liquid-Gas Relative Permeabilities	Water-Oil Relative Permeabilities
------------------------------------	-----------------------------------

Sl	Krg	Krog	Sw	Krw	Krow
0.00	1.0000	0.0000	0.00	0.0000	1.0000
0.05	0.8444	0.0013	0.05	0.0033	0.9209
0.10	0.7310	0.0046	0.10	0.006	0.8361
0.15	0.6464	0.0107	0.15	0.009	0.7427
0.20	0.5742	0.0199	0.20	0.0122	0.6413
0.25	0.4994	0.0332	0.25	0.0153	0.5369
0.30	0.4458	0.0510	0.30	0.0185	0.4261
0.35	0.3973	0.0735	0.35	0.0223	0.3342
0.40	0.3454	0.1020	0.40	0.0266	0.2581
0.45	0.2964	0.1362	0.45	0.0326	0.1919
0.50	0.2429	0.1767	0.50	0.0395	0.1411
0.55	0.2011	0.2236	0.55	0.0483	0.0999
0.60	0.1656	0.2773	0.60	0.0598	0.0648
0.65	0.1311	0.3383	0.65	0.0768	0.0464
0.70	0.0988	0.4072	0.70	0.1063	0.0318
0.75	0.0733	0.4843	0.75	0.1491	0.0229
0.80	0.0514	0.5698	0.80	0.2159	0.0143
0.85	0.0350	0.6639	0.85	0.3134	0.0107
0.90	0.0178	0.7667	0.90	0.4649	0.0071
0.95	0.0088	0.8788	0.95	0.6736	0.0036
1.00	0.0000	1.0000	1.00	1.0000	0.0000

Table 13(e). - Liquid-gas and water-oil relative permeabilities for layers 13 and 14

Liquid-Gas Relative Permeabilities			Water-Oil Relative Permeabilities		
Sl	Krg	Krog	Sw	Krw	Krow
0.00	1.0000	0.0000	0.00	0.0000	1.0000
0.05	0.8444	0.0013	0.05	0.0025	0.8516
0.10	0.7310	0.0046	0.10	0.0049	0.7032
0.15	0.6464	0.0107	0.15	0.0074	0.5658
0.20	0.5742	0.0199	0.20	0.0098	0.4680
0.25	0.4994	0.0332	0.25	0.0118	0.3848
0.30	0.4458	0.0510	0.30	0.0153	0.3150
0.35	0.3973	0.0735	0.35	0.0195	0.2541
0.40	0.3454	0.1020	0.40	0.0267	0.2013
0.45	0.2964	0.1362	0.45	0.0372	0.1582
0.50	0.2429	0.1767	0.50	0.0512	0.1269
0.55	0.2011	0.2236	0.55	0.0696	0.0997

0.60	0.1656	0.2773	0.60	0.0954	0.0769
0.65	0.1311	0.3383	0.65	0.1289	0.0529
0.70	0.0988	0.4072	0.70	0.1696	0.0368
0.75	0.0733	0.4843	0.75	0.2288	0.0207
0.80	0.0514	0.5698	0.80	0.3069	0.0123
0.85	0.0350	0.6639	0.85	0.4140	0.0092
0.90	0.0178	0.7667	0.90	0.5620	0.0062
0.95	0.0088	0.8788	0.95	0.7625	0.0031
1.00	0.0000	1.0000	1.00	1.0000	0.0000

Table 13(f). - Liquid-gas and water-oil relative permeabilities for layers 2, 5, 7 and 12

Liquid-Gas Relative Permeabilities			Water-Oil Relative Permeabilities		
SI	Krg	Krog	Sw	Krw	Krow
0.00	0.7	0.	0.00	0.0000	0.7
1.00	0.	0.7	1.00	0.7	0.

Pattern selection should be based on such considerations as well investment resources, well productivity, reservoir structure, etc. In this study, the injector was set in the center of four 20-acre squares surrounded by eight producers. This formed an 80-acre inverted 9-spot pattern. One-fourth of an 80 acre 9-spot pattern was used in our simulation, and initial oil, water, and pore volume in place are $2.3397\text{E}7 \text{ ft}^3$, $3.4001\text{E}7 \text{ ft}^3$, and $5.7399\text{E}7 \text{ ft}^3$, respectively.

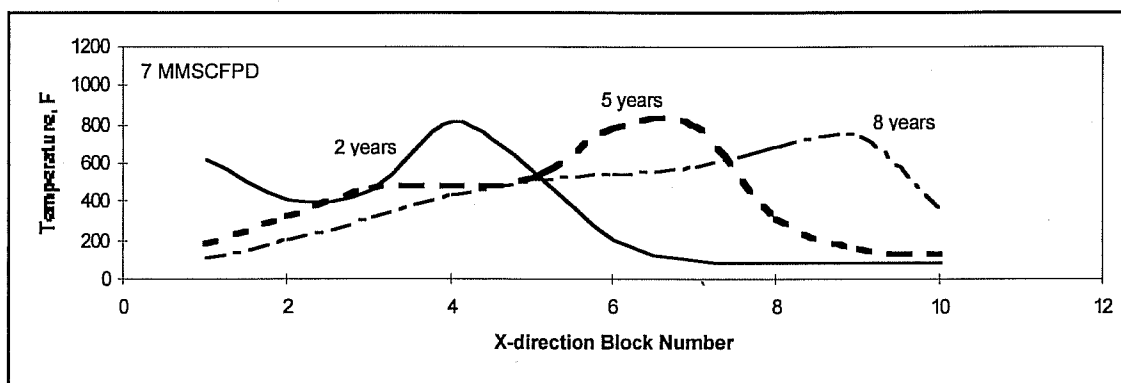
Choosing a grid system is always one of the most critical tasks. A total of nine primary equations (six mass balances, one energy balance, and two mole-fraction constraints) need to be solved simultaneously at each node. Computer time rises dramatically as the total number of nodes increases. The number of nodes in the grid system was minimized without sacrificing simulation accuracy. The maximum grid number allowed for STARS is 13440, and the product of block number and components is limited to 26880. A $10 \times 10 \times 14$ grid, with a block size of $93.338 \text{ ft} \times 93.338 \text{ ft} \times \text{thickness}$, was utilized. For such large grid blocks the block temperature corresponds to the average temperature instead of the combustion front temperature. This resulted in failure of the block to ignite and caused unrealistically high heat losses in our early simulations. To get around this difficulty, the heat loss parameters were lowered sufficiently to enable average temperature to reach combustion temperature at the combustion front.

4.3.2 Sensitivity Studies and Results

Many parameters can influence the predicted performance. Gaining this information will help in the project design and economic evaluation. Our study focused on the operational parameters as well as the reservoir and fluid parameters such as, injection rate, air enrichment, cracking reaction kinetics, wet versus dry combustion, phase equilibrium constant, and well spacing.

The effect of injection rate on the recovery was investigated for three different rates, 10 MMSCFPD (11.48 Scf/Dft²), 7 MMSCFPD (8.03 Scf/Dft²) and 5 MMSCFPD (5.74 Scf/Dft²). Air was injected simultaneously into all 14 layers. The injection pressure was kept just above the reservoir pressure (1981 psi). Ignition time varies with the injection rate. In this study, external heat was provided for the first two years, long enough to ensure that ignition had been established. All simulation runs were limited to 10 years to avoid excessive run time.

The temperature distribution of plane Y=1 and Z=3 was captured in Figure 2. It shows the location of the combustion front at various times and injection rates. A higher injection rate results in a higher combustion front temperature due to greater oxygen availability. This greater availability of oxygen accelerated the burning rate of fuel. Since the combustion front cannot advance until all the fuel is consumed, accelerated consumption of fuel translated into higher predicted peak temperature and rapid advancement of combustion front through the reservoir.



←
5 MMSCFPD
Fig. is missing

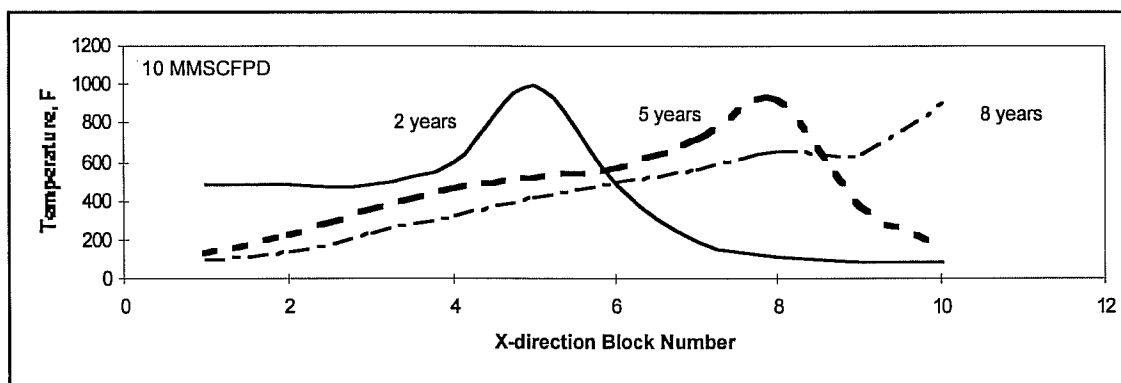


Figure 2. - Position of combustion front for various injection rates

In the eighth year the position of the combustion front for 5 MMSCFPD is in grid block 7, while for 7 MMSCFPD is in block 9, and for 10 MMSCFPD is in block 10, indicating breakthrough. Note higher temperatures during the early time period in block 1 are caused by the external heat added into the block. Sharp temperature decrease in block 1 after two years is due to the heat loss to the cold injection air and the surrounding while external heaters were turned off.

Figure 3 presents the effect of injection rates on cumulative oil production, cumulative oil recovery and air/oil ratio (AOR). Higher injection rate can accelerate the oil production, therefore, correspond to higher oil recovery rates. Oil recovery in this study refers to volumetric oil recovery expressed as a percentage of initial oil in place. As injection rate increases from

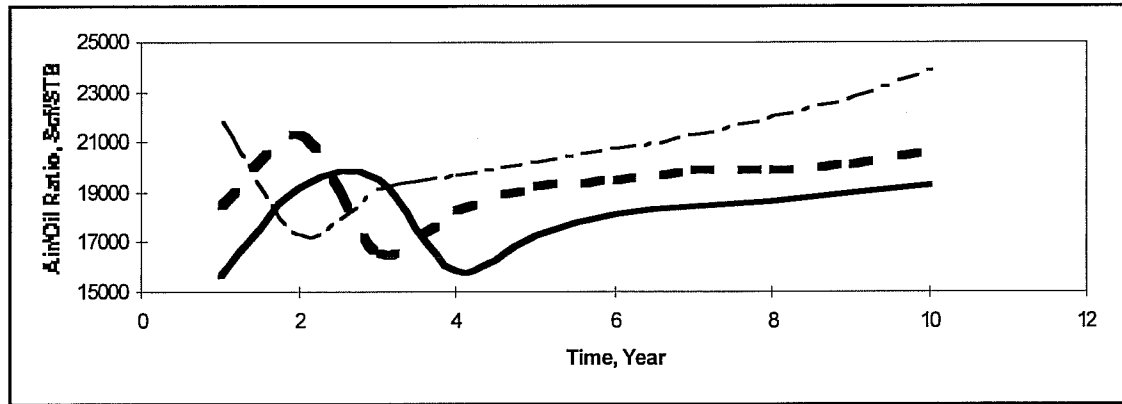


Figure 3. - Effect of injection rates on cumulative oil production, oil recovery and AOR

5 MMSCFPD to 10 MMSCFPD, the cumulative oil recovery increases from 19.6% to 32.9% in 10 years.

The accelerated oil production rate and increased oil recovery at higher injection rate are caused by: (1) the availability of large volumes of combustion gas to displace the oil from the pores, (2) greater distillation and cracking effect due to higher temperature, and (3) enhanced swelling and solvent effect resulting from the generation of large volumes of CO₂ and lighter ends. It is also believed that the higher temperature caused the water near the combustion front to vaporize much more rapidly, accelerated the build up of steam bank ahead of the combustion front and contributed to the increased recovery.

AOR values for all three runs are lower than 24 Mscf/bbl, the upper limit being considered economically. However, 7 MMSCFPD case has much lower AOR compared to that of 10 MMSCFPD case, and slightly higher AOR and 6.4% additional oil recovery than that of 5 MMSCFPD case. No breakthrough occurred in the 10 year period run and this 7 MMSCFPD case appeared to be the best case.

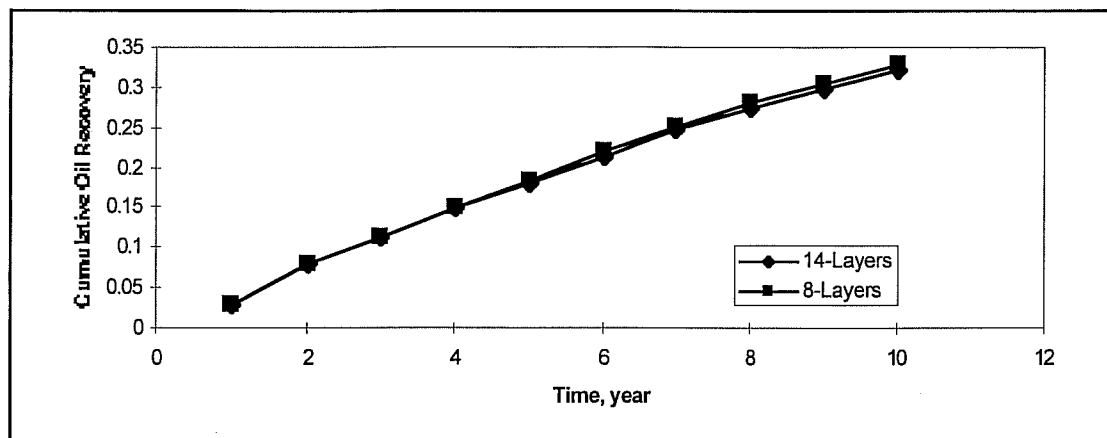


Figure 4. - Comparison of cumulative oil recovery--14-layer vs. 8-layer (10 MMscf/D air inj.)

Since all these runs are very time consuming, one run was performed to study the possibility of reducing computation time without sacrificing the accuracy. Air was injected into eight high permeability layers by shutting in the six low permeability layers (NE and NF layers plus four silt layers). The result shows that computation time can be reduced by almost 40%, while ultimate oil recovery remains essentially the same as the case of injections into all 14 layers, as shown in Figure 4. Extinction radius calculation, which will be discussed later, also shows that these six layers couldn't maintain combustion. All this indicates that the low permeability NE and NF sands and silt layers contribute very little toward the oil production.

Reductions of the oxygen content from the injection gas can result in incomplete burn, promote Low Temperature Oxidation (LTO) reactions, lower the peak temperature and recovery. Thus, enriching the injection air with oxygen was investigated and compared with normal air injection (21%). For comparison on equal amount of oxygen basis, the air injection rates were adjusted to maintain the same total oxygen for both enriched air and normal air. The effect of enriched air was investigated by injecting 30% and 40% (by volume) oxygen content air separately and the results were compared with normal air injection.

Figure 5 shows the comparison among these three cases. Though the peak oil production was accelerated with enriched air injection (i.e. the peak daily production rates occurred 4 and 2 years earlier, respectively, compared to the normal air injection), the final cumulative oil recovery was only marginally higher.

The slightly higher oil overall recovery with enriched air can be attributed to the somewhat higher CO₂ and steam production. The increased steam production is the result of more rapid evaporation of connate and produced water.

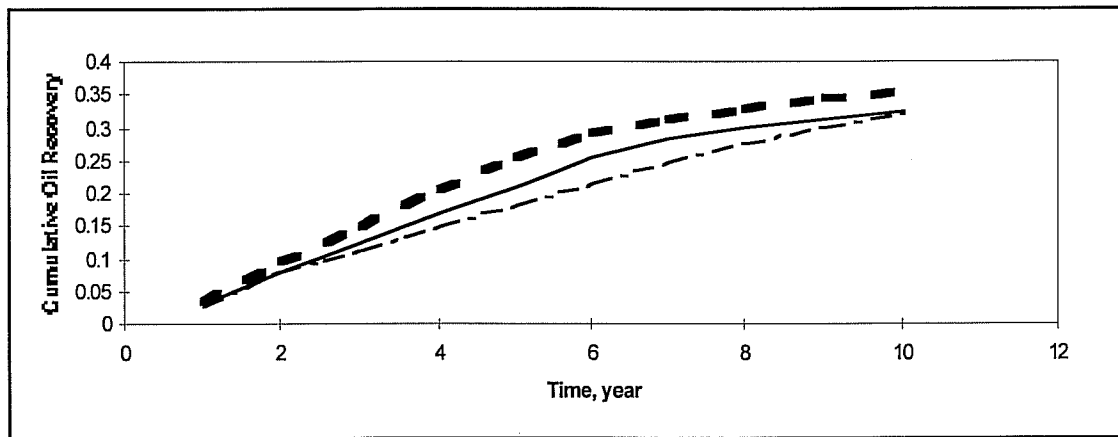
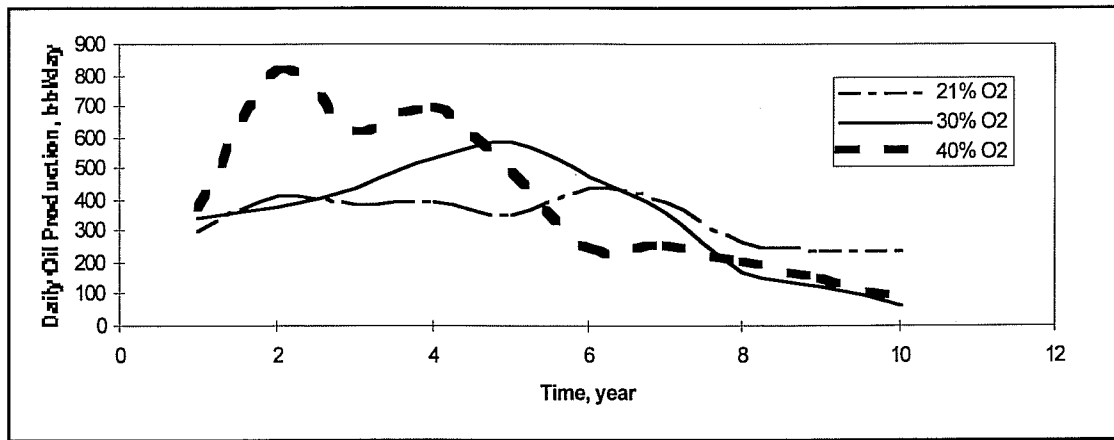


Figure 5. - Effect of enriched oxygen on daily oil production and oil recovery

The kinetic model employed in the simulator is that of Arrhenius:

$$R_A = A \exp (-E/RT) \quad \text{Equation 1}$$

where A is pre-exponential factor, E is activation energy and R is universal gas constant. Increasing A values can accelerate the combustion reaction rates. Conducting this study can give us the insight of the role of the kinetics or reaction rate played in the combustion process. Three runs were made to evaluate the effect of pre-exponential factor on oil recovery. The cases studied were: $A=1.0E05$ (base case), $A=1.0E08$, and $A=1.0E11$. Figure 6 shows that the oil recovery rate in this study is not controlled by the kinetics of the combustion or reaction rate. The pre-exponential factor increased by one thousand times over the base case had resulted in oil recovery 1.16% OIP decrease, while a million times increase in the pre-exponential factor resulted in only 0.93% decrease in oil recovery.

In terms of heat reaching the displacement front, the dry combustion process is less efficient because much of the heat released by the burning oil remains behind the combustion front. To improve this

situation, water is injected simultaneously with the air after initial combustion has been established. Water, with a specific heat of approximately four times that of air, can recover

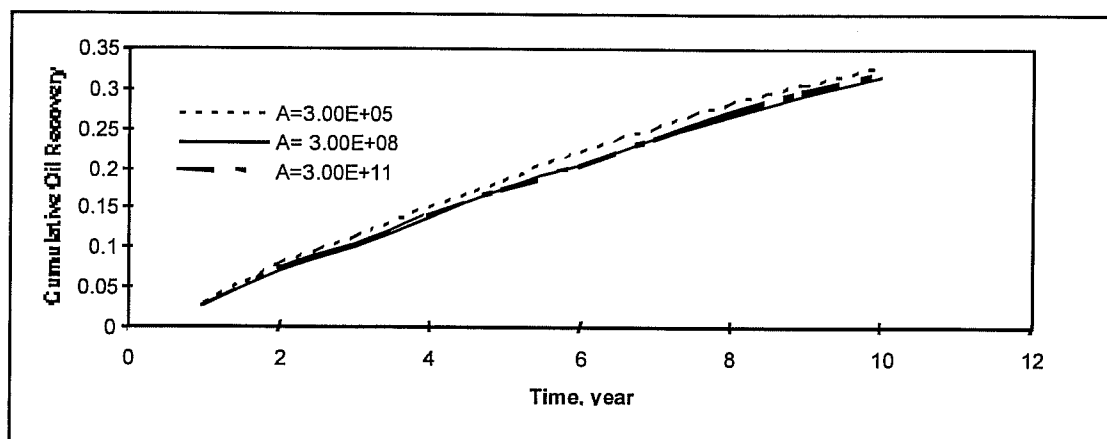


Figure 6. - Effect of kinetics of cracking reaction (10 MMscf/D air injection)

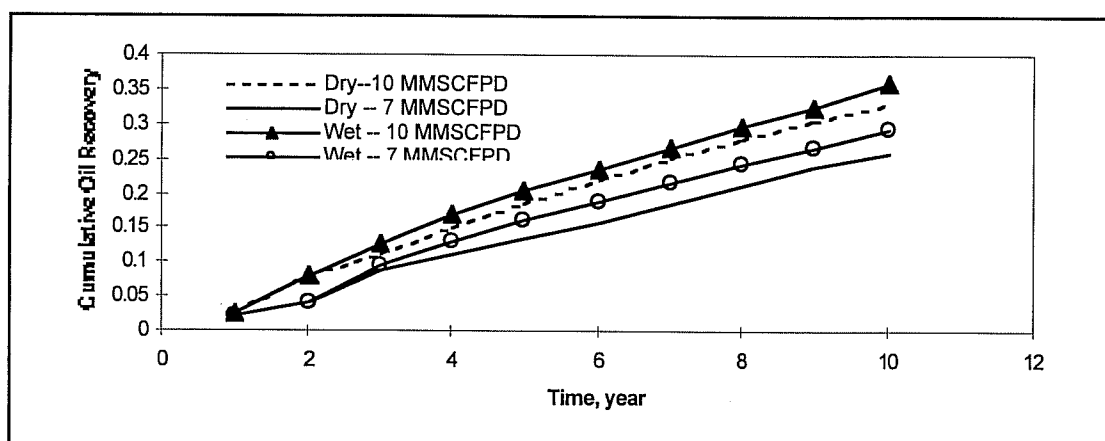


Figure 7. - Oil recovery in wet combustion is superior to the corresponding dry combustion

part of the heat remaining behind the combustion zone and carry that heat downstream beyond the combustion zone either as superheated steam or saturated steam.

To further understand the effect of the injection water, we simulated the following two cases. Same amounts of water, 1000 STB/D, were simultaneously injected with the air at the end of two years dry combustion, the air injection rates for these two cases were 10 MMSCFPD and 7 MMSCFPD, respectively. Simulation results were compared with the corresponding dry combustion runs.

Figure 7 shows that at constant water injection rate, the oil recovery is a function of air injection rate. The recovery in both cases was superior to the corresponding dry combustion cases. The additional

recovery due to wet combustion was around 3.5%. Higher recovery is the result of the more rapid combustion front movement, the increased utilization of energy, and increased volume of fluid injected.

The air requirement is lower in wet combustion process because of the lower amount of coke deposited and lower amount of fuel consumed, which resulted in the lower AOR, as presented in Figure 8.

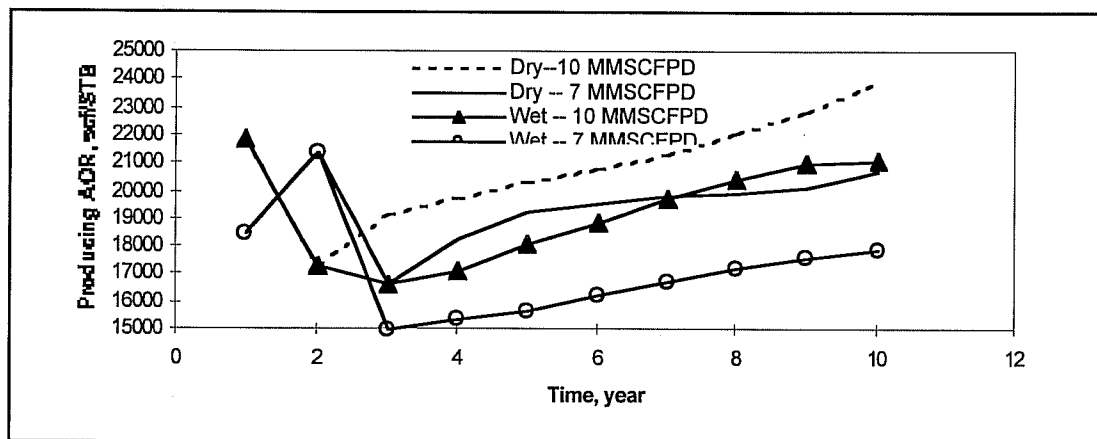


Figure 8. - Comparison of producing AOR for wet and dry combustion

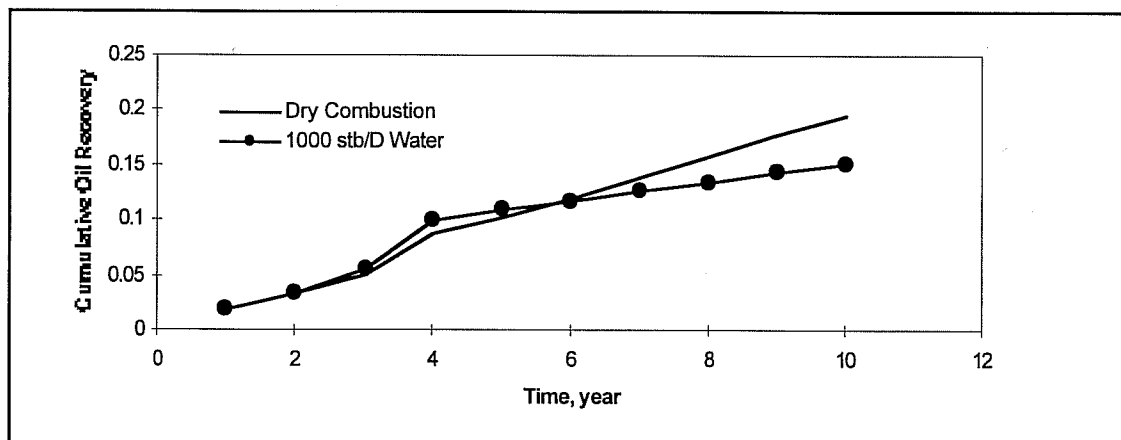


Figure 9. - Effect of the amount of water injected on oil recovery (5 MMscf/D air injection)

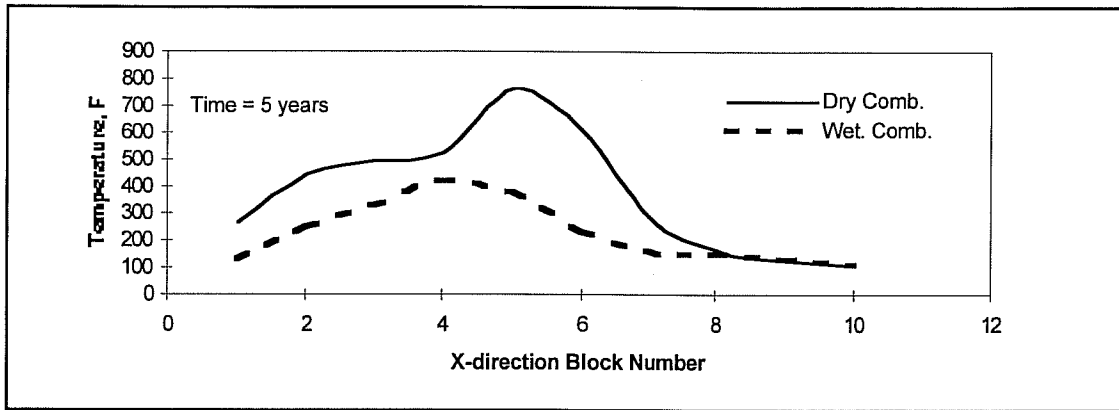


Figure 10. - Effect of wet combustion on temperature distribution (5 MMscf/D air injection)

The contradictory behavior occurred when we lowered the air injection rate to 5 MMSCFPD. The ultimate oil recovery dropped to 15.2% OIP, 4.4% lower than that of the corresponding dry combustion, as presented in Figure 9. Figure 10 captures the profile of the temperature distribution at the fifth year. It clearly shows that the combustion front moved much more slowly and temperature was much lower than that of dry combustion. Apparently this high water injection partially quenched the combustion, which resulted in the lower oil recovery rate. Figure 11 is the snapshot of the saturation profile at the same time. Note that oil saturation was zero in the burned zone. This distribution also indicated that less oil was produced in this high water injection case. Thus, there appears to be a minimum air injection rate for a given water injection rate, below which, the recovery is likely to decline.

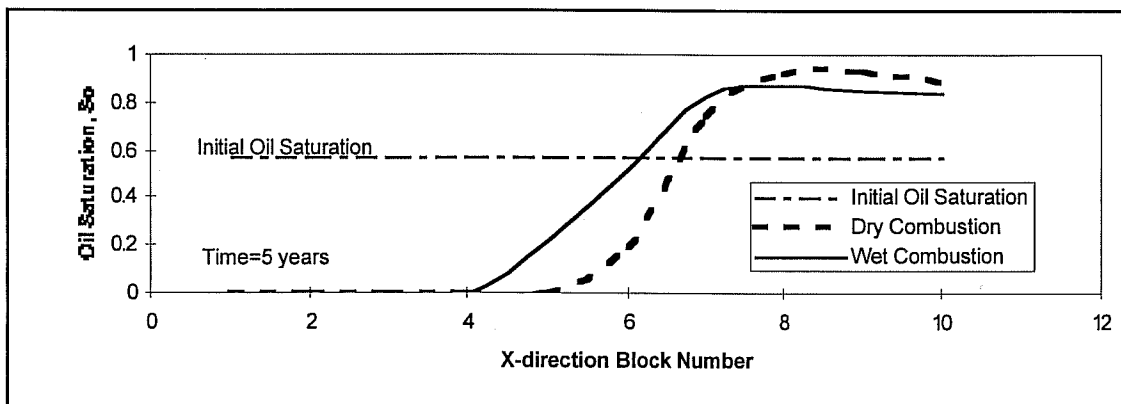


Figure 11. - Effect of wet combustion on oil saturation (5 MMscf/D air injection)

Providing accurate phase equilibrium constants, K , is always troublesome. An initial attempt was made to calculate K -values by using CMG WINPROP. Unfortunately, the K -values converged to the trivial solution. To examine the effect of this K -value, studies were conducted by introducing two sets of K -values: one was adopted from STARS used as base K values, the other was generated from Schrader

Bluff crude composition and an equation of state (EOS). Table 14 shows the two sets of K-values for pressure 1915 psi and 2015 psi, and temperature from 77 °F to 927 °F with 50 degrees intervals.

Table 14. - Two sets of K values

Base K Values				The EOS generated K values			
Heavy Oil		Light Oil		Heavy Oil		Light Oil	
2.51e-9	2.39e-9	1.54e-4	1.46e-4	9.78e-20	8.89e-20	0.009103	0.008268
2.23e-8	2.12e-8	4.80e-4	4.56e-4	2.35e-16	2.14e-16	0.019943	0.018115
1.54e-7	1.46e-7	0.00128	0.00122	6.83e-14	6.21e-14	0.038548	0.035013
8.5e-7	8.08e-7	0.00304	0.00289	5.12e-12	4.65e-12	0.067585	0.061388
3.91e-6	3.72e-6	0.00648	0.00616	1.53e-10	1.39e-10	0.109676	0.099618
2.63e-5	2.50e-5	0.01260	0.012	2.37e-9	2.15e-9	0.167211	0.151878
8.42e-5	8.00e-5	0.01790	0.017	2.26e-8	2.06e-8	0.242239	0.220025
2.42e-4	2.30e-4	0.02310	0.022	1.50e-7	1.37e-7	0.336388	0.305541
4.10e-4	3.90e-4	0.02950	0.028	7.52e-7	6.83e-7	0.450855	0.409511
5.89e-4	5.60e-4	0.03470	0.033	3.01e-6	2.73e-6	0.586406	0.532632
8.84e-4	8.40e-4	0.04000	0.038	1.00e-5	9.12e-6	0.743414	0.675242
0.00166	0.00158	0.04520	0.043	2.89e-5	2.63e-5	0.921906	0.837366
0.00284	0.0027	0.05050	0.048	7.38e-5	6.70e-5	1.121608	1.018756
0.00389	0.0037	0.05680	0.054	0.00017	0.000154	1.342004	1.218941
0.00558	0.0053	0.06310	0.060	0.000359	0.000326	1.582379	1.437273
0.00768	0.0073	0.06940	0.066	0.000705	0.000641	1.841869	1.672968
0.01050	0.0100	0.07680	0.073	0.001301	0.001181	2.119497	1.925137
0.01790	0.0170	0.08840	0.084	0.00227	0.002062	2.414210	2.192825

The EOS generated K values were much higher for the light oil and lower for the heavy oil than the base K values. In other words, the EOS made the oil lighter. This presumes that most light oil will evaporate before it burns. Thus, the amount of residual oil available for burning and cracking was lowered, the rate of advancement of combustion front will be increased and oil recovery will be higher.

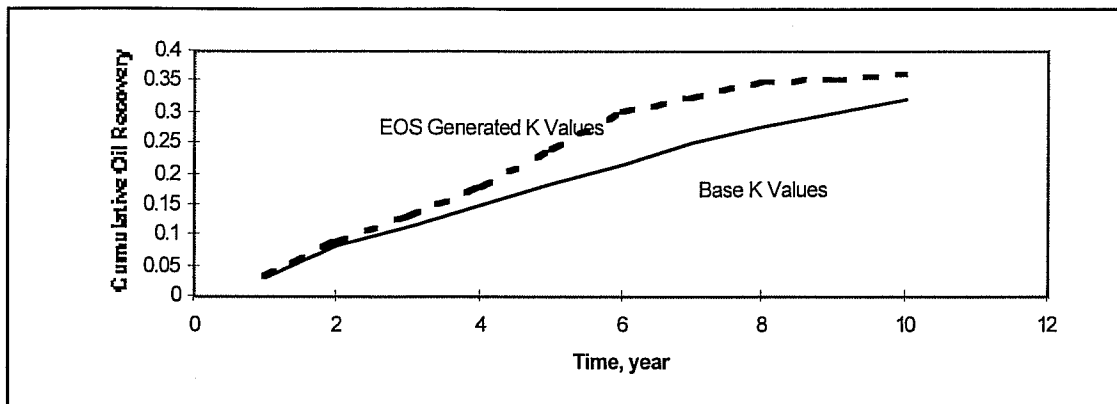


Figure 12. - Effect of phase equilibrium K-values on oil recovery (10 MMscf/D air injection)

Figure 12 illustrates oil recoveries by incorporating these two sets of K-values. The EOS generated K values resulted in additional 4% oil recovery over the base K values, which clearly underscored the importance of estimating this parameter correctly.

To study the effect of well spacing,
 In this study, the air injection rates were kept the same at 10 MMSCFPD while the well spacings were arbitrarily changed to 40 and 160 acres, respectively. Smaller well spacing resulted in higher flux which translated to higher oil recovery. Figure 13 gives the comparisons of oil recovery among three different well spacings. As expected, the 40 acres well spacing has the highest oil recovery.

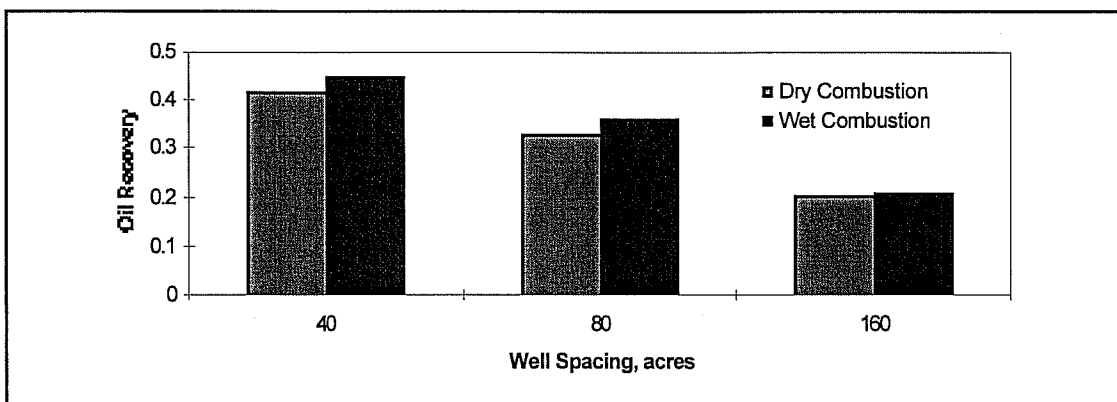


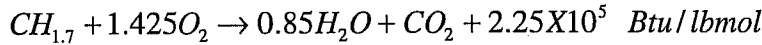
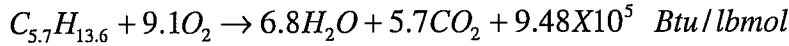
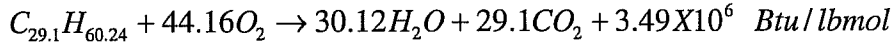
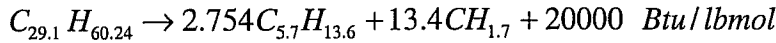
Figure 13. - Well spacing sensitivity study (10 MMscf/D air injection)

4.4 Extinction Radius Calculations

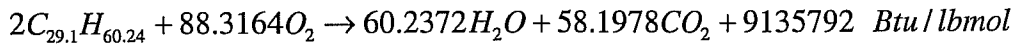
The extinction radius is defined as the radial distance (from the injection well) beyond which it is no longer possible to support combustion. For a combustion process to succeed, the extinction radius at any given injection rate must exceed the spacing between the injector and producer. The extinction radius is a function of air injection rate and rock-fluid properties.

A spread sheet program was developed. Details are discussed below.

Four chemical reactions, cracking of heavy oil and oxidation of heavy oil, light oil, and coke, can be written as,



Multiplying the last equation by 13.4 and adding to the summation of the first three equations, one can get



Knowing the amount of oxygen consumption or heavy oil cracking enable the calculation of the total reaction heat, Q. This reaction heat is equal to the heat loss to the surrounding rock and heat absorbed by the mixture, which includes unoxidized oxygen, nitrogen, CO₂, H₂O (connate and produced), and oil (heavy and light oils). The energy balance equation is expressed as,

$$Q = \sum (nC_p)_i (T - T_0) + (T - T_0)t / (h / KA) \quad \text{Equation 2}$$

where T₀ is initial reservoir temperature, t is the time, A is the area, and K is the rock conductivity. Reaction heat Q and mixture moles, n_i, are functions of time; C_p is specific heat (Btu/lb) and h is pay thickness (ft).

Since average radial velocity, U, is equal to

$$U = r/t = Q_1 / (2\pi rh) = Q_0 (P_0 / P_1) (T_1 / T_0) / (2\pi rh) \quad \text{Equation 3}$$

Where Q₀ P₀, P₁, T₁, T₀ and h is the injection rate, initial injection pressure, reservoir pressure, reservoir temperature, initial injection temperature and pay zone thickness, respectively. Rewriting this equation and expressing time t as a function of radius gives,

$$t = (2\pi r^2 h) / [Q_0 (P_0 / P_1) (T_1 / T_0)] \quad \text{Equation 4}$$

Substituting this equation into the energy balance equation and using a trial-and-error method, the extinction radius is calculated with assumed minimum supporting combustion temperature.

Assuming the injection rate for each layer is proportional to its permeability. Figure 14 shows the extinction radius in each layer as a function of injection rates. In each layer, a higher injection rate results

in a higher extinction radius. In six low permeability layers, the combustion couldn't be maintained and therefore these layers contribute very little toward the oil production.

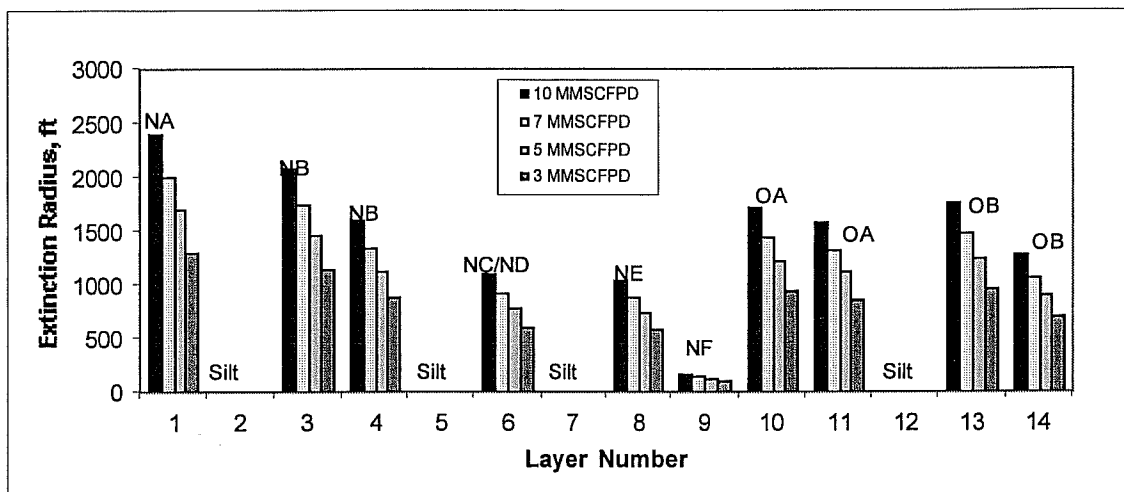


Figure 14. - Extinction radius at various injection rates

In this study, the injector was set in the center of four 20-acre squares surrounded by eight producers. Hence, the extinction radius should be greater than 934 feet. Figure 14 indicates that a minimum air injection rate of 5 MMSCFPD must be maintained to implement the successful combustion.

4.5 Summary

This CRADA project was conducted to identify the most promising recovery processes for Schrader Bluff Milne Point, Alaska. In-situ combustion was evaluated more extensively and results discussed in more detail in this section. The following summarizes the results of this evaluation.

A laboratory study of in-situ combustion determined that Schrader Bluff crude oil has favorable burn characteristics. A stable front can be maintained and recovery efficiencies are good. Wet combustion, a process combining in-situ combustion with water injection, appears to perform better than dry combustion. A first estimate of air requirements, burn rates, etc., were determined.

Results of a simulation study of in-situ combustion were consistent with observed behavior in the laboratory.

The simulation study suggests that in-situ combustion cannot be maintained in the low permeability sands (NE, NF, silt layers).

Extinction radius calculations indicated that to implement a successful 80 acre spacing in-situ combustion project, a minimum of 5 MMscf/day air injection rate is required.

No pronounced advantage in using high oxygen content air is predicted for the Schrader Bluff reservoir. Enriched air will accelerate peak oil production but has minimal effect on the overall oil recovery.

The pre-exponential factor of the combustion kinetics has only marginal effect on predicted oil recovery. However, the phase equilibrium K values have significant impact on the predicted ultimate oil recovery.

Wet combustion causes higher oil recovery and requires lower AOR than that of dry combustion. AOR values for both dry and wet combustion are within the acceptable range. However, high water injection and/or low air injection rate may partially quench the combustion and reduce the recovery.

5. Recovery by Gas Injection

5.1 Background

5.1.1 *Miscible vs. Immiscible Recovery at Schrader Bluff*

[continue]

5.1.2 *EOR and CO₂ Sequestration*

[continue]

5.1.3 *Phase Behavior at Schrader Bluff (3-Hydrocarbon Phases)*

The shallow late Cretaceous Schrader Bluff region of the Milne Point field, north slope Alaska contains in excess of 2 billion barrels of original oil in place (OOIP) with API gravities typically falling between 18-21.5° and viscosity from 30 to 70 cp. Commercial production from Schrader Bluff began in 1991. A waterflood was initiated in 1992 and average production rates were about 350 BOPD per well, which is low by North Slope standards and render the resource uneconomic.

To save this resource from premature abandonment, initial model screening was performed and gas injection (CO₂, lean gas and NGL) appears promising. Multiple-contact miscible or near miscible gas flooding was found to have the potential to achieve a significant amount of incremental oil over conventional waterflooding. Moreover, injecting CO₂ could reduce greenhouse gas emissions, and thus, benefit the environment.

The efficiency of a displacement of oil by CO₂ depends on a variety of factors, including phase behavior of CO₂/crude-oil mixtures generated during the displacement, densities and viscosities of the phases present, relative permeabilities to individual phases, and a host of additional complications such as dispersion, viscous fingering, etc. In a viscous reservoir like Schrader Bluff, the dominant phase behavior mechanisms affecting reservoir performance are viscosity reduction and oil phase swelling.

Field research and laboratory tests for oil in Schrader Bluff and analogous fields like Kuparuk and West Sak formation have been carried out. The occurrence of liquid/liquid and liquid/liquid/vapor phase behavior in CO₂/oil was observed. Displacements of oil by CO₂ were found to be able to develop miscibility or near miscibility by extraction of hydrocarbon components into a CO₂-rich phase when liquid/liquid phase behavior occurred even though CO₂ was immiscible at reservoir conditions.

Interpretations of the effects of phase behavior on displacement efficiency are often contradicted by the complexity of the behavior of CO₂/crude-oil mixture. Rathmell *et al.*, Hutchinson and Braun believed that CO₂ flooding behaved much like a vaporizing gas drive. Vapor phase CO₂ mixes with oil in place and extracts light and intermediate hydrocarbons. After multiple contacts, the CO₂-rich phase vaporizes enough hydrocarbons to develop a composition that can displace oil efficiently. The data reported by them are based on the reservoirs where reservoir temperature is above 120°F and only liquid-vapor equilibrium is shown. For Schrader Bluff field, reservoir temperature is below 120°F and mixtures of CO₂ and oil exhibit multiple liquid phases. Metcalfe and Yarbrough argued the process should be condensing gas drive. Kamath *et al.* found that an increase in the solubility of liquid phase CO₂ in crude oil at

temperature near the critical temperature of CO₂ (88°F) caused more efficient displacements of oil by CO₂. Huang and Tracht found that swelling and stripping of hydrocarbons from the oil by a CO₂-rich liquid phase were the dominant mechanisms for low temperature liquid/liquid region. Gas condensing into a liquid phase that then develops miscibility was confirmed by Chang *et al.* in a micromodel study. Zick believed that a combination of condensing/vaporizing gas drive mechanism was responsible for the high displacement. Reservoir temperature and displacement pressure determine which mechanism will control the displacement. He argued that above the minimum miscibility pressure (MMP), the condensing/vaporizing mechanism could generate displacement that was effectively miscible, although true miscibility might not actually be developed. When the pressure slightly below the MMP, so called near miscible condition, the loss in oil recovery is not great and might be offset economically by the reduction in mass of CO₂ required and better CO₂ sweep efficiency.

Since reservoir temperature is usually considered constant for a typical gas injection project, pressure becomes the key factor to affect the CO₂/crude oil phase behavior. Further investigation was conducted by Shyeh-Yung. He concluded that four mechanisms would affect CO₂ mixture phase behavior: (1) the ability of CO₂ to extract components from crude oil decreases as pressure decreases. Less oil will be recovered by extraction and miscibility may not develop dynamically, (2) interfacial tension between the CO₂-rich phase and crude oil increases as the pressure decreases, making displacement of crude oil less efficient, (3) at lower pressure, less CO₂ will dissolve in oil to increase oil volume, and oil recovery due to swelling will be reduced, and (4) lower CO₂ solubility also results in less oil viscosity reduction as pressure lowers.

5.1.4 Evaluation of Gas Injection

Fully compositional simulations of CO₂/NGL injection processes previously performed with commercial simulators VIP and GEM were often unstable being unable to obtain converged solutions. The results of the current investigation show that the problem in part was caused by the presence of three hydrocarbon phases. The reservoir temperatures and pressures typical of Schrader Bluff are in the phase region of CO₂ where a second liquid phase and a gas phase simultaneously form. PVT swelling tests have verified the conditions at which three hydrocarbon phases are simultaneously present. At 80 mole% CO₂-NGL and 4340 psi, the phase behavior resulted in a multiple phase system forming an asphaltic phase that settled to the bottom of the sample column. An oil-rich second phase and a gas-rich third phase formed quickly above the first phase. The third phase becomes lighter in color and more transparent as pressure was decreased until at 1200 psia and below, an effervescent CO₂ gas phase formed.

Commercial compositional simulators like VIP and GEM do not include methodology to incorporate these phase conditions and require that the EOS be simplified. The degree of error introduced by this simplification is felt to be potentially significant.

In order to understand and characterize the error resulting from the simplification, UTCOMP is chosen in this study. To our knowledge UTCOMP, an isothermal three-dimensional compositional simulator developed by the University of Texas at Austin, is the only existing simulator that can predict fluid flow performance with three hydrocarbon phases.

Initial objective was to use the same data sets employed in GEM and VIP, run them with UTCOMP, and compare results with three different simulators. Unfortunately, UTCOMP was not operational with those data sets because of the problem issues involved in the UTCOMP simulator. Discussion was conducted with BP engineers and a 1D common data set was established. BP engineers agreed to perform VIP runs (both 1D and 2D) under the same condition and model configurations based on the common data set and provide the results for the comparisons. Sadly, until now, results of VIP runs are still unavailable.

A description of UTCOMP and a number of simulation runs (both 1D and 2D) are reported first in this section. Estimated oil recoveries are given as a function of injection gas compositions. One 2D water flooding case was compared with that of GEM run. Please note the result should be considered qualitative rather than quantitative because the conditions for two runs are not exactly the same. In the next section, history match laboratory slim tube test results will be shown to verify the capability and reliability of UTCOMP and followed by extensive 1D sensitive studies conducted based on the successful matching slim tube test data set.

5.2 Recovery Estimates (simulation screening)

5.2.1 UTCOMP

A detailed description of UTCOMP can be found in Chang's Ph.D. dissertation. Briefly, UTCOMP can simultaneously simulate a maximum of four phases, an aqueous phase and three hydrocarbon phases (oil phase, gas phase and second non-aqueous liquid). Water is allowed only in the aqueous phase and all components except water exist in hydrocarbon phases. The solution of UTCOMP is analogous to IMPES (the gridblock pressures are solved implicitly while the component moles rather than phase saturations are obtained explicitly). A finite-difference method that is third-order correct in space is employed by UTCOMP to reduce numerical dispersion and grid orientation effects when solving the material balance equations. The stability of this third-order method has been dramatically improved by adding a flux limiter that makes its total variation diminishing. Phase behavior is calculated using either the Peng-Robinson equation of state or a modified version of the Redlich-Kwong equation of state. A rigorous Gibbs stability test is done before all flash calculations to determine the number of coexisting phases present, and a phase identification test is done after all flash calculations to consistently label each phase for subsequent property calculations. Physical phenomena such as dispersion, capillary pressure, interfacial tension and relative permeability are modeled in the simulator.

Unlike GEM or VIP, UTCOMP is not a commercial simulator, and UTCOMP is less user-friendly than VIP or GEM. Besides preparing input data file for UTCOMP, users must change the numerical setting in the source code each time to make a new case run. The user's guide is not updated for the current UTCOMP version. Probably the biggest issue is the volume shift factor. UTCOMP allows users to input a volume shift factor in the input file, but the program itself is not functional with that value. Since volume shift factor affects the fluid properties like density, modification, tune fluid parameters so that volume shift factor becomes zero, has to be done to minimize the impact of this factor.

5.2.2 1D Simulation (UTCOMP)

Problem issues were discussed with BP engineers. A 1D common data set was established. The pertinent data for this common data set are given as follows: a grid system of 1 x 50 x 1 was used to

represent the field. Each grid block has an identical length of 12.5 ft. The width and height for this field are 50 ft and 58.1 ft, respectively. One production well and one injection well are located in opposite corners. Schrader Bluff oil was assumed in the field and was lumped and treated as a twelve-component hydrocarbon mixture. Table 15 shows the compositions of Schrader Bluff oil. Table 16 shows the defined compositions of the oil and solvents (CO₂, NGL, and lean gas) after the lumping. The phase behavior was determined using the Peng-Robinson equation-of-state (EOS). Fluid description parameters are given in Table 17. Note the parameters have been tuned so that volume shift factor becomes zero. The capillary pressure was assumed to be negligible, and the impact of interfacial tension on phase-relative permeability curve was neglected. The Stone II model was used to generate the four-phase relative permeability values. Initial temperature was constant at 86°C. Initial oil, water and gas saturation were set at 0.75, 0.25 and 0, respectively. Residual saturation for water, oil and gas were assumed as 0.25, 0.3 and 0.05, respectively.

Table 15. - Composition of Schrader Bluff oil

Component	Oil, mole%	Component	Oil, mole%	Component	Oil, mole%
Nitrogen	0.054	Nonanes	2.457	Tricosanes	1.692
Carbon Dioxide	0.221	Decanes	2.494	Tetracosanes	1.244
Methane	30.27	Undecanes	2.576	Pentacosanes	1.185
Ethane	0.275	Dodecanes	3.013	Hexacosanes	1.21
Propane	0.214	Tridecanes	3.393	Heptacosanes	0.931
Iso-Butane	0.148	Tetradecanes	3.428	Octacosanes	1.054
n-Butane	0.388	Pentadecanes	3.034	Nonacosanes	1.104
Iso-Pentane	0.352	Hexadecanes	2.839	triacontanes	0.821
n-Pentane	0.374	Heptadecanes	2.677	C31	0.905
Hexanes	0.9	Octadecanes	2.739	C32	0.725
Benzene	0.028	Nonadecanes	2.134	C33	0.652
Heptanes	1.537	Eicosanes	2.357	C34	0.625
Toluene	0.186	Henicosanes	1.768	C35	0.595
Octanes	2.118	Docosanes	1.663	C36	13.621

Table 16. - Defined compositions of twelve-component oil and solvent (mole%)

Component	Oil, mole%	NGL, mole%	Lean Gas, mole%	CO ₂ , mole%
CO ₂	0.221	0	0	100
C1	30.324	0	97.14	0
C2	0.275	0	0.52	0
C3	0.214	2.315	0.22	0
NC4	0.536	41.993	1.11	0
NC5	0.726	27.771	0.52	0
C6	0.928	14.845	0.24	0
C7-C9	6.298	13.077	0.24	0

C10-C13	11.476	0	0	0
C14-C19	16.851	0	0	0
C20-C35	18.531	0	0	0
C36+	13.621	0	0	0

Table 17. - Fluid component description parameters

Component	Pc, psi	Tc, °R	Vc, ft ³ /lb-mole	MW, lbm/lb-mole	OM	Parach, dynes- cm ^{1.25} /gm-mole
CO ₂	1071.6	547.57	0.116	44.01	0.225	126.4912
C1	667.8	343.04	1.66	16.04	0.013	39.8432
C2	707.8	549.76	2.486	30.07	0.0986	83.7369
C3	616.3	665.68	3.387	44.10	0.1524	126.7644
NC4	550.7	765.32	4.086	58.12	0.201	168.8961
NC5	488.6	845.37	4.944	72.15	0.2539	210.1921
C6	483.77	923	5.294	84	0.2583	244.3968
C7-C9	415.41	1040.3	8.112	109.16	0.3165	314.9718
C10-C13	255.39	1199.6	12.92	153.26	0.4255	431.9548
C14-C19	207.82	1337.4	20.93	356.2	0.577	859.9934
C20-C35	172.63	1515.3	32.27	502.14	0.766	1055.794
C36+	110	1907	67.10	894.34	1.1322	1117.661

Note: OM: Pitzer acentric factor, Parach: Parachor for component

Figure 15 shows the predicted oil recovery of pure CO₂ injection at two different reservoir pressures. In both cases, the CO₂ was injected at a constant rate of 0.05% pore volume (PV) per day and the simulation was terminated after 1.2 PV was reached. Constant bottomhole pressure was maintained for the production well. Oil recovery at high reservoir pressure (1984 psi) is 57%, while for the low pressure (820 psi) case is 49%. Table 18 lists an average saturation comparison between these two cases. Water saturation for the two cases is more or less the same at 0.25. For the high pressure case, the injected CO₂ immediately condensed into second liquid phase. This condensation process lowers the oil viscosity, thus increases the oil recovery. For the low pressure case, condensation process is not fully completed, and thus, four phases coexist. Although gas saturation for the low pressure case is very low, the oil recovery is about 8% lower than that of high pressure case.

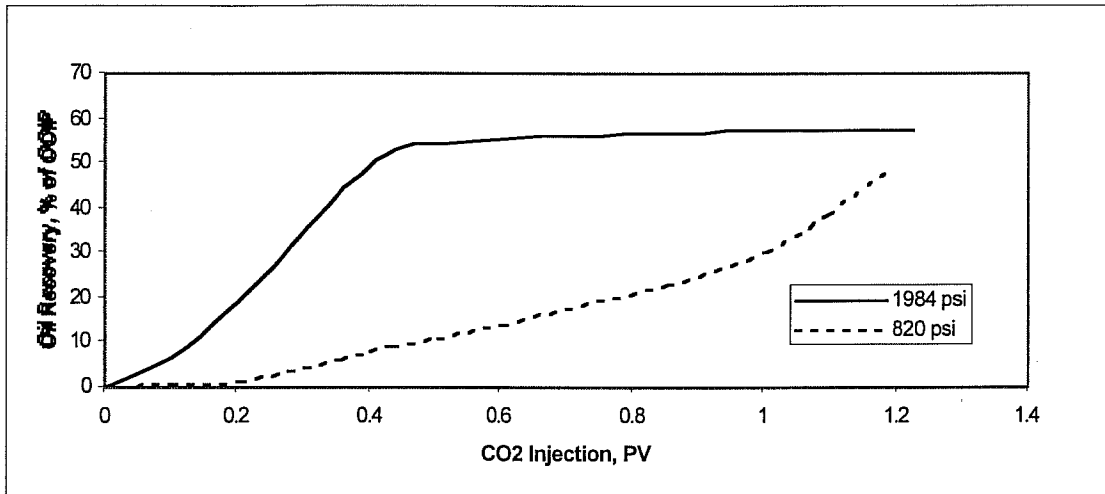


Figure 15. - CO₂ Injection, simulated 1D Flow at various pressures

Please note that the convergence for the low pressure case run was very difficult to achieve because of the coexistence of four phases. Extremely low time step (0.001 day) was used in the simulation. Results show slight oscillation in the average gas and second liquid phase (see Table 18). After carefully examining the simulation result at 1.2 PV, we found that currently in place moles for the component C10-C13 (8510 moles) was greater than that of original in place (7450 moles). Clearly there was problem in the numerical calculation although no single warning message was given by UTCOMP. The result for this case should be considered least reliable.

Table 18. - Average saturation for pure CO₂ injection at high and low pressures

PV	High Pressure (1984 psi)				Low Pressure (820 psi)			
	S _w	S _o	S _g	S _{2nd Liq.}	S _w	S _o	S _g	S _{2nd Liq.}
0.0005	0.25	0.75	0	0	0.25	0.677	0.073	0
0.10	0.25	0.669	0	0.081	0.25	0.676	0.066	0.008
0.20	0.25	0.573	0	0.177	0.25	0.666	0.054	0.030
0.40	0.25	0.352	0	0.398	0.25	0.622	0.072	0.056
0.50	0.25	0.336	0	0.414	0.25	0.600	0.090	0.060
0.61	0.25	0.329	0	0.421	0.25	0.582	0.102	0.066
0.71	0.25	0.326	0	0.424	0.25	0.556	0.114	0.080
0.87	0.25	0.323	0	0.427	0.25	0.535	0.049	0.166
1.02	0.25	0.321	0	0.429	0.25	0.507	0.049	0.194
1.2	0.25	0.319	0	0.431	0.25	0.500	0.019	0.231

Figure 16 shows the oil recovery of 100% NGL injection at two different reservoir pressures. In both cases, NGL was injected at a constant rate of 0.05% PV and the simulation was terminated after 1.2 PV was reached. Since NGL has excellent miscibility, it completely mixes with oil in place and oil recovery for both cases are extremely high. No second liquid phase effect was found in these two cases.

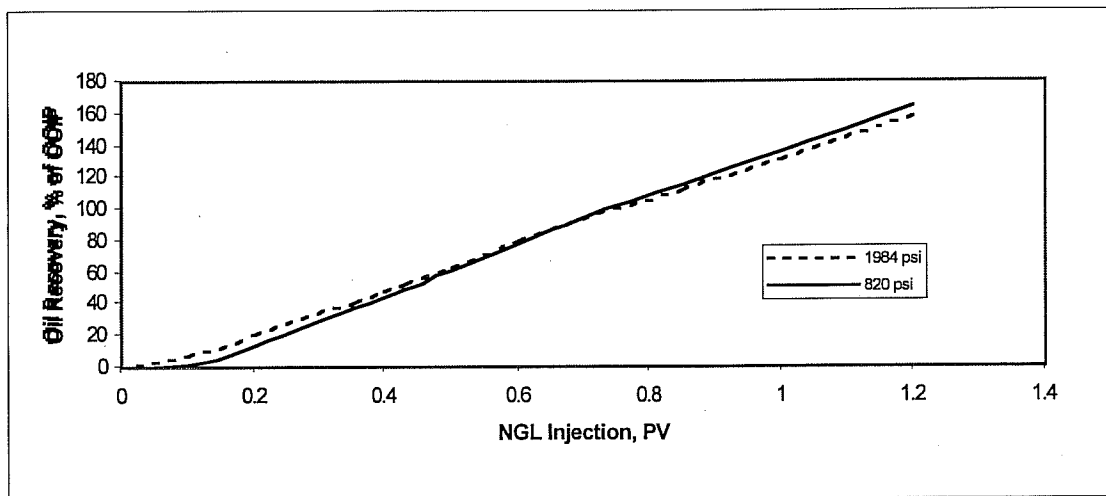


Figure 16. - NGL injection, simulated 1D flow at various pressures

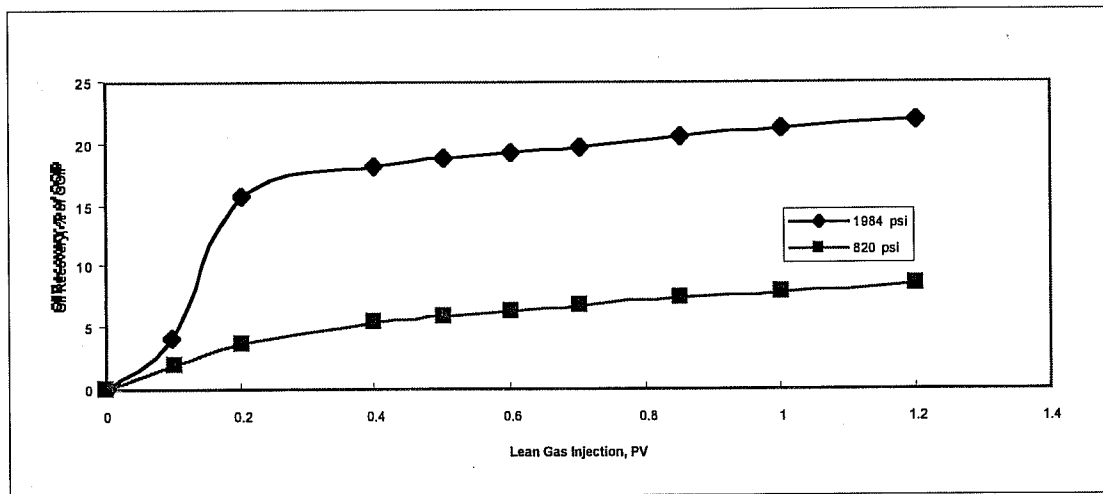


Figure 17. - Lean gas injection, simulated 1D at various pressures

Figure 17 shows the simulation result after NGL was replaced by Schrader Bluff lean gas. The oil recovery is much lower comparing with that of NGL. Unlike NGL, lean gas is mainly made of C_1 (about

96%). It has poor miscibility at the injection condition and thus leads to immiscible process and results in poor oil recovery. Again, there is no second liquid phase effect in either of these two cases.

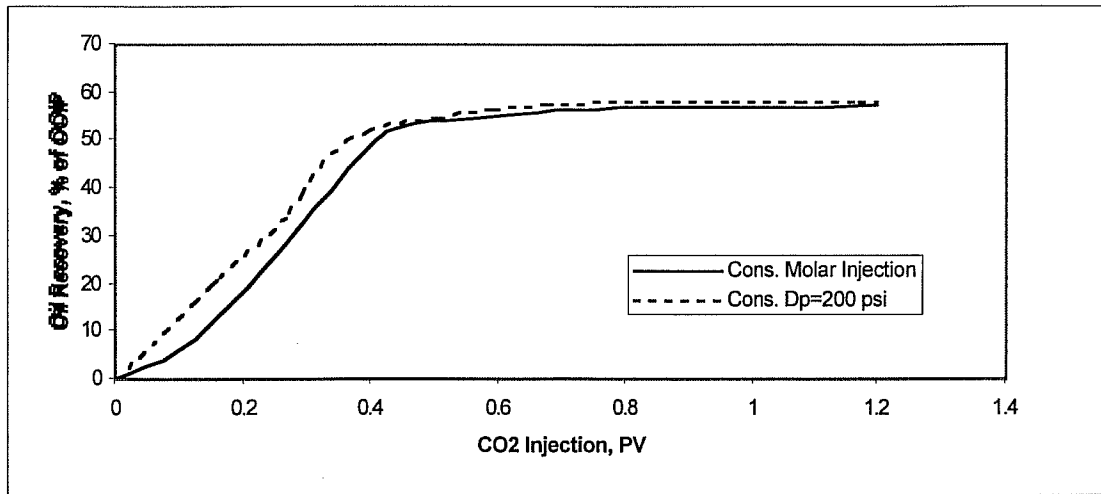


Figure 18. - Comparison of two CO₂ injection methods (reservoir pressure = 1984 psi)

In the constant PV injection case, the differential pressure can be quite large at times, making phase behavior variable and complicated across the 1D grid. The effect of this variation on production was compared to a fixed pressure case (production well at constant pressure, injection well maximum pressure at 200 psi above production well). The result for the CO₂ high pressure case is compared in Figure 18. While the total oil recovery at 1.2 PV injection is nearly identical (less than 1% difference), the time to achieve this recovery is quite different. The constant injection case takes 2400 days to achieve an oil recovery of 58% of OOIP, while the constant pressure case takes 3547 days, about 50% longer. The results are shown in Figure 19.

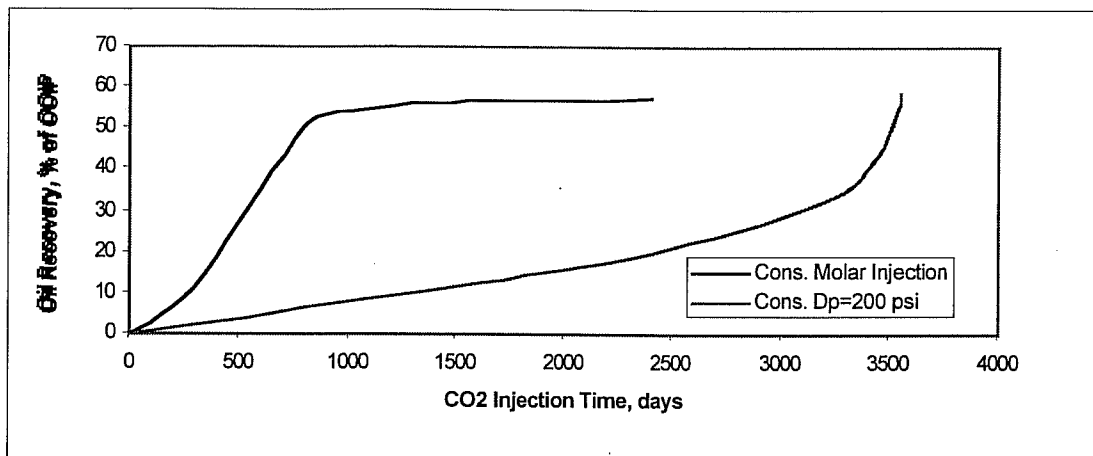


Figure 19. - Injection time comparison between two CO₂ injection methods (P=1984 psi)

A centroid simplex mixture design was constructed to optimize the selection of solvent mixtures (CO₂, NGL, Schrader Bluff lean gas) and plot the function of predicted oil recovery as a function of solvent mixture. Oil recovery was determined at 1.2 PV injected. Injection rate was fixed at 0.05% PV/day. All other parameters were based on the common data set. Two production well pressures were considered, 1984 psi and 820 psi.

Because injected hydrocarbon solvents contributed to the total oil recovery after breakthrough, an estimate of produced solvent was subtracted out from the recovery estimates. The assumption was made that a given injection component was produced when the quantity injected exceeded the original amount in-place. Final oil recovery was estimated by first subtracting out the moles of injected hydrocarbons by component that was produced, and converting the total to volume (bbl) and calculating the overall recovery estimate. By doing so, one expects to obtain a more consistent basis for comparison between the range of solvent mixtures. Using this assumption, recoveries with injection of pure NGL were nearly 100% (99-100%), as one would expect. Original values predicted by UTCOMP for this case was greater than 150% of OOIP, because injected solvent contributed to the oil recovery estimate.

The centroid simplex-lattice design was the basis of the design selection. However, point selection was modified to minimize error in the regions of anticipated greatest change. Design-Expert by Stat-Ease was used to develop the experimental design. Tables T and U give the design point selection for the high pressure and low pressure cases, respectively. Results were modeled using canonical polynomials. The different models were compared and those selected gave the most reasonable fit (full cubic for high pressure case, special cubic for low pressure case).

Table 19. - Mixture model design, high pressure case (1984 psi)

Observation No.	CO ₂ (mole fract)	NGL (mole fract)	Resid Gas (mole fract)	Recovery (% OOIP)
1	1	0	0	57.1

2	0	1	0	99
3	0	0	1	21.3
4	0.5	0.5	0	94.4
5	0.4	0	0.6	30.5
6	0	0.5	0.5	98.4
7	0.685	0.15	0.165	73.1
8	0.15	0.7	0.15	98.6
9	0.33	0.34	0.33	93.5
10	0.25	0.25	0.5	88.2
11	0.55	0.1	0.35	61.8
12	0.5	0.3	0.2	91
Model Coefficient	A	B	C	

$$\text{Recovery} = 57.15*A + 99.1*B + 21.33*C + 65.84*AB - 25.14*AC + 153.33*BC + 378.17*ABC + 44.57*AB(A-B) - 20.74*AC(A-C) - 153.95*BC(B-C)$$

$$R^2 = 0.9994$$

Table 20. - Mixture design, low pressure case (820 psi)

Observation No.	CO ₂ (mole fract)	NGL (mole fract)	Resid Gas (mole fract)	Recovery (% OOIP)
1	1	0	0	29.7
2	0	1	0	99.1
3	0	0	1	7.6
4	0.5	0.5	0	94.8
5	0.4	0	0.6	11.8
6	0	0.5	0.5	71.7
7	0.5	0.3	0.2	78.3
8	0.3	0.6	0.1	97.4
9	0.1	0.6	0.3	98.2
10	0.33333333	0.33333333	0.33333333	57.8
11	0.685	0.15	0.165	47.1
12	0.15	0.7	0.15	99
13	0.25	0.25	0.5	34.3
Model Coefficient	A	B	C	

$$\text{Recovery} = 30.4*A + 101.8*B + 5.5*C + 135.8*AB - 26.8*AC + 85.5*BC - 126*ABC$$

$$R^2 = 0.960$$

The model fit was not very good for the low pressure case. Unlike the high pressure case, the estimated recovery for the pure CO₂ case at low pressure as calculated from the mole composition data (29.7) did not agree with the overall result (49.0) given by UTCOMP. Problems for this simulation run are discussed previously. This is particularly critical because the pure component cases are more influential points in the matrix design. The influence of this error on the overall matrix model is likely to be even greater than that suggested by the lower overall correlation coefficient ($R^2 = 0.960$). An

experimental determination of this point (slim tube run of pure CO₂ at 820 psi) would greatly improve the reliability of the predictions for low pressure situations, and is very strongly recommended.

A contour plot of these models are given in figures 20 and 21. Minimum miscibility pressure (MMP) is defined as the pressure at which the recovery is 90% of OOIP at 1.2 PV gas injection. To achieve a multiple-contact miscible process at high pressure (1984 psi), oil recovery should be greater than 90%. One can inject 1.2 PV of NGL-lean gas mixture solvent, or NGL- CO₂ mixture solvent or a combination of NGL, CO₂ and lean gas as long as their compositions are obtained from the left side of 90% oil recovery line.

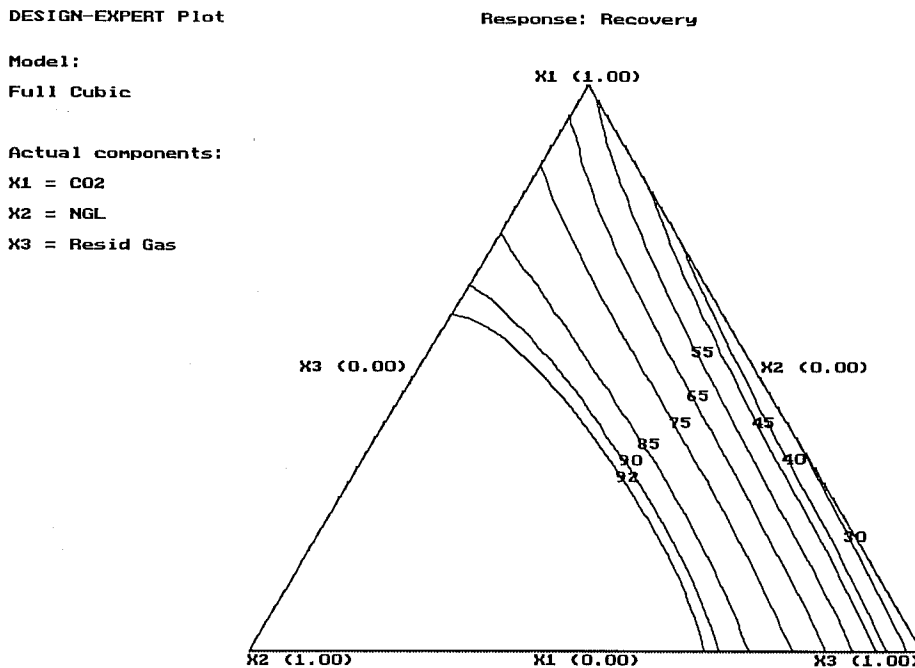


Figure 20. - Contour map of recovery as a function of solvent composition, 1984 psi

The results from VIP runs supposedly provided by BP engineers are still unavailable, comparison between these two simulators is unable to conduct.

Model:

Special Cubic

Actual components:

X1 = CO2

X2 = NGL

X3 = Resid Gas

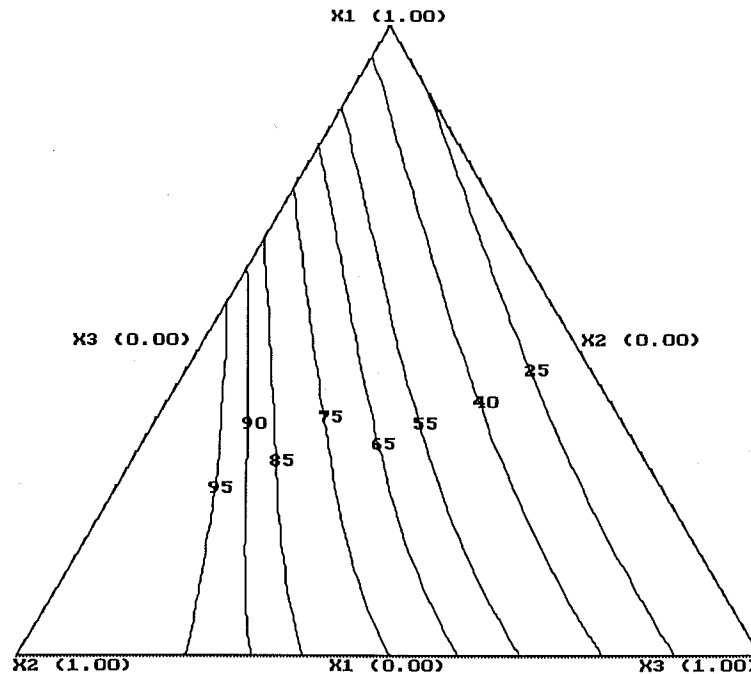


Figure 21. - Contour map of recovery as a function of solvent composition, 820 psi

5.2.3 2D Simulations

The simulation runs were extended to two-dimensional cases. All runs were based on 20-acre, one half of 40-acre spacing. A 20 x 14 grid system was used in this study. The reservoir descriptions were based on a 36 layer model developed by BPX and lumped into 14 layers. Input data for reservoir description, component properties, rock fluid data, and well configuration are the same as those used in the GEM 2D run with two major modifications. First, twelve-component oil used in the common data set was employed instead of ten-component oil to avoid problems caused by the volume shift factor. Second, a new set of relative permeability values developed by BPX was used to replace the one with approximate compositional consistency. Since UTCOMP doesn't have the table input option, the relative permeability values have to be curve fit to one of the models (Bake model, modified Stone II model, Corey model, and modified Corey model). Details of each model can be found in the Appendix B. Table 21 lists the input parameter curve fit for the modified Stone II model.

Table 21. - Relative permeability input parameters from Stone II model

Exponent Values		End Point Values	
e_{row}	3	K_{row}^o	1.06
e_{rog}	2.414	K_{rog}^o	0.132
e_{rw}	3.06	K_{rw}^o	0.39
e_{rg}	3.61	K_{rg}^o	1

The initial objective was to use UTCOMP simulator to evaluate the impact of three hydrocarbon phases. BP engineers shall use VIP to make runs under the same condition and model configurations used in UTCOMP and compare the results with UTCOMP run. Unfortunately, results of VIP runs are still unavailable. To get around this, a simple water flooding run was made and its oil recovery is compared with that of previous GEM run. Since the condition and model configurations were not exactly the same, the focus becomes whether UTCOMP can deliver the similar result. Figure 22 clearly shows the capability and credibility of UTCOMP. UTCOMP predicted almost identical oil recovery pattern though the difference between these two predictions increased during late time period.

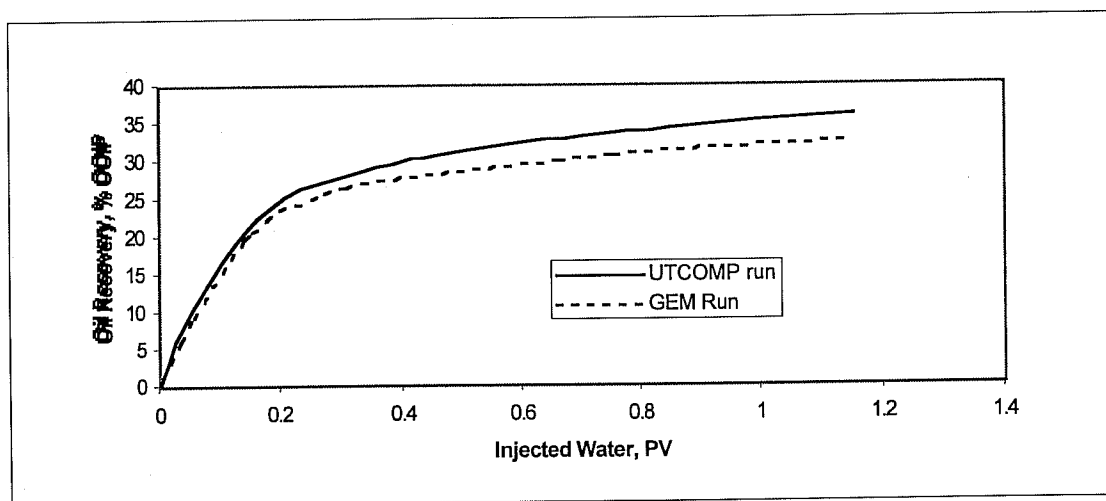


Figure 22. - Oil recovery prediction by UTCOMP and GEM

Another way to study the effect of the CO₂ rich second liquid phase on oil recovery is to take advantage of UTCOMP input option. UTCOMP allows users to choose a maximum number phases allowed in the simulation through input parameter NP. NP equal to 3 means only three phases—water, oil and gas phases are allowed, while NP equal to 4 means additional second liquid phase is also included. Figure 23 shows the comparison between these two cases. Note that all other input data are exactly the same. Clearly the case with CO₂ second liquid phase has outperformed the other case. It predicted about 5% of OOIP higher oil recovery at the 1.2 PV.

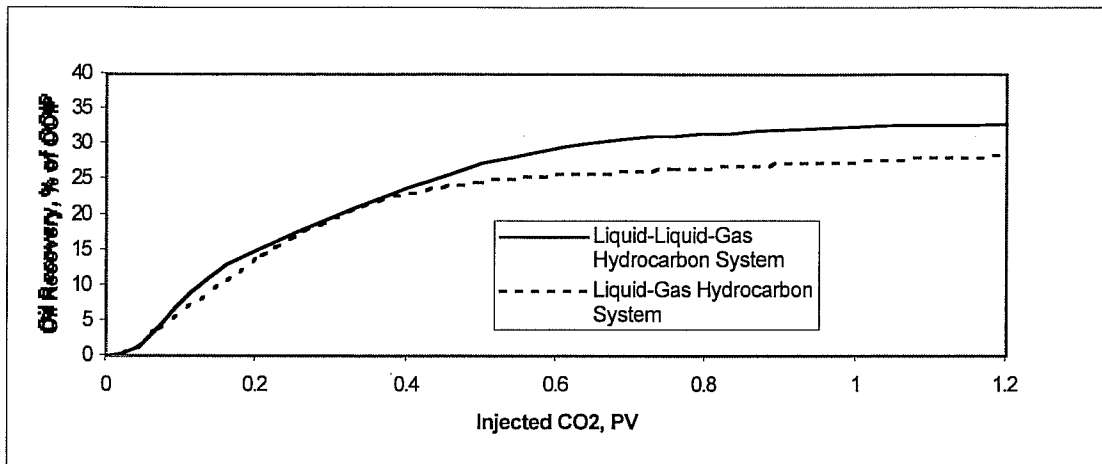


Figure 23. - Effect of CO₂ rich second liquid phase on oil recovery

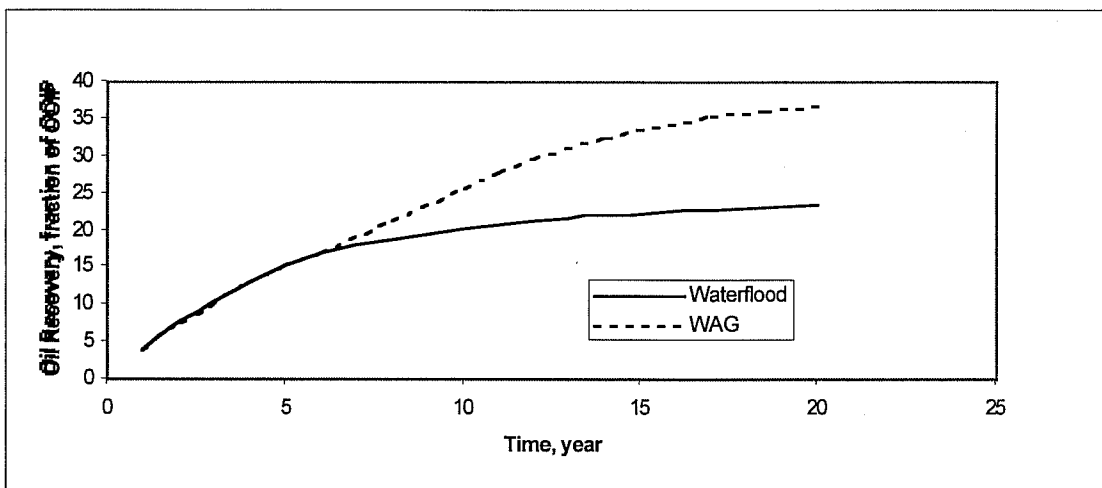


Figure 24. - Oil recovery for 1:1 WAG process

Figure 24 shows oil recovery for 1:1 WAG process. The injection rate is maintained the same at 1.1% PV/year. The yield was 36.6% of OOIP after 20 years. This is an increase in the oil production of 13.3% of OOIP compared to the water injection scenario. However, the extra oil does not appear until the 6th year.

To further demonstrate the credibility of UTCOMP, history match slim tube test result is shown in the next section. Extensive 1D sensitive studies based on the matching slim tube test data set are followed.

5.3 Multi-phase CO₂ Fluid Flow (compositional simulation)

Experiment: Slim Tube Test

A slim tube test utilizing a 77.5 mole% CO₂-22.5 mole% NGL injection solvent was performed on the oil, a recombined sample from Schrader Bluff E-20 separator fluids. The recombination was made to the same GOR as the original oil (138 scf/stb). The slim tube is 60 ft long with an internal diameter of 0.18 in. The slim tube was packed with sandstone giving a permeability and porosity of 25 Darcy and 23.3%, respectively. The temperature was maintained at 92°F. The outlet end of the tube was maintained at an initial pressure of 1950 psi. After charging the slim tube with recombined oil, solvent was injected at a constant rate of 0.247 standard pore volume (PV) per day. The test was terminated when a total of 1.4 PV (five and half days) solvent was injected into the tube.

The gas broke through at 0.85 PVI (pore volume injected). Total oil recoveries were 93.5% at 1 PVI, and 98.9% at 1.2 PVI. Residual oil was recovered from the slim tube using toluene (extracting from the slim tube, distilling the wash and analyzing the separated fluids for toluene). Residual oil was 6% of the original oil in place (OOIP).

5.3.1 Simulation: Slim Tube History Match Study

A history match study was conducted using UTCOMP. The recombined oil composition was lumped and treated as a twelve-component hydrocarbon mixture, same as used in the common data set. The phase behavior was determined using the Peng-Robinson equation-of-state (EOS). A grid of 1x50x1 in the x, y, and z directions was used. Each block has the same length of 1.2 ft. The solvent (77.5 mole% CO₂ -22.5 mole% NGL) was injected at block (1,1,1) at a rate of 0.247 PV/day. The outlet end of the tube at block (1,50,1) was set at the initial pressure of 1950 psi. The capillary pressure was assumed to be negligible, and the impact of interfacial tension on phase-relative permeability curve was neglected. The modified Corey's model was used to generate the four-phase relative permeability values.). All other input parameters are adopted from the common data set.

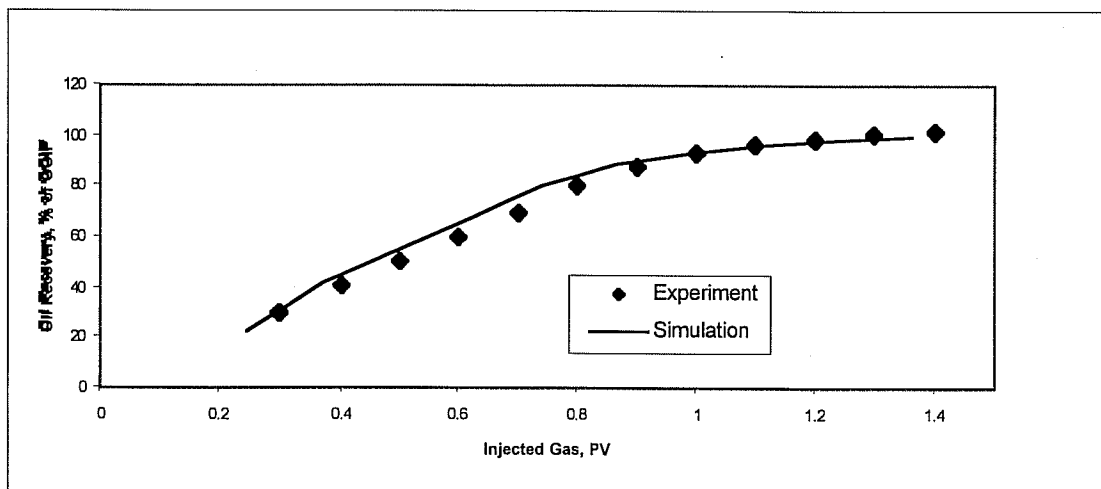


Figure 25. - History match of E-20 slim tube test

Figure 25 shows a comparison between slim tube test data and UTCOMP simulation results. Oil recovery (percentage of OOIP) is plotted as a function of solvent PVI. Simulation results slightly overestimated the oil recovery in the early period and matched the oil recovery after gas breakthrough. The recoveries were 93.5% at 1 PVI, matching the slim tube test data, and 98% at 1.2 PVI, less than 1% lower than the experimental test result. Overall, simulation results agree well with test data, all within $\pm 2\%$ of OOIP.

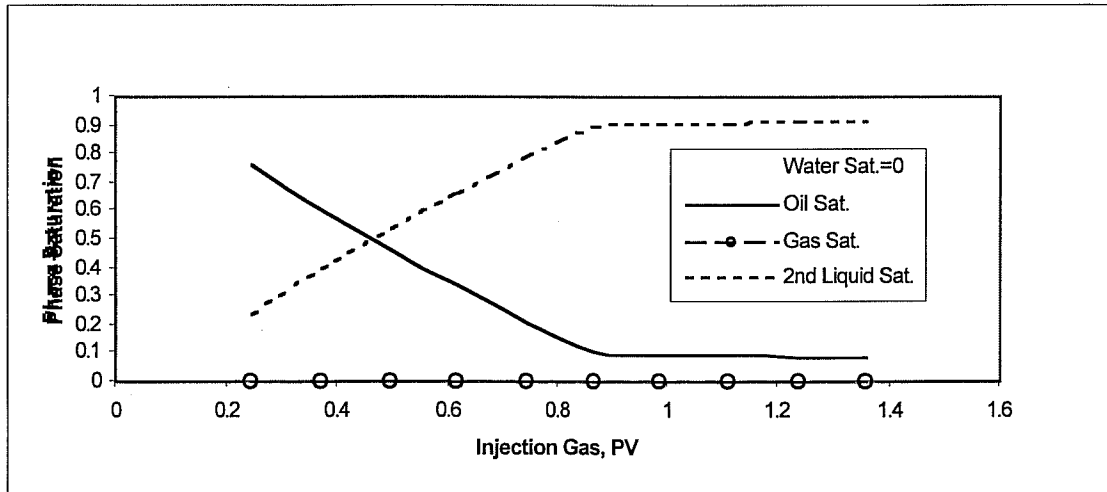


Figure 26. - Slim tube average saturation vs. injection pore volume

Slim tube average saturations are plotted in Figure 26. Figure 26 shows the formation of a CO_2 -rich second liquid phase in the slim tube initially upon injection of solvent. As more solvent was injected, the original oil was gradually replaced. Oil saturation gradually decreased to residual saturation of 6%, while the second liquid phase saturation gradually increased to 94%. Water saturation was zero during this test. A very small amount of gas phase (less than 0.1%) co-existed with oil and second liquid phases initially, but disappeared after the first injection day.

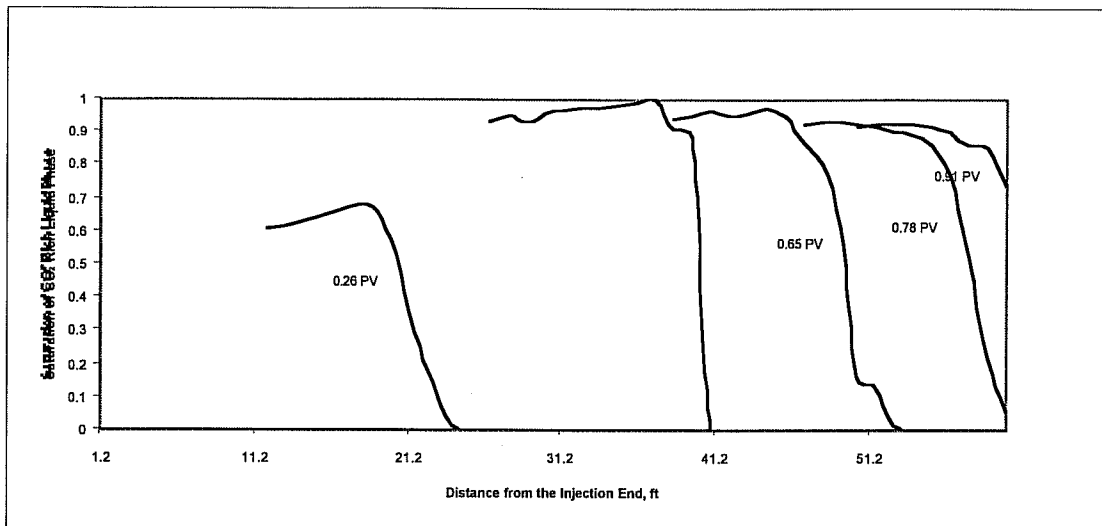


Figure 27. - Distribution of CO₂ rich second liquid phase saturation

Other parameters were similarly well matched. Figure 27 shows distributions of CO₂ rich liquid phase saturations along the tube. As solvent injection continued, the injection frontal zone moved gradually towards the production end. Gas breakthrough occurred between 0.78 PVI and 0.91 PVI, consistent with the experimental test indication of 0.86 PVI. After gas breakthrough, the differential pressure across the slim tube dropped from above 100 psi to 3 psi, matching the slim tube experimental data of 135 psi before gas breakthrough to 5 psi after gas breakthrough.

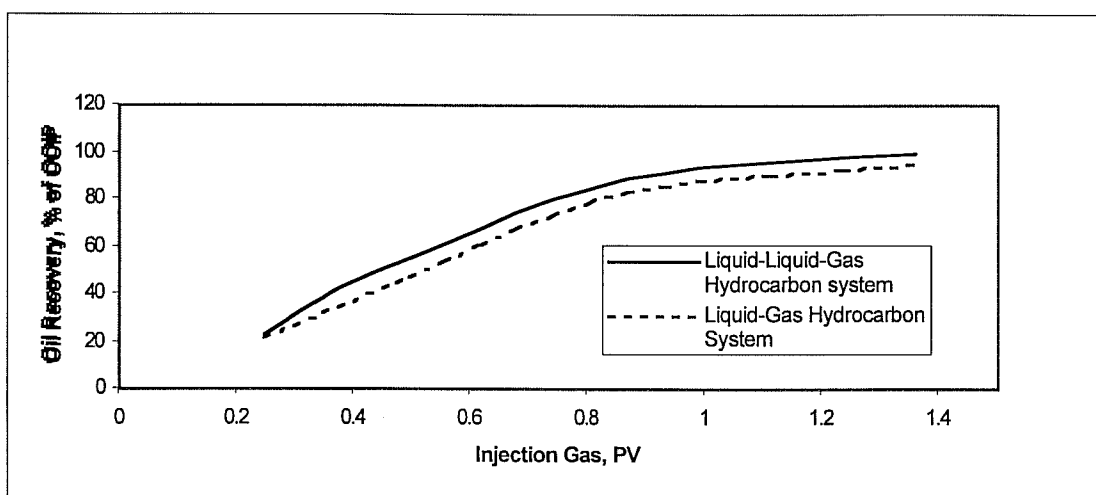


Figure 28. - Effect of CO₂ rich phase on oil recovery

To study the effect of the CO₂-rich second liquid phase on oil recovery, input parameter NP (maximum number of phases allowed) was adjusted to allow only three phases--water, oil and gas phases. The CO₂-rich second liquid phase was lumped into the gas/oil phase to approximate the results from the simplification done with commercial simulators. Figure 28 compares oil recovered with and without the simplifications. The case with simplification predicted 5% of OOIP lower than that of the four-phase case, consistent with the results of 2D simulation discussed in the previous section. This result clearly underscores the important contribution of the CO₂-rich phase and the potential error from simplified systems.

Extensive 1D sensitive studies based on the matching slim tube test data set were conducted to better understand the parameters that possibly affect the oil recovery.

5.3.2 *Four-phase Relative Permeability (Sensitivity Study)*

Relative permeability is a major factor that affects the oil recovery. In general, relative permeability is a function of saturation, wettability, pore structure and capillary number. Its primary impact on oil recovery is through fluid mobilities and fractional flows. Unfortunately, no reliable experimental four-phase (water-oil-gas-second liquid phase) relative permeability data are available, and only a few sets of experimental three-phase (water-oil-gas) relative permeabilities for a specific type of porous medium are available in the literature. Due to the scarcity of reliable data, theoretical models were solely relied on to predict flow behavior.

In UTCOMP, the relative permeability is defined with fitting parameters of various models. Because look-up tables are not an option, the relative permeability table for Schrader Bluff was curve fit to each of the models for this study. In this work, Baker model, modified Stone II model, Corey model, and modified Corey model were used.

Baker and modified Stone II model use the two-phase oil-water and oil-gas data to predict the three-phase oil relative permeabilities. The three-phase water and gas relative permeabilities are assumed to be the same as those of two-phase flow. Gas and water three-phase relative permeabilities are assumed to be functions of their own saturations only, whereas those of the oil phase is assumed to be a function of two saturations. For four-phase flow, the oil relative permeability is shared by the oil and second liquid phases in proportion to their relative volumes.

For Corey's model and modified Corey's model, phase relative permeabilities depend only on their own saturations.

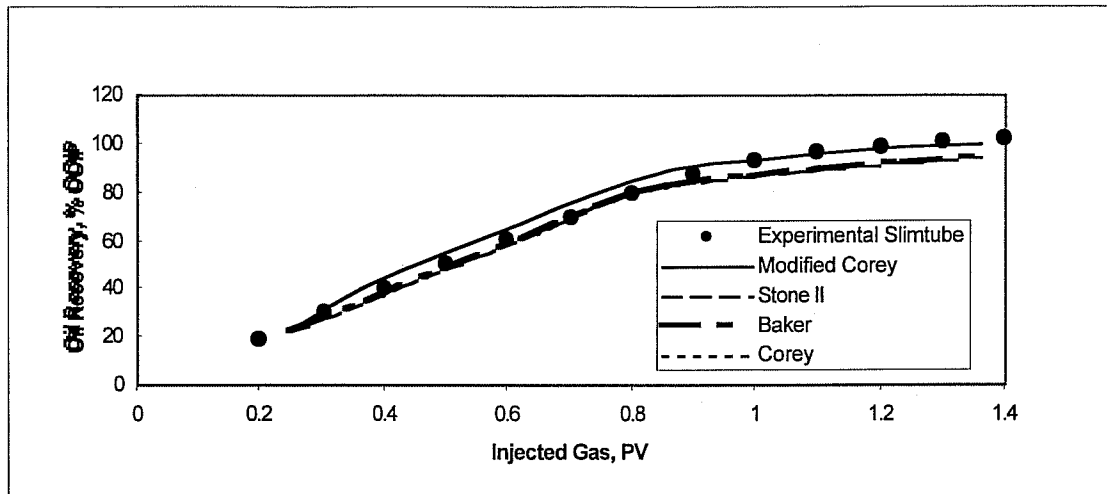


Figure 29. - Effect of relative permeability models on oil recovery

Figure 29 compares oil recovery between slim tube test and UTCOMP simulation results for the four permeability models. Stone II, Baker and Corey models gave almost identical oil recoveries. Oil recovery was slightly underestimated by about 1% before gas breakthrough, 1% better than that of modified Corey's model. However, all models predicted about 7% lower oil recoveries than the experimental test result after gas breakthrough, comparing 1% difference predicted by modified Corey's model. Overall, the modified Corey's model appears to give the best simulation result.

5.3.3 Effects of Temperature and Pressure (Sensitivity Study)

Phase behavior and oil composition effects on fluid properties (densities, viscosities, etc.) influence local displacement efficiency. During CO₂ flooding, the CO₂ mixes with oil in place and extracts light and intermediate hydrocarbons. After multiple contacts, the CO₂ rich phase develops a composition that can completely displace contacted oil. Since the number of phases present in CO₂-oil systems depends on pressure and temperature, reservoir temperature and pressure sensitive studies were performed in this simulation study.

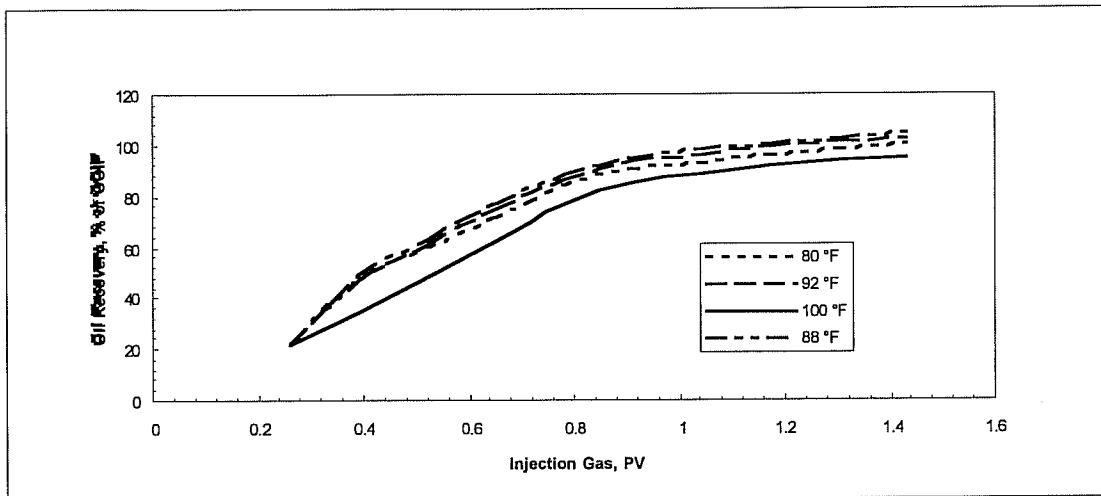


Figure 30. - Oil recovery at various reservoir temperature (0.26 PV/day)

Temperature was found to influence the oil recovery efficiency. Schrader Bluff reservoir temperature varies from 80°F to 100°F, which includes the critical temperature of CO₂ (88°F). Figure 30 shows the oil recovery at various reservoir temperatures. The injection rate in these cases was kept constant at 0.26 PV per day. Oil recovery was the highest at 88°F and decreased as the temperature increased or decreased from the critical temperature. Higher recovery results from the increased solubility of the liquid phase CO₂ in crude oil at or near the CO₂ critical temperature. This swelling process lowers the viscosity of oil liquid phase and results in a more efficient displacement of oil by CO₂.

Pressure was also found to affect the results of a gas injection project. For a typical gas injection project, the reservoir temperature is usually considered constant; thus pressure becomes more practical to be adjusted to improve the efficiency of CO₂ injection.

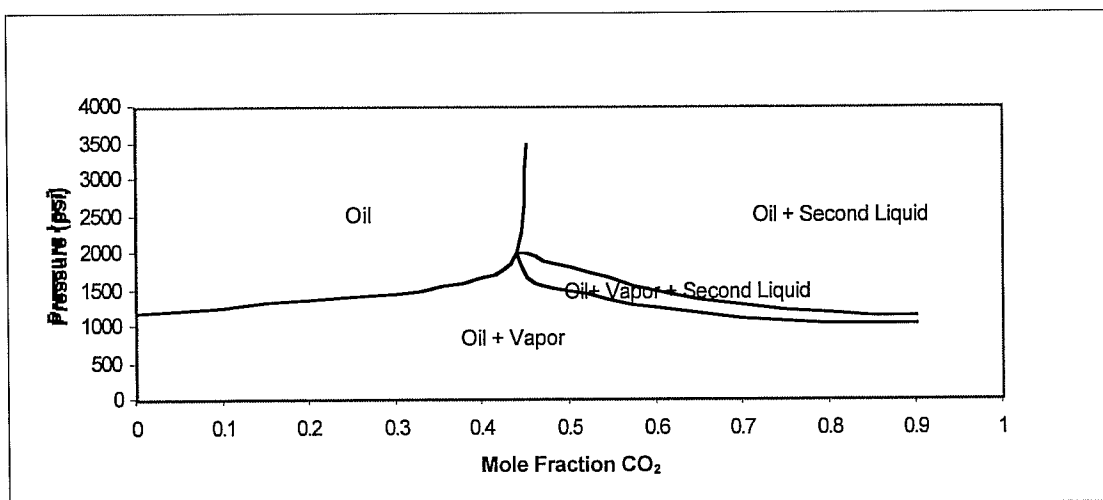


Figure 31. - CO₂/oil phase equilibrium at 92° F

To better understand the pressure effect on oil recovery, we used UTCOMP to generate the phase behavior plot. By assigning each block different pressures with the same CO₂/oil mixture, one time step flash calculation can be used to estimate the bubble point/dew point. P-X diagram can then be generated by repeating this process. Figure 31 shows the CO₂/oil phase equilibrium at reservoir temperature 92°F. A three-phase liquid-second liquid-vapor region appears at pressures ranging from 1100 to 2000 psi and CO₂ concentrations higher than about 44 mole%. CO₂/oil mixture changes from an oil-vapor region to a three-phase liquid-second liquid-vapor region and then to an oil-second liquid phase as pressure increased with CO₂ concentration higher than 44 mole percent. The three-phase region occurs over a fairly narrow pressure region from a few psi to about 400 psi.

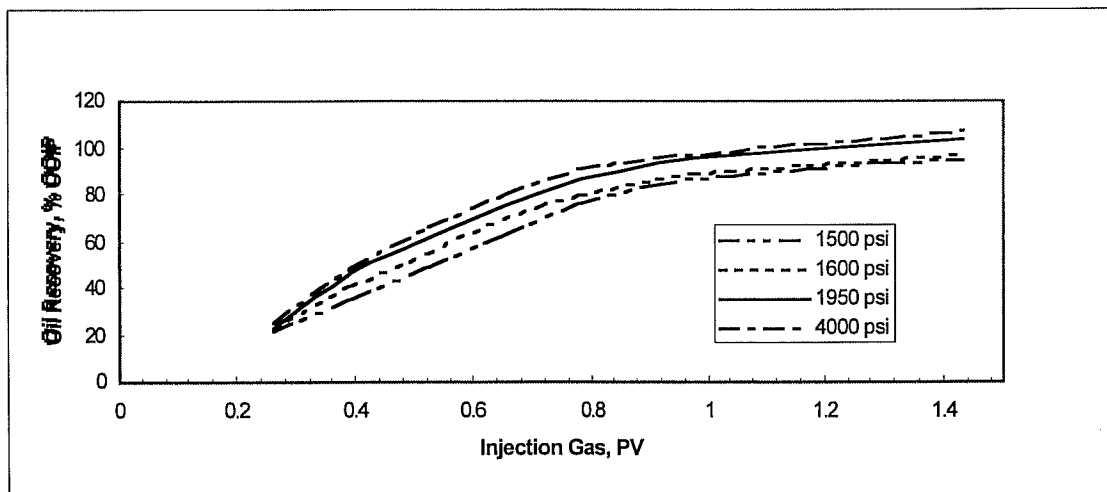


Figure 32. - Oil recovery at various reservoir pressures (0.26 PV/day)

Figure 32 shows the oil recovery at four different reservoir pressures at the same injection rate of 0.26 PV/day. Higher injection pressures result in higher oil recoveries. As the CO₂/oil phase changes from a three-phase to an oil-second liquid phase region, oil recovery is increased about 5%. Inside the oil-second liquid phase region, further increase pressure has minimal impact on the oil recovery.

5.3.4 Mechanism of Displacement

When CO₂ and oil are mixed, two physical changes occur that lead to improved oil recovery. First, the CO₂ –oil mixture has a lower viscosity than the original oil, which increases the mobility. Second, the high solubility of CO₂ in oil causes significant swelling, which forces oil to move because of volume expansion.

Mechanisms for CO₂ mixing during flow processes vary but generally fall into the following three categories: (1) vaporization (vaporizing the intermediate components from the oil phases to the CO₂-rich

phase), (2) condensation (condensing the intermediate component, predominantly ethane through butane, from CO₂ phase to liquid phase), and (3) a combination of vaporization and condensation. Which mechanism will control the displacement depends on the reservoir temperature, pressure, and compositions of gas and reservoir oil.

For the case of this study, gas saturations are low to zero throughout the slim tube (see Figure 26), and the displacement process mostly resembles a liquid-liquid extraction process. The primary mechanism then should be condensation of CO₂ into the liquid phase, rather than vaporization. This conclusion is consistent with the observations reported by R.S. Metcalfe and Lyman Yarborough, Shelton and Yarborough, and by Huang and Tracht.

If we use the definition of minimum miscibility pressure (MMP) as the pressure at which the recovery is 90% of OOIP at 1.2 PV gas injection, MMP should be around 1500 psi (see Figure 32). Since the slim tube pressure above 1950 psi, the displacement for the slim tube is considered as a multiple-contact miscible process.

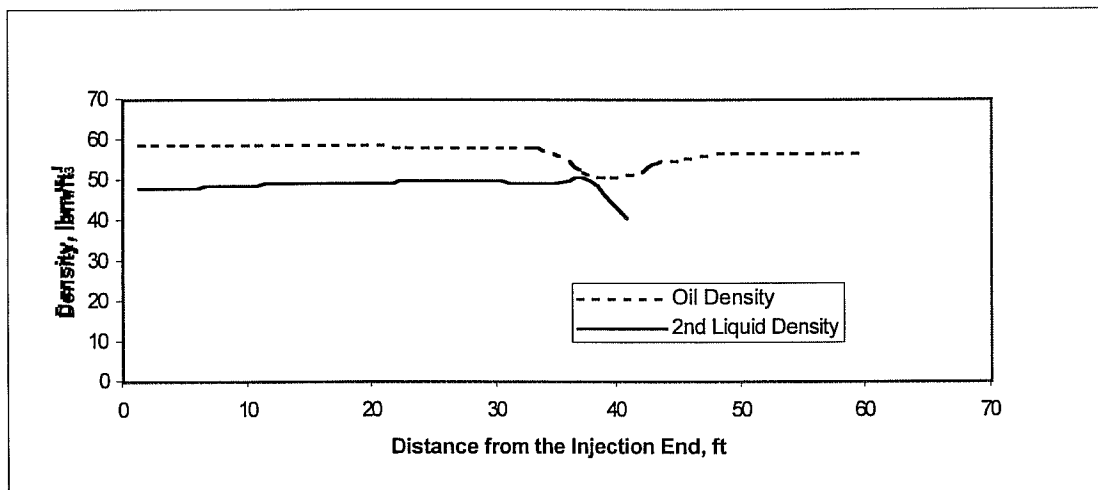


Figure 33. - density profile for the CO₂ rich and oil phases

Extraction between two liquid phases can substantially increase the viscosity and density of the CO₂ rich phase, while dissolved CO₂ can reduce the viscosity and density of the hydrocarbons remaining in the oil-rich liquid. Figure 33 shows the density profile along the slim tube at 0.49 PV. Clearly, the density of the CO₂ rich liquid phase increases along the injection path and reaches the highest in the mixing zone. Density differences between two liquid phases decrease from 10 lbm/ft³ to 1.5 lbm/ft³ at the mixing zone.

5.3.5 Conclusions

Following conclusions can be drawn from this study.

UTCOMP can accurately predict four-phase systems and simulation results match well with slim tube experiment data, all within $\pm 2\%$ of OOIP.

Relative permeabilities have an important effect on oil recovery. Due to the scarcity of reliable experimental data, theoretical models were used to generate four-phase curves. Studies show that modified Corey's model appears to be the best.

The number of phases present in CO₂-oil systems depends on the reservoir temperature and pressure. Oil recovery has the highest recovery at 88°F. Oil recovery increases as the pressure is increased and as the temperature approaches the CO₂ critical temperature.

The simulation runs show that lumping the CO₂-rich second liquid phase into the gas/oil phases, reduces oil recovery (5% of OOIP for Schrader Bluff). A similar error is possible with commercial simulators unable to simulate four-phase systems.

5.4 Summary

[continue]

6. Asphaltene Precipitation Potential

6.1 Background

Currently, oil is being produced from Schrader Bluff by waterflood and no asphaltene problems have been reported from the field operations. So why is this a concern?

The asphaltene content of West Sak oil, taken from the same formation in an adjacent field, has been measured at about 5 wt% (DeRuiter et al., 1990). PVT tests of the Schrader Bluff oil have shown that under destabilizing conditions an asphaltic phase forms. Conditions known to destabilize asphaltenes include the introduction of certain solvents such as carbon dioxide, propane, butane, pentane, etc. Since these solvents are among those being considered for enhanced oil production, it is possible that the proposed EOR methods will also introduce asphaltene deposition problems. Such problems have been observed in other field projects where CO₂ and light hydrocarbon solvents like NGL's are used.

6.1.1 Chemical nature of asphaltenes

It is not the intention of this report to discuss in detail the nature of asphaltenes, asphaltene behavior, and deposition mitigation methods. Two excellent sources for additional information can be found in books by Yen and Chilingarian (1994) and Bunger and Li (1981) both containing many chapters by different authors. Typically, asphaltenes from crude oil is identified as that material precipitating out when excess amounts of paraffinic solvents such as pentane or heptane are added. Asphaltenes are considered soluble in aromatic solvents like toluene and benzene, which excludes the carbenes and carboids. Asphaltenes are typically a dark, amorphous powder, with specific gravity in excess of 1 and having relatively high molecular weights (generally greater than 1000 amu).

However, the determination of specific properties of asphaltenes can be complicated by the procedure used to generate them: the material is usually a mixture of many chemically non-unique species. Further, Thanh et al. demonstrated that a high concentration of microcrystalline waxes can co-precipitate with asphaltenes from the addition of n-pentane (Thanh et al., 1999). Not only does this make material characterization difficult, but well treatments may be incorrectly designed if all of the deposit were assumed to be asphaltenes when wax deposits are also present.

Measurement of molecular weight values of asphaltenes is also very difficult. Asphaltenes are often insoluble in the very solvents used to measure molecular weights. Secondly, the presence of other species such as co-precipitated wax or resins will introduce error in the values measured. Molecular weight values of asphaltenes are often in dispute, since values can vary depending on the method and conditions of the measurement. Furthermore, asphaltenes are known to associate in solution, particularly with resins. Some methods of measurement will not be able to easily differentiate asphaltene molecules from the much larger macro-molecules in solution. The same material measured by different means can have molecular weights that vary from 600 to 300,000 amu (Speight and Moschopedis, 1981).

Despite these difficulties, its presence is financially important. In crude oils where the resin to asphaltene ratio approaches 1, the stability of asphaltenes become very sensitive to changing temperature, pressure, and composition of the crude oil. For these cases, significant amounts of deposit in the

production equipment will result as the reservoir pressure declines towards the crude oil bubble point. However, below the bubble point loss of the lightest hydrocarbon components will result in increased stability in the crude oil and further flocculation of asphaltenes is not expected. This behavior can be explained thermodynamically with the changing solubility and molar volume parameters of the crude oil.

Even if no precipitation problems are present on initial production, the injection of solvents like CO₂, propane rich NGLs, etc., can result in the reduction of overall solubility parameter of the crude oil and resulting destabilization of asphaltenes. Other phase changes may also contribute if resins and asphaltenes are partitioned differently in multiple liquid phases.

Finally, the asphaltenes remaining in the oil during production and transportation to the refinery must be treated or separated as part of the crude oil upgrading process. Such processes are very energy intensive, add substantial cost to the refining process, and reduce the overall value of the crude oil. So, while the material is difficult to characterize because it is a mixture of chemically non-unique species, its presence and properties must be understood.

6.1.2 Solubility Characterization Methods

As already explained, asphaltenes by definition precipitate from crude oil in the presence of excess pentane but are soluble in aromatic solvents like toluene and benzene. Because asphaltenes are defined functionally rather than chemically, solution stability as a function of solvent has been extensively studied. Not surprisingly, for a given crude oil the amount of material precipitated depends on the solvent used and the quantity of solvent added—even here one does not obtain a unique result. Because the value is functionally dependent, the "asphaltene content" for a given crude oil is somewhat arbitrary. Comparing asphaltene content of crude oils must always consider the method used to derive the value.

Many researchers including Hirschberg et al. use Flory-Hildebrand theory to characterize the stability of asphaltenes in crude oil (Hirschberg et al., 1982). Stability is based on the Hildebrand solubility parameter for the solute and solvent. As the differences between the solute and solvent increase, the solute becomes less stable in the solvent and at some point flocculates or separates out. This approach has been very effective in characterizing polymer solutions and is frequently applied to prediction models for asphaltenes. The effects of temperature, pressure, and hydrocarbon composition may be related to asphaltene solubility using this theory.

A number of studies have compared the relative amounts of asphaltenes precipitated from crude oil as a function of solvent solubility parameter (SP) (for example, Speight, 1994). In general, as the hydrocarbon chain of the solvent is increased (SP increases), the amount precipitated is less for any given amount of solvent. Thus, propane is likely to precipitate much more asphaltenes and at an earlier point than that of n-heptane. Methane and ethane would be even worse, except that the solubility limit of methane and ethane in the crude oil for a given pressure and temperature usually is reached before the precipitation point for the respective solvents.

Wiehe characterized a two-dimensional mapping of solvents to characterize the solubility of asphaltenes in heavy oil (Wiehe, 1995 & 1996). The solvent solubility parameter was separated into the complexing solubility component (i.e., hydrogen bonding forces) and the field force solubility component

(i.e., van der Waals and dipole interactions). Solubility is measured as a function of solvents with varying complexing and force field solubility components, and a solubility region is mapped for a given crude oil. Thus, the effect of different solvents with similar overall solubility parameters are more accurately characterized. The overall assessment using this approach suggested that while solvent complexing was important in maintaining solubility of asphaltenes, the dominant interaction was not hydrogen bonding. Solubility behavior was principally related to aromaticity and molecular weight.

While many studies evaluate the effect of solvent, most confine the solvent selection to a class of saturated hydrocarbons. While correlation of solubility to solvent selection can be observed, the effect is confounded by the restriction of solvents tested. Speight reported one of the few sets of data that included a broader range of solvent types, comparing asphaltene solubility in wt% (Speight, 1994). Speight concluded that the correlation to solubility parameter only holds for hydrocarbon solvents, and severe variance appears between different series of solvents (ketones, ethers, etc.). Although comparison was only made to solvent solubility parameter, other solvent properties may be similarly compared to determine which properties best correlate.

A dataset was assembled based on the solubility of asphaltenes from the Athabasca Bitumen as measured by Speight (Mitchell and Speight, 1973; Speight, 1994). The reported data were obtained from ^{from} high solvent/crude oil ratios, as is typically done for obtaining an estimate of crude oil asphaltene content. The wt% precipitate was converted to wt% soluble based on estimation of asphaltene content using n-pentane (standard procedure). As can be seen in the figures, this turns out to be very arbitrary, as some solvents precipitate even more asphaltenes. In the figures, these will show up as negative wt% soluble.

A few solvent values were added to the list from Wiehe's data (Wiehe, 1996). These are solvents with 100 wt% soluble asphaltenes. Other solvents were not added, because the wt% precipitate was not reported and because the hydrocarbon was different (Cold Lake Bitumen). Overall, the results were consistent between the two sets of data.

Solvent properties were then obtained from the literature and plotted against the following physical properties: Hildebrand's Solubility Parameter (Hoy, 1970; Wiehe, 1996; dielectric constant (CRC, Lange's Handbook), dipole moment (CRC, Lange's Handbook), refractive index, molar polarizability, and density. Jill Buckley had shown that the point at which asphaltene flocculation could be accurately tied to refractive index values of crude oil/solvent system (Buckley, 1996).

Figure 34 shows a plot of wt% asphaltenes vs. Hildebrand's Solubility Parameter. The major group of outlier points are those of ketone and ester solvents. The extreme outlier points (n-pentanol and ethylene glycol) are also shown in this plot. Clearly, a reasonable correlation can be shown with the solubility parameter, provided the solvent is non-polar in nature. This is consistent with the limitations of the theory applied to asphaltenes by Hirschberg and others (Hirschberg et al. 1982; 1984; Chung, 1992; Anderson, 1999). Solution theory needs to be modified for highly polar or associating solvents.

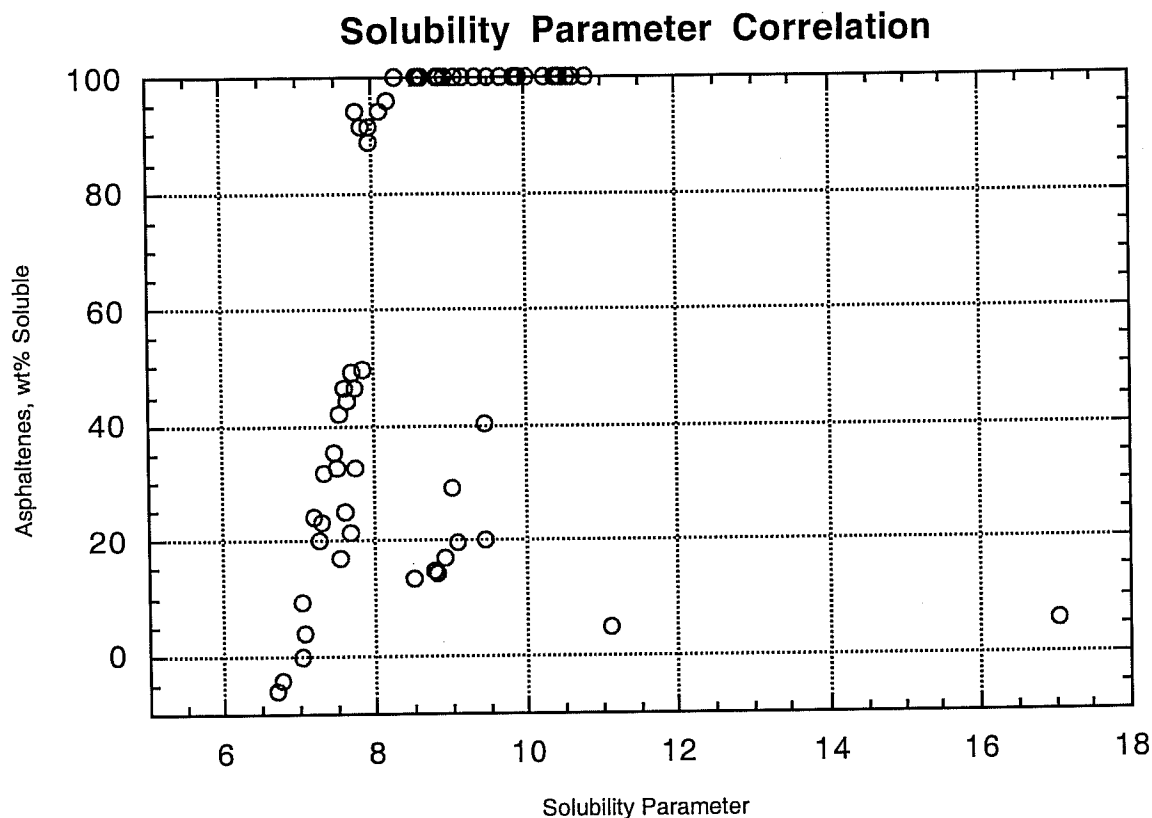


Figure 34. - Comparison of Hildebrand's solubility parameter and wt% soluble asphaltenes of Athabasca bitumen for a range of solvents

The other plot of interest is that of solvent density for the same data set (see Figure 35). Since the solvent ratio to crude oil is very high, the solvent density effectively estimates the fluid density at which the asphaltene solubility is measured. Oil density as a function of PVT conditions are correlated and fine-tuned using presently available equations-of-state (EOS). If a correlation to density could be justified, asphaltene stability could be quickly estimated using standard EOS software, since variation of oil density from variation in temperature, pressure, etc., and the addition of gas solvents such as CO₂ are all readily determined.

It isn't immediately obvious that any correlation exists in Figure 35. However, looking at the specific data points one can see a series of curves corresponding to each homologous series of solvent types by chemical functionality. The cyclic hydrocarbons (saturated, aromatic), alkanes/alkenes, dialkyl ethers, ketones, and esters each group themselves in a regular fashion. In general, an increase in solvent density corresponds to an increase in asphaltene solubility, where the curve is shifted by the nature of the solvent.

This is consistent with observed behavior in the field. It is the lighter crude oils (lower density) that are most likely to show asphaltene deposition problems from pressure depletion during primary production. Rarely do the heavy (more dense) asphaltic crude oils show this problem in the field. As pressure drops, the fluid density similarly drops.

Resins are cyclic aromatic compounds are generally believed to associate with asphaltenes providing solution stability. The density plot clearly shows that cyclic solvents do add stability, where a lower solvent density is required to precipitate asphaltenes from solution. The exceptions to this trend in Figure 35 are alcohols, the points designated as circles in squares. Table 22 shows the slope and intercept values to the lines of Figure 35. More extensive work is needed looking at asphaltene solubility as a function of solvent (crude oil mixture) density for a variety of oils, densities, and phase conditions.

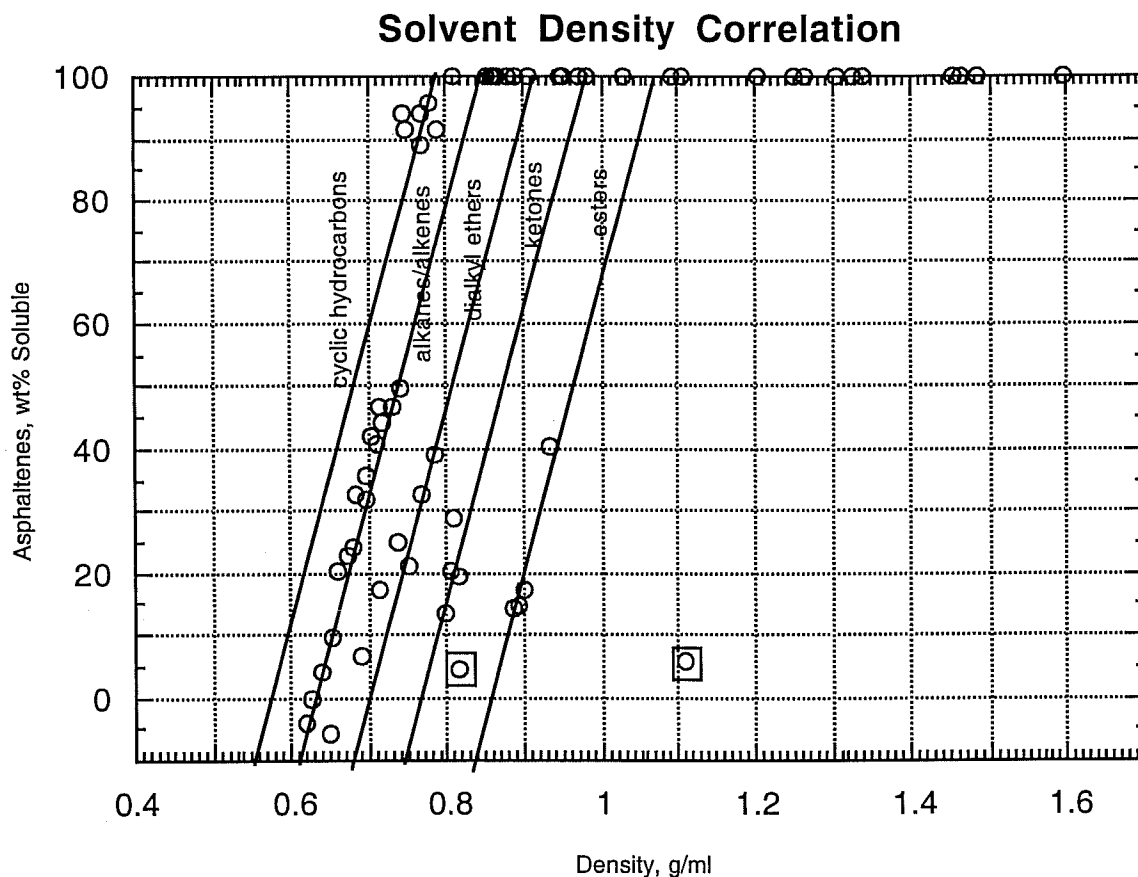


Figure 35. - Comparison of solvent density and wt% soluble asphaltenes of Athabasca bitumen for a range of solvents

In principle, one could apply this relationship to a crude oil by measuring the density and onset of asphaltene flocculation and setting this value to the solvent constant.

Solubility (wt%) = 517.8(density, g/ml) + solvent constant (see Table 22), where minimum is set at 0 wt% and maximum is set at 100 wt%.

Table 22. - Input parameters for linear approximation of asphaltene solubility

slope	517.8	Athabasca Oil
Solvent constant:	-302.4	cyclic hydrocarbons
	-326.2	linear hydrocarbons
	-357.3	dialkyl ethers
	-393.5	ketones
	-447.9	esters
	not valid	alcohols

6.1.3 Solubility prediction methods

A number of models have been developed for predicting the conditions at which asphaltenes flocculate and for predicting how much will precipitate out. A couple of the recent papers illustrate approaches to this task (Chung, 1992; Nghiem et al., 1998), and Andersen and Speight (Andersen et al., 1999) provide an excellent overview of the approaches typically taken to model asphaltene phase behavior.

To clarify terminology, "flocculation" is referred to as the process of solid formation from a thermodynamic equilibrium of a solution. However, once formed these solids may remain suspended or deposit on the solid matrix (rock) of the reservoir. The latter deposition process is referred to as precipitation. "Plugging" is considered the process of solid asphaltene particles depositing specifically at the pore-throat of reservoir rock pores in sufficient amounts to stop fluid flow. This distinction is often needed because conditions may be favorable to flocculation but have minimal impact on fluid flow of crude oil in the reservoir. Reasons for minimal impact include slow precipitation rates and minimal plugging effects. That is, particle density and size enable the flocculated asphaltenes to flow with the crude oil and remain suspended for relatively long time periods.

Prediction models have tended to follow one of several basic approaches that assume the asphaltene particles behave reasonably well according to: (a) solution thermodynamics, (b) colloidal particle theory, or (c) micellization stabilization in solution. The solution thermodynamic theory approach requires that the flocculation-solution process be reversible. Unfortunately, cases have been reported that show this to be true for some crude oil systems and to be not true (at least in a reasonable time-frame) for other crude oil systems. Additionally, most models assume the asphaltenes to be a single solid-phase pseudo-

component. This assumption is grossly in error, particularly when waxes and resins with very different chemical properties co-precipitate with the asphaltenes. Unfortunately, obtaining the detailed properties of individual asphaltene components making up the material group classified as asphaltenes for a given crude oil is usually beyond the scope of most experimental studies. The complexity of identifying asphaltene components is further increased by the variation of amount and type of asphaltenes precipitated as a function of the particular solvent added, the amount of solvent added in proportion to the crude oil, and the contact time of the solvent. Consequently, developed models usually simplify the problem to a manageable degree of complexity by assuming asphaltenes formed from solution can be suitably represented as a single pure component.

In general, one of the major difficulties in modeling asphaltene precipitation is the lack of the required physical characterization data of the asphaltene being studied. This has led Andersen and Speight to conclude that "In all models a number of parameters are tuned to obtain best fits to the experimental data . . . Even though the models are based on thermodynamic concepts, they remain empirical because of the number of parameters used in the calculations." Prediction of asphaltene flocculation behavior is therefore limited to the conditions actually studied for a particular crude oil and cannot be reliably predicted apriori using currently available models. The discussion of the previous section reviewing the effect of different solvents was an attempt to identify simpler reliable empirical methods of measuring and predicting asphaltene solution stability.

Of the models describing a thermodynamic process, most adapt the Hildebrand solubility parameter concept. The Flory-Huggins equation is used to estimate the maximum volume fraction the asphaltenes remain in solution. This is the approach used to evaluate Schrader Bluff as discussed later in this section. Required input parameters include asphaltene molar volume, asphaltene solubility parameter, crude oil molar volume, and crude oil solubility parameter. The molar volume is dependent on molecular weight and density, and is calculated for the Schrader Bluff case as described later.

[continue] insert general equations for different versions; discuss in more detail particular models; etc.

Quantitative asphaltene molecular weight, asphaltene solubility parameter values, and crude oil solubility parameter values are difficult to obtain accurately. As mentioned earlier, molecular weights can vary widely depending on the method and conditions used to measure it. Solubility parameter is a function of molar volume and molar internal energy of vaporization, both of which would be very difficult to obtain for asphaltenes. More typically one estimates this value based on precipitation data using different solvents with specified solubility parameter. Alternatively, these values are simply tuned to obtain a good overall match to experimental data with whatever model is being used.

Tuned equation-of-state models may be used for crude oil molar volume estimates. Most typically, one must obtain experimental conditions at which asphaltenes are formed, tune the model parameters including asphaltene molecular weight and solubility parameter to fit the data, then extrapolate to other conditions of interest that do not extend too far from the conditions measured. Increasing the number of model parameters in more sophisticated models require access to more unique experimental data for parameter optimization and do not necessarily result in more useful or more accurate predictions.

In summary, several approaches have been taken to model the flocculation behavior of asphaltenes in crude oil. While the theoretical basis of these models may be sound, the applicability of these models are no better than that of empirical models. The input data required for them are usually not quantifiable or easily measured for asphaltenes, and the models are based on assumptions that are clearly wrong. The most obvious of these erroneous assumptions is that asphaltenes behave like a single pure component in solution.

6.1.4 *Summary of activities done on this project* [continue]

6.2 **Comparison of Schrader Bluff with other Fields**

In considering whether the injection of CO₂ and light hydrocarbon solvents will precipitate asphaltenes, several previous studies have enough in common with Schrader Bluff to warrant a separate discussion. The following paragraphs include discussions of field cases that help to determine to what degree asphaltenes are likely to be a problem and how it might be mitigated.

The geological formations containing the oil of Schrader Bluff are the same sands as ^{those} that of the adjacent West Sak and Ugnu formations. The oil and rock properties are likely to be very similar, with the exception that West Sak and Ugnu are up dip and the reservoir temperatures are lower. Several studies have been published on West Sak and Ugnu evaluating gas injection processes (DeRuiter et al., 1990; Zick, 1986; MacAllister et al., 1985; Sharma et al., 1989).

In PVT studies of West Sak, static PVT swelling studies were conducted with methane, carbon dioxide, ethane, propane, and n-butane solvents (DeRuiter et al., 1990). Propane and n-butane were shown to be first-contact miscible. At high concentrations, propane and n-butane also precipitated solid asphaltic materials. To the extent soluble, asphaltene precipitation was not evident in the presence of the other solvents. The asphaltenes was determined to represent about 5 wt% of the original oil.

In the case of propane, asphaltic phase precipitated at propane concentrations of 50 wt% and above. The asphaltic phase precipitated at n-butane concentrations of 70 wt% and above. It is expected that the n-butane with solubility parameter value slightly higher and consistent with alkane solvent series sensitivity to asphaltene that as the alkane chain-length is increased less asphaltenes are precipitated from a given crude oil. A gas mixture (35% ethane, 34% propane, and 31% n-butane) was also tested, and similarly produced a lower asphaltic phase. Because the other single solvents are not first-contact miscible, their solubilities are not high enough to reach the concentrations in the crude oil needed to similarly destabilize the asphaltenes. Therefore, no problems were observed in the static PVT cell with these solvents.

A flow experiment (slim tube) was conducted with these solvents. In the gas mixture case, a residual amount of asphaltic material was recovered from the slim tube after the solvent injection was complete (oil recovery near 100%). However, the amount of asphaltic material was small relative to the amount evidenced in the static PVT experiment. No mention of any asphaltic material was made for the carbon dioxide and ethane injection experiments. Ethane was shown to develop miscibility with West Sak oils, but no asphaltene precipitation problems are noted.

Gondouin suggests that miscible displacement by such gases as CO₂ is not applicable to West Sak and that reservoir plugging by asphaltenes is likely to reduce overall recoveries (Gondouin, 1991). A modified thermal recovery process was proposed to address some of the unique issues relating to the arctic environment for this approach.

In summary, PVT and slim tube studies of West Sak oil, which is similar to Schrader Bluff oil, suggests that carbon dioxide is immiscible at reservoir conditions. Whether or not asphaltene problems will severely impact operations in the field has not been fully determined. Hydrocarbon solvents with propane and n-butane are miscible with West Sak oil, and asphaltene precipitation was demonstrated for these solvents. However, the presence of asphaltenes in flow experiments with these miscible hydrocarbon solvents was slight and was not sufficient to measurably reduce the nearly complete recovery of crude oil for at least one set of experiments.

The Kuparuk EOR Project is another field example worth mentioning (Zick, 1986; Rienbold et al., 1992; Godbole et al., 1992; Hoolahan et al., 1996). There are many reservoir properties that are very similar to Schrader Bluff, and many of the concerns in designing and scaling up of the Kuparuk EOR project are the same as those presently being evaluated for Schrader Bluff. Geographically, the Kuparuk River Unit is neighboring Schrader Bluff on the North Slope of Alaska. All issues associated with working in the Arctic climate will be the same. Gas solvent choice and availability will have the same constraints. The formation porosity and thickness are approximately the same for both reservoirs. The depth of the Kuparuk EOR Project is somewhat deeper at 6000 ft vs. about 4000 ft for Schrader Bluff. Although being deeper helps with higher reservoir temperature and higher reservoir pressure limits, fluid and PVT properties are not that different.

There are many similarities with the oil properties. As with Schrader Bluff, the oil viscosity exceeds the recommended amount for a miscible gas injection process. The API Gravity for Kuparuk River Unit varies from 18° to 24° API while that of Schrader Bluff varies from 14° to 21° API. The recommended lower limit for miscible gas injection processes is 24° API due to the more extreme differences in mobility between the injected solvent and the crude oil. As with Schrader Bluff, Kuparuk River Unit oil is under-saturated, although the relative amounts of light ends (C1 to C6) are higher for Kuparuk than for Schrader Bluff. As with Schrader Bluff, the asphaltene content is relatively high (3 wt% to 17 wt% of C7+ fraction), and was a concern for the EOR project.

At least 2 primary concerns for the Kuparuk EOR Project relevant to Schrader Bluff were carefully examined: (1) 3-hydrocarbon phases were dominant in the EOR process and effects of fluid flow were unknown, and (2) the lower liquid phase concentrated the asphaltenes with precipitation evident in the laboratory PVT studies. Extensive, PVT, slim tube, coreflood, single and multi-contact experiments were conducted in the laboratory to evaluate these issues and provide the needed information for simulation and scale-up studies. Unlike other published studies, the P-X diagram for Kuparuk oil had a relatively large L-L-V region and experimental studies showed that the asphaltenes concentrated in the lower liquid phase. The formation of the more dense asphaltic liquid phase was observed to be reversible, and oil recoveries were described by the near-miscible condensing/vaporizing mechanism for enriched gas displacement. Flow experiments in the laboratory (and further supported in the field test) showed that the asphaltenes did not significantly plug at pore-throat locations and or impede fluid flow. The impact of the

three hydrocarbon phases is no longer considered a concern because: (1) all 3 phases are light and reasonably similar in physical properties, (2) the heaviest, most dissimilar phase occurs at relatively low saturations, (3) the 3 phases appear for a small range of compositions, and (4) no laboratory or field results have indicated any major problems with fluid flow (Hoolahan et al., 1996). Success of the initial small EOR project at Kuparuk has subsequently been expanded and now represents one of the largest of its type in the world.

Extensive experience with CO₂ injection and potential asphaltene problems also provides some useful information for Schrader Bluff. Huang determined for a West Texas crude that injecting CO₂ into a reservoir with higher amounts of asphaltenes in the crude oil could lead to deposition in the reservoir rock resulting in an increase of oil wettability and a reduction in overall oil recovery (Huang, 1992). In Huang's experiments, asphaltene content in excess of 4.6 wt% was sufficient to cause these problems. Furthermore, using slim tube experiments to estimate MMP values could be misleading when asphaltene problems are present because of deviated performance of fluid flow. Oil recovery curves departed from ideal behavior and mobilizing oil was more difficult. As a result, the classic slim tube criteria for determining miscibility may be in error relative to the asphaltene free crude oil. At least one of the oils analyzed by Huang had similarities to Schrader Bluff: viscous oil (14 cp at 120° F), similar in density (20.2° API), and higher amounts of asphaltenes (14 wt%), although the latter is a bit higher than Schrader Bluff. CO₂ is a solvent under consideration for Schrader Bluff and has caused some problems for a West Texas crude oil.

As with Schrader Bluff, a multiple phase region (L-L-V) can form in the reservoir with the injection of solvents like CO₂ (Creek et al., 1990). Although not explicitly stated, Creek et al. also show that coincident with the formation of the multiple hydrocarbon phases is the precipitation of asphaltenes (50 mole% CO₂). This was similarly observed with Schrader Bluff crude oil where SARA measurements clearly showed the selective partition of asphaltene into the lower more dense phase due to the doubled asphaltene/resin ratio. Anomalous behavior of oil recovery for slim tube displacement tests of the Permian Basin crude were attributed to the presence of these multiple phases.


~~Two other papers have been published that discuss more generally the behavior of asphaltene~~ deposition on hydrocarbon fluid flow. Rassamdana et al. summarized the field performance of an enriched hydrocarbon injection project over an 11 year period (Rassamdana et al., 1997). Some of the production wells had difficulty with asphalt precipitation, even though the asphaltene content of the field was relatively low [continue amount, look up AIChE J., v. 41, p. 10 (1996)]. They reported an unusual pattern in field production. Initially, the injectivity of the fluid decreased as expected and was attributed to plugging from the precipitation of asphalt. However, after some time period, an oscillation of increased followed by decreased injectivity and permeability persisted for the remainder of the observation period. It was explained that the plugging contributed to an increase in reservoir delta-P, and this increased pressure resulted in a reversal of the trend. The implication was that at least in the reported field asphaltene precipitation does not necessarily result in the ultimate plugging of the reservoir, and that the problem could be managed so long as asphaltene deposition in the production equipment could be managed.

delete spaces

Ali et al. conducted a detailed laboratory and simulation study (Ali et al., 1997). Results from this study suggested that although flocculation is dependent on well established conditions (temperature, pressure, solvent composition, etc.), adsorption and plugging of the asphaltene particles are a strong function of flow rate. Most of the asphaltene deposition was observed to occur at the highest flow rate, suggesting that in a reservoir the greatest reduction in permeability is likely to occur in the near wellbore region. This is contrary to fines migration where the greatest plugging is expected at the lower flow rates and where gravity segregation is likely to have the greatest impact. Apparently, in the case of asphaltenes the increased flow rate also increases particle interactions, particle trapping, aggregation, etc. at the pore throat region.

In summary, evidence of field experience shows that for gas injection processes containing CO₂ or enriched hydrocarbon components (propane, butane), asphaltene destabilization may result. Much of the difficulty with asphaltene destabilization has been in mitigating the asphaltene deposition in the production equipment. Reduction in reservoir permeability and gas injectivity is possible, but overall the effect on field performance can usually be tolerated. If present, the greatest damage is likely to occur in the near wellbore region where solvent remediation can be applied.

6.3 PVT Studies of Schrader Bluff Oil

Two PVT studies have been conducted with Schrader Bluff recombined oil. The reports are included in the Appendices of this report. While doing the standard swelling, differential liberation, ^{etc.} etc., measurements, observations are made when asphaltenes are visibly apparent. Since these tests were conducted with different solvents at different pressures and temperatures, useful information can be obtained on the relative stability of the asphaltenes. Furthermore, this information may be used in modeling studies (following subsection) to predict under what conditions asphaltenes may become a problem to the production operations. 

A series of non-destructive swelling experiments were conducted at 92° F on Schrader Bluff recombined oil and Prudhoe Bay Miscible Injectant (MI). Composition of the MI is given in the original report (see Appendix G). As the mole% MI was increased, saturation pressures steadily increased, and up to 60 mole% solvent the behavior is similar to typical black oils. At 80 mole% MI a dark asphaltic phase was observed to coat the cell walls. With increasing pressure, the liquid volume containing the asphaltic material decreased. At 8900 psia the liquid volume disappeared and only the solid particles remained on the wall. The temperature was then increased. At 248° F and 10,000 psia the asphaltenes appeared to go into solution. These particles reappeared on cooling to 92° F. As pressure was lowered to 6427 psia, a second liquid phase reappeared as a condensate.

Destructive swelling tests were conducted at 80 mole% to measure the density, composition and SARA of the individual phases. The lower liquid containing the asphaltic material was found to have less of the light ends (<C5) and more of the heavier ends and the density was slightly higher. The SARA was more revealing. Table 23 below summarizes the results from the SARA test. Clearly shown is the selective partitioning of asphaltenes into Liquid 1 the lower layer. This is in direct contrast with the aromatics and polars (groups containing crude oil resins). that partitioned nearly equally between the 2 liquid phases. Resins are known to be critically important for stabilizing asphaltenes, and in this case it is

evident that the ratio of asphaltenes to resins effectively doubled in the lower phase. The SARA results indicate such a change is sufficient to destabilize the Schrader Bluff asphaltenes.

Table 23. - SARA of phases in MI swelling study for Schrader Bluff

Sample	Saturates, wt %	Aromatics, wt %	Polars wt%	Asphaltenes, wt%
Liquid 1	33.8	42.1	13	11.1
Liquid 2	44.1	42	12.7	1.2
Gas	49	40.3	10.6	0

Liquid 1 is the asphaltic liquid phase initially present

Liquid 2 is the upper condensate phase that drops out at lower pressures

Similar swelling tests were conducted at 92° F using Schrader Bluff recombined oil and a CO₂/NGL solvent mixture in the ratio of 77.5 mole% to 22.5 mole%. As before, non-destructive swelling tests were conducted of 20 mole% to 80 mole% solvent at 92° F. As before, swelling behavior was typical for black oil through 60 mole% solvent, but at 80 mole% solvent and 4340 psia an asphaltic phase forms. Destructive swelling tests were not conducted to measure composition and SARA information. As pressures are lowered from 9000 psia to 1200 psia the number of phases change from 1 to 4 hydrocarbon phases (3 liquids, 1 gas). For lower solvent mixtures (20, 40, and 60 mole% solvent) only 2 phases (liquid, gas) are formed with gas saturation points increase with increasing solvent from 1634 to 2062 psia respectively.

It is clear from the PVT swelling studies that the phase behavior of light solvents (CO₂, Prudhoe Bay MI, NGL) become complex at Schrader Bluff reservoir temperatures and high solvent concentrations. The presence of such complex phase behavior is also likely to be the primary cause of potential asphaltene deposition problems. PVT swelling studies show that asphaltene particles drop out of the crude oil at high solvent concentrations, and SARA measurements of these phases suggest selective partitioning of asphaltenes into the more dense phase in contrast to the crude oil resins results in a destabilized condition sufficient to precipitate out asphaltenes. Additional flow tests are recommended.

A slimtube test with Schrader Bluff oil and the CO₂/NGL solvent mixture has been conducted at 92° F. Although not quantified, fluid flow problems were encountered suggesting that asphaltene plugging may have contributed to the experimental difficulties.

6.4 Model Predictions Asphaltene Behavior for Schrader Bluff Oil

6.4.1 Introduction

To obtain a better understanding of what factors are likely to increase the potential for asphaltene precipitation, including injection of solvents like carbon dioxide, model predictions were made. Available information from this project such as PVT studies and published information from the literature were taken. Although a variety of models are available, the Hirschberg model was adapted for this study, because it was intended to be an initial evaluation. The advantage of the Hirschberg model is that the

input parameters required are limited to 2 for asphaltenes--molar volume and solubility parameter; and the asphaltenes are simplified to 1 pseudo-component of the crude oil mixture. Molar volume and solubility parameter are also needed for the heaviest components of the crude oil, which in this study was assigned to the C36+ fraction. More detailed calculations using refined EOS models could be used in a follow-up study if warranted. As indicated previously in this report, to date all models used for characterizing and predicting asphaltene precipitation are empirical.

6.4.2 Describe model and basis of input

The Hirschberg model is adequately described in the literature and will not be fully presented here (Hirschberg et al., 1984). However, application of this model requires some discussion to explain what was the basis for estimating the input parameters.

Information was provided based on GC compositional analysis. That is, the crude oil composition (mole%) was determined through carbon number 35, and the rest was lumped into carbon 36. The asphaltene fraction was lumped separately into one pseudo-component. The molar volume of the C36 fraction was based on a correlation to the molecular weight; therefore this empirical parameter for the C36 fraction was tweaked using the molecular weight value. Other values entered to fit available data include C36 solubility parameter, asphaltene molecular weight, asphaltene density, and asphaltene solubility parameter. Temperature and pressure was entered as appropriate for the data being evaluated.

For each of the components C1 through C35 and CO₂, including the injection solvent, estimates were made for molecular weight, molar volume, and solubility parameter based on available correlations. Model calculations assumed one phase was being analyzed and that the solvent added was initial contact miscible. Obviously, this is not always true. However, one must know separately the conditions limits of solubility and only analyze for asphaltene stability at the appropriate conditions.

Molecular weights for the respective carbon numbers were assigned according to Katz, et al. Crude oil s are being analyzed by GC analysis, and it is presumed that for a given carbon number assigned from the GC peaks, a range of isomers are included. Consequently, the molecular weight values are adjusted slightly.

There are several correlations for estimating molar volumes of each constituent. For the pressure and temperature variation studies, molar volumes for all but the C36+ and asphaltene components were estimated using the Redlich-Kwong EOS (Chueh & Prausnitz, 1967). Simplified mixing rules were used for calculating the molar volume of the crude oil, which does not work well with polar components like carbon dioxide and hydrogen sulfide. That is, the mixture coefficient $a = (\sum(\text{mole}\% \cdot a_i^{0.5}))^2$ and $b = \sum(\text{mole}\% \cdot b_i)$ for respective components i (Redlich & Kwong, 1981). Components C36+ and asphaltenes were considered noncompressible and their molar volumes were determined based on estimated molecular weight and density values.

For the West Sak study, a simpler approach was used for estimating molar volumes. As before molar volumes of the C36+ and asphaltene fractions are based on molecular weight and density values. For C3 through C35 fractions, the correlation to component molecular weight developed by Won was used (Won, 1986). Values for nitrogen, carbon dioxide, methane and ethane were estimated based on hypothetical

dissolved liquid volume at 25°C (Barton, 1983). Unlike the previous method, this approach to estimating molar volumes are fixed and approximate values at standard conditions. Variation in pressure or temperature has a direct effect on molar volume, and these changes would not be properly reflected by this approach.

The solubility parameter for the C36+ and the asphaltene fractions are entered values and are adjusted to fit experimental data. For C6 and greater, the correlation for hydrocarbons by Bradford is used (Bradford & Thodos, 1966). For C1 through C6, this correlation is used for reduced temperatures less than 1.0. However, when reduced temperature exceeds 1, the larger of two values are chosen. One set of values is obtained as follows: C3 or less including nitrogen and carbon dioxide is obtained from gas solubility data (Prausnitz and Shair, 1961) and extrapolated for C4 and C5 (Blanks & Prausnitz, 1964). The other set of values is calculated according to Giddings and coworkers for compressed gases. (Giddings et al., 1968). The solubility parameter for the crude oil mixture is estimated by multiplying the respective solubility parameter of the component by its molar volume fraction and summing the components in the crude oil.

Thus, for the Schrader Bluff study, which considers the effect of pressure and temperature, temperature affects on molar volume and on solubility parameter are accounted for. The pressure effect on molar volume is accounted for, but the pressure effect on the solubility parameter is ignored. Direct effect of pressure on the solubility parameter is minor relative to the affect on molar volume, which itself affects the solubility parameter and is accounted for in the above calculations.

The approximations introduce some error. In particular, the EOS method of estimating volume is not properly corrected for carbon dioxide and will be somewhat in error. Mixing rules to estimate the crude oil mixture volume from the individual components is somewhat simplified and not exact. The Redlich-Kwong EOS used is not as rigorous as the more commonly used ones today, including the Peng-Robinson fine-tuned with interaction coefficients. And finally, the correlation methods used for molar volume and solubility parameter are somewhat approximate. However, considering the larger errors introduced and empirically corrected for the C36+ and asphaltene fractions (molecular weight, density, solubility parameter), the above approximations were considered adequate for this study.

6.4.3 West Sak

DeRuiter et al. published a study about the solubility and displacement behavior of gas solvents with West Sak crude oil (DeRuiter et al., 1990). Although not exactly the same, West Sak oil is of the same origin as that from the "O" sands of Schrader Bluff. Sufficient information is made available concerning asphaltene stability that an evaluation based on information from this study is useful.

The following table shows the oil composition. (Oil A, paper)

Table 24. - Composition of West Sak for asphaltene modeling study

Comp.	Mole%	Comp.	Mole%	Comp.	Mole%
N ₂	0.000%	C11	2.600%	C25	1.800%

CO ₂	0.000%	C12	2.600%	C26	1.800%
C1	0.000%	C13	2.600%	C27	1.800%
C2	0.000%	C14	2.600%	C28	1.800%
C3	0.000%	C15	3.000%	C29	1.800%
iC4	0.000%	C16	3.000%	C30	1.400%
nC4	0.000%	C17	3.000%	C31	1.400%
iC5	0.000%	C18	3.000%	C32	1.400%
nC5	0.000%	C19	3.000%	C33	1.400%
C6	0.500%	C20	2.400%	C34	1.400%
C7	0.500%	C21	2.400%	C35	1.000%
C8	0.500%	C22	2.400%	C36+	39.781%
C9	0.500%	C23	2.400%	Asphaltenes	1.219%
C10	2.600%	C24	2.400%		

Asphaltene density was assumed to be 1.22 g/ml and mwt. was initially set at 2500 amu. Although seemingly arbitrary, asphaltene precipitation predictions are relatively insensitive to this value relative to the other parameters entered for the Hirschberg model, and using an average value for asphaltenes is not unreasonable here. Mole% asphaltene content was adjusted to give 4.9 wt% (given in paper). C36+ mwt. was adjusted to give overall oil density of 0.9433 (given in paper), and turns out to be 1044 amu. Density of the C36+ fraction is calculated based on the molecular weight and mole% C36+ was automatically adjusted to give 100% for the total mixture.

Using the Hirschberg model, it is assumed that at 40:1 vol. ratio of n-pentane, at least 95% of asphaltenes are precipitated (conditions for measuring asphaltene content of crude oil). The asphaltene solubility parameter is adjusted to get this value (mole% = 99.6 n-pentane). The solubility parameter for asphaltenes was determined to be $9.69 \text{ (cal/cm}^3)^{0.5}$ and the solubility parameter for the crude oil was determined to be about $8.66 \text{ (cal/cm}^3)^{0.5}$.

Taking the above information and using the EOS to estimate molar volumes, asphaltene stability with respect to propane and butane at 500 psi was estimated to compare with the results of the study. Propane and butane are considered miscible at these conditions (500 psi and 65° F). The paper indicated that precipitation appeared for n-butane at 70wt% and above. The above model predicts that at 70 wt% n-butane, 98% of asphaltenes is precipitated. The paper indicated that at 50 wt% propane precipitation occurred. The model predicts that at 50 wt% propane virtually 100% of asphaltenes is precipitated. While the trend is correct (less propane than butane required to precipitate asphaltenes), the model predicts based on the above input that precipitation occurs sooner than reported in the paper. (ca. 20 wt% propane and ca. 40 wt% butane). Due to the approximate nature of both experimental and prediction methods in this study, nothing further is concluded.

If the asphaltene solubility parameter were adjusted slightly to $9.7 \text{ (cal/cm}^3)^{0.5}$, then the asphaltene precipitation predicted for propane appears at about 25 wt% and for butane at about 50 wt%. Although not definitive, the evaluation of West Sak oil suggests that the solubility parameter of the asphaltenes is approximately $9.7 \text{ (cal/cm}^3)^{0.5}$, considering all other assumptions made.

6.4.4 Schrader Bluff (PVT)

Some limited information is available on the asphaltene characteristics of the live Schrader Bluff crude oil (see Appendices G & H). Based on assumptions developed in the West Sak study, an evaluation was made of the Schrader Bluff live crude oil to varying conditions (pressure, temperature, composition), including the injection of gas solvents.

Composition of the crude oil (E-20 well) is given in Table 25 below. Benzene was lumped into the C6 component and toluene was lumped into the C7 component.

Table 25. - Composition of Schrader Bluff for asphaltene modeling study


Comp.	Mole%	Comp.	Mole%	Comp.	Mole%
N ₂	0.099%	C11	2.722%	C25	1.197%
CO ₂	0.288%	C12	2.919%	C26	1.146%
C1	35.430%	C13	3.407%	C27	1.078%
C2	0.348%	C14	3.183%	C28	1.110%
C3	0.266%	C15	3.314%	C29	0.936%
iC4	0.181%	C16	2.947%	C30	0.982%
nC4	0.420%	C17	2.652%	C31	0.861%
iC5	0.373%	C18	2.441%	C32	0.772%
nC5	0.385%	C19	2.217%	C33	0.725%
C6	0.923%	C20	2.126%	C34	0.667%
C7	1.763%	C21	1.818%	C35	0.634%
C8	2.199%	C22	1.710%	C36+	7.673%
C9	2.358%	C23	1.411%	Asphaltenes	0.250%
C10	2.708%	C24	1.361%		

As can be seen in the table, the light hydrocarbons is primarily methane, and the crude oil is depleted of the C2 to C6 components.

The C36+ mwt was set to 1044, as was determined for the West Sak study. The asphaltene mwt was assigned the value of 2500, and the solubility parameter set to 9.7. Density of asphaltenes was assumed to be 1.22 g/ml, and that of C36+ was estimated based on correlation with molecular weight. Based on a SARA test of a swelling study, it is estimated that asphaltenes in the live crude oil is about 2.8 wt% of total. Mole% is adjusted accordingly. As before, C36+ mole% is adjusted to make up the difference to a total of 100% for the crude oil. The initial temperature is set at 92° F, the same as for the PVT swelling study from which the data is taken; the initial pressure is set at 1618 psi, bubble point for the crude oil.

Unfortunately, the predicted results don't match the laboratory data; the model predicts that at these conditions asphaltenes will not be soluble in the crude oil. In order to obtain solubility one must lower the asphaltene solubility parameter to at least 9.24. If one goes back to the West Sak study and sets the asphaltene solubility parameter to 9.2, precipitation begins for propane at just over 55 wt%, but for butane no asphaltene precipitation is predicted, which is inconsistent with laboratory measurements in that study. In the West Sak study, if one sets the solubility parameter so that asphaltene precipitation starts to form at 50 wt% for propane (asphaltene solubility parameter = 9.27), the result is the same. At these conditions, no asphaltene precipitation occurs with the addition of n-butane. Adjustment of asphaltene molecular weight within reasonable parameter does not correct this inconsistency.

To evaluate the sensitivity of Schrader Bluff crude oil to the injection of solvent gases, the PVT study was used to set the minimum conditions (asphaltene solubility parameter set to 9.23). Evaluating up to 60 mole% Prudhoe Bay MI at the saturation pressure confirms that asphaltene flocculation is not predicted as was observed in the laboratory. Asphaltenes were observed at 80 mole% Prudhoe Bay MI, but not saturation pressure was observed. At 4113 psi, no asphaltene precipitation is predicted for 80 mole% or 90 mole% PB MI.

If one trusts the predictions, the suggestion is that the presence of asphaltene solids is related to the phase changes that occur in the presence of high concentrations of PB MI. Indeed, at 80 mole% PB MI, the first observance of 2 liquid hydrocarbon phases is noted. Furthermore, the SARA of these phases showed that while the asphaltenes concentrated in the lower liquid phase, the resins ^{are} equally in the lower and upper liquid phases. That is, the resin to asphaltene ratio in the lower liquid phase is reduced by a factor of about 2, the exact value changing as a function of pressure. 

If one extends the model predictions further by replacing the PB MI with pure carbon dioxide, the result is the same. No precipitation of asphaltenes is indicated for carbon dioxide. In the case of propane, asphaltene precipitation is predicted above ca. 70 mole% (ca. 30 wt%) at 3000 psi, and ca. 35 mole% (ca. 10 wt%) at 1618 psi. In the case of n-butane, no asphaltene precipitation is predicted. The model predictions suggest that asphaltene flocculation observed in the PVT swelling study is not the result of solution destabilization due to changing solvent solubility properties. At least the prediction result is consistent with the hypothesis that asphaltene destabilization occurs for Schrader Bluff principally when multiple liquid hydrocarbon phases are present.

Another PVT swelling study with E-20 oil was conducted with a CO₂/NGL mixture in the ratio of 77.5 mole% to 22.5 mole%, respectively. Similar to other reported results, asphaltenes were not observed until the solvent reached 80 mole% and the pressure was reduced to below the saturation pressure. It was at this pressure that the first occurrence of multiple liquid hydrocarbon phases is observed and the first occurrence of solid asphaltenes in the lower more dense phase. The Hirschberg model using the above parameters predicted that at the saturation pressure of 4340 psi, no asphaltene precipitation is indicated for the solvent mixture up to 99.9 mole% solvent.

A qualitative approach to evaluating the potential asphaltene problem of Schrader Bluff may be followed using Figure 35. It is assumed that the solvent density was very nearly the mixture density of the

experiments used to generate the plot, and that for a solvent of a particular type the solubility could be estimated based on the resulting density of the solvent/crude oil mixture.

Secondly, the crude oil density of Schrader Bluff crude oil is 0.818 g/ml at the saturation pressure of 1618 psi., and because no asphaltenes drop out of the crude oil (no solvent) at those conditions, one can assume the asphaltenes to be 100 wt% soluble at 0.818 g/ml, 92° F, and 1618 psi. Even though the plot of Figure 35 is not specific to Schrader Bluff, it should be at least approximately correct. Based on that, one can see that any appreciable reduction of oil density is likely to result in asphaltene flocculation. For the CO₂/NGL swelling experiment and using the Redlich-Kwong EOS described earlier, the solution density is estimated at 0.796 g/ml for the 60 mole% solvent (2062 psi, saturation pressure), and 0.778 g/ml for the 80 mole% solvent (4340 psi, saturation pressure). Although not definitive, this result is suggestive that reduction of crude oil density with higher concentrations of solvent may be contributing to the destabilization of asphaltenes in the Schrader Bluff oil.

6.4.5 Summary

Models for predicting asphaltene flocculation are generally empirical at best, since some of the data required for their use are not easily or accurately obtainable. The models used in this study are based on assumptions and approximations, and some of the input parameters were arbitrarily assigned to fit the predictions to the available laboratory measurements. Consequently, no conclusions from the model study should be accepted without further confirmation from laboratory measurements.

The model study does suggest that if confined to a single liquid phase system, solvent mixtures such as Prudhoe Bay MI and CO₂/NGL are not likely to cause significant asphaltene precipitation problems for Schrader Bluff crude oil. Pure propane is predicted to cause problems at high solvent concentrations, as was observed in the laboratory for West Sak crude oil. Multiple liquid phase systems were not studied using the Hirschberg model and sophisticated EOS calculations. By inference, model predictions suggest that flocculation of asphaltenes occur due to the formation of complex phase behavior at higher solvent concentrations.

6.5 Summary

In summary, very limited information is available concerning the relative stability of asphaltenes in Schrader Bluff as a function of temperature, pressure, and composition. Significant amounts of asphaltenes are known to be present, injection of high concentrations of solvents typically used for EOR recovery processes have been observed to precipitate asphaltenes from the crude oil. The extent of plugging expected in the reservoir, and the resulting impact on fluid flow and crude oil recovery are still not well defined.

It is interesting to note that both laboratory and predicted results suggest the formation of asphaltene solids from Schrader Bluff is coincident with the formation of multiple liquid hydrocarbon phases. This can be explained by the observation that when present, asphaltenes selectively partition into the lower more dense phase, but the resins partition equally between both liquid phases. The resulting resin/asphaltene ratio changes as a result. It is known that asphaltene stability in crude oil depends on this ratio—values near 1 result in asphaltene flocculation being sensitive to changes in other conditions, such as pressure, while values much higher than 1 tend to render the asphaltenes more stable.

7. Conclusions

8. Bibliography

8.1 General

- Ali, M.A. and M.R. Islam: "The Effect of Asphaltene Precipitation on Carbonate Rock Permeability: An Experimental and Numerical Approach," SPE Paper 38856, Pres. 1997 SPE Annual Technical Conference, San Antonio, Texas, 5-8 October 1997.
- Anderson, S.I.: "Flocculation Onset Titration of Petroleum Asphaltenes," *Energy and Fuels* v. 13, pp. 315-322, 1999.
- Anderson, S.I. and J.G. Speight: "Thermodynamic Models for Asphaltene Solubility and Precipitation," *J. Pet. Sci. & Eng.* V. 22, pp. 53-66, 1999.
- Barton, A.F.M.: *Handbook of Solubility Parameters and Other Cohesion Parameters*, p. 219, CRC Press, Boca Raton, Florida, 1983.
- Bidinger, C.R. and J.F. Dillon: "Milne Point Schrader Bluff: Finding the Keys to Two Billion Barrels," SPE Paper 30289, Pres. Int. Heavy Oil Symposium, Calgary Canada, 19-21 June 1995.
- Blanks, R.F. and J.M. Prausnitz: "Thermodynamics of Polymer Solubility in Polar and Nonpolar Systems," *I&EC Fundamentals*, v. 3(1), pp. 1-8, February 1964.
- Bradford, M.L. and G. Thodos: "Solubility Parameters of Hydrocarbons," *Can. J. Chem. Eng.*, pp. 345-348, Dec. 1966.
- Buckley, J.S.: "Microscopic Investigation of the Onset of Asphaltene Precipitation," *Fuel Science and Technology Int.*, V. 14(1&2), pp. 55-74, 1996.
- Bunger, J.W. and N.C. Li (ed.): *Chemistry of Asphaltenes*, Advances in Chemistry Series 195, American Chemistry Society, Washington, D.C., 1981.
- Chang, Y., G.A. Pope and K. Sepehrnoori: "A Higher-Order Finite Difference Compositional Simulator," *J. Pet. Sci. Eng.* No. 1, pp. 35-50, November 1990.
- Chang, Y.: "Development and Application of an Equation of State Compositional Simulator," Ph.D. Dissertation, University of Texas, Austin, 1990.
- Chueh, P.L. and J.M. Prausnitz: "Vapor-Liquid Equilibria at High Pressures: Calculation of Partial Molar Volumes in Nonpolar Liquid Mixtures," *AIChE J.*, v. 13(6), pp. 1099-1107, November 1967.

- Chung, T.H.: "Thermodynamic Modeling for Organic Solid Precipitation," SPE Paper 24851, Pres. SPE Annual Technical Conference, Washington, D.C., October 4-7, 1992.
- Creek, J.L. and J.M. Sheffield: "Phase Behavior, Fluid Properties, and Displacement Characteristics of Permian Basin Reservoir Fluid- CO₂ Systems," SPE/DOE Paper 20188, Pres. SPE/DOE 7th Symposium on Enhanced Oil Recovery, Tulsa, Oklahoma, 22-25 April 1990.
- DeRuiter, R.A., L.J. Nash, and M.S. Wyrick: "Solubility and Displacement Behavior of Carbon Dioxide and Hydrocarbon Gases with a Viscous Crude Oil," SPE Paper 20523, Pres. SPE 65th Annual Technical Conference, New Orleans, LA, 23-26 September 1990.
- Giddings, J.C., M.N. Myers, L. McLaren, and R.A. Keller: "High Pressure Gas Chromatography of Nonvolatile Species," Science, v. 162, pp. 67-73, 4 October 1968.
- Godbole, S.P., K.J. Thele, and E.W. Reinbold: "EOS Modeling and Experimental Observations of Three-Hydrocarbon-Phase Equilibria," SPE Paper 24936, , Pres. SPE 67th Annual Technical Conference, Washington, D.C., 4-7 October 1992.
- Gondouin, M. and J.M. Fox III: "The Challenge of West Sak Heavy Oil: Analysis of an Innovative Approach," SPE Paper 22077, Pres. Int. Arctic Technology Conf., Anchorage, AK, 29-31 May 1991.
- Grigg, B.R., and W.R. Siagian: "Understanding and Exploiting Four-Phase Flow in Low-Temperature CO₂ Floods," SPE Paper 39790, Pres. 1998 SPE Permian Basin Oil and Gas Recovery Conference, Midland, Texas, 25-27 March 1998.
- Hallam, R.J., T.D. Ma, and E.W. Reinbold: "Performance Evaluation and Optimization of the Kuparuk Hydrocarbon Miscible Water-Alternating-Gas Flood," 1995 New Developments in Improved Oil Recovery, H.J. DeHaan (ed.), Geological Society Publication No. 84, pp. 153-164, 1995.
- Hirschberg, A./, L.N.J. de Jong, B.A. Schipper, and J.G. Meyers: "Influence of Temperature and Pressure on Asphaltenes Flocculation," SPE Paper 11202, Pres. SPE Annual Tech. Conf., New Orleans, Louisiana, 26-29 September, 1982.
- Hirschberg, A./, L.N.J. de Jong, B.A. Schipper, and J.G. Meyers: "Influence of Temperature and Pressure on Asphaltenes Flocculation," Soc. Pet. Eng. J., pp. 283-293, June 1984.
- Hoolahan, S.P., G.S. McDuffie, D.G. Peck, and R.J. Hallam: "Kuparuk Large Scale Enhanced Oil Recovery Project," SPE Paper 35698, Pres. SPE Western Regional Meeting, Anchorage, Alaska, 22-24 May 1996.
- Hoy, K.L.: "New Values of the Solubility Parameters from Vapor Pressure Data," J. Paint Technology, v. 42(541), pp. 76-118, February 1970.
- Huang, E.T.S. and J.H. Tracht: "The Displacement of Residual Oil by Carbon Dioxide," SPE Paper 4735, Pres. 1974 Symposium on Improved Oil Recovery, Tulsa, 22-24 April 1974.

- Huang, E.T.S.: "The Effect of Oil Composition and Asphaltene Content on CO₂ Displacement," SPE/DOE Paper 24131, Pres. SPE/DOE 8th Enhanced Oil Recovery Conference, Tulsa, Oklahoma, 22-24 April 1992.
- Kamath, K.I., J.R. Comberati and A.M. Zammerilli: "The Role of Reservoir Temperature in CO₂ Flooding," Pres. U.S. DOE Fifth Annual Symposium on Enhanced Oil and Gas Recovery, Tulsa, 22-24 August 1979.
- Kamath, V.A., J. Yang, and G.D. Sharma: "Effect of Asphaltene Deposition on Dynamic Displacements of Oil by Water," SPE Paper 26046, Pres. SPE Western Regional Meeting, Anchorage, Alaska, 26-28 May 1993.
- Kuo, S.S.: "Prediction of Miscibility for the Enriched-Gas Drive Process," SPE Paper 14152, Pres. 60th Annual Technical Conference and Exhibition of the SPE of AIME, Las Vegas, Nevada, 22-25 September 1985.
- Lim, M.T., G.A. Pope, K. Sepehrnoori, and Y. Soni: "Grid Refinement Study of a Hydrocarbon Miscible Gas Injection Reservoir," SPE Paper 38060, Pres. 1997 SPE Asia Pacific Oil and Gas Conference, Kuala Lumpur, Malaysia, 14-16 April 1997.
- MacAllister, D.J. and R.A. DeRuiter: "Further Development and Application of Simulated Distillation for Enhanced Oil Recovery," SPE Paper 14335, Pres. SPE 60th Annual Technical Conf., Las Vegas, NV, 22-25 September 1985.
- Metcalf, R.S. and L. Yarborough: "The Effect of Phase Equilibria on the CO₂ Displacement Mechanism," SPE Paper 7061, Pres. SPE-AIME Fifth Symposium on Improved Methods for Oil Recovery, Tulsa, 16-18 April 1978.
- Mitchell, D.L. and J.G. Speight: "The Solubility of Asphaltenes in Hydrocarbon Solvents," Fuel v. 52, p. 149-152, April 1973.
- Nghiem, LX., D.A.Coombe, and S.M. Farouq Ali: "Compositional Simulation of Asphaltene Deposition and Plugging," SPE Paper 48996, Pres. SPE Annual Technical Conference, New Orleans, Louisiana, 27-30 September 1998.
- Prausnitz, J.M. and F.H. Shair: "A Thermodynamic Correlation of Gas Solubilities," AIChE J., pp. 682-687, December 1961.
- Rassamdana, H., N. Mirzaee, A.R. Mehrabi, and M. Sahimi: "Field-Scale Asphalt Precipitation during Gas Injection into a Fractured Carbonate Reservoir," SPE Paper 38313, Pres. SPE Western Regional Meeting, Long Beach, California, 25-27 June 1997.
- Rathmell, J.J., F.I. Stalkup, and R.C. Hassinger: "A Laboratory Investigation of Miscible Displacement by CO₂," SPE Paper 3483, Pres. SPE-AIME 46th Annual Fall Meeting, New Orleans, 3-6 October 1971.
- Redlich, O. and J.N.S. Kwong: "On the Thermodynamics of Solutions. An Equation of State. Fugacities of Gaseous Solutions," SPE Reprint Series no. 15, pp. 52-63, 1981.

- Rienbold, E.W., S.W. Bokhari, S.R. Enger, T.D. Ma, and S.M. Renke: "Early Performance and Evaluation of the Kuparuk Hydrocarbon Miscible Flood," SPE Paper 24930, Pres. SPE 67th Annual Technical Conference, Washington, D.C., 4-7 October 1992.
- Sharma, A.K., S.L. Patil, V.A. Kamath, and G.D. Sharma: "Miscible Displacement of Heavy West Sak Crude by Solvents in Slim Tube," SPE Paper 18761, Pres. SPE California Regional Mtg., Bakersfield, California, 5-7 April 1989.
- Shelton, J. L. and L. Yarborough: "Multiple Phase Behavior in Porous Media During CO₂ or Rich-Gas Flooding," J. Pet. Tech. pp. 1171-1178, Sept. 1977.
- Speight, J.G. and S.E. Mischopedis: "On the Molecular Nature of Petroleum Asphaltenes," Chemistry of Asphaltenes, Advances in Chemistry Series 195, Bunger, J.W. and N.C. Li (ed.), pp. 1-15, American Chemistry Society, Washington, D.C., 1981.
- Speight, J.G.: "Chemical and Physical Studies of Petroleum Asphaltenes," Asphaltenes and Asphalts, 1, Yen, T.F., and G.V. Chilingarian (ed.), pp. 7-65, Elsevier Science, 1994.
- Speight, J.G.: "The Chemical and Physical Structure of Petroleum: Effects on Recovery Operations," J. Pet. Sci. & Eng., v. 22, pp. 3-15, 1999.
- Strycker, A. and S. Wang: "Gas Injection for Schrader Bluff," U.S. DOE Report TRWPT/CRADA-003-2 (OSTI: ID 8017), May 1999.
- Taber, Joseph J., F. David Martin, and R.S. Seright: "EOR Screening Criteria Revisited," SPE/DOE Paper 35385, pres. SPE/DOE Tenth Symposium on Improved Oil Recovery, Tulsa, Oklahoma, 21-24 April 1996.
- Thanh, N.X., M. Hsieh, and R.P. Philp: "Waxes and Asphaltenes in Crude Oils," Organic Geochemistry, v. 30, p. 119-132, 1999.
- Wiehe, I.A.: "Polygon Mapping with Two-Dimensional Solubility Parameters," Ind. Eng. Chem. Res., v. 34, pp. 661-673, 1995.
- Wiehe, I.A.: "Two-Dimensional Solubility Parameter Mapping of Heavy Oils," Fuel Science and Technology Int., v. 14(1&2), pp. 289-312, 1996.
- Williams, C.A., E.N. Zana and G.E. Humphrys: "Use of the Peng-Robinson Equation of State to Predict Hydrocarbon Phase Behavior and Miscibility for Fluid Displacement," SPE Paper 8817, Pres. First SPE/DOE Symposium on Enhanced Oil Recovery, Tulsa, 20-21 April 1980.
- Won, K.W.: "Thermodynamics for Solid Solution-Liquid-Vapor Equilibria: Wax Phase Formation from Heavy Hydrocarbon Mixtures," Fluid Phase Equilibria, v. 30, pp. 265-279, 1986.
- Yen, T.F., and G.V. Chilingarian (ed.): Asphaltenes and Asphalts, 1, Elsevier Science, 1994.
- Zick, A.A.: "A Combined Condensing/Vaporizing Mechanism in the Displacement of Oil by Enriched Gases," SPE Paper 15493, Pres. SPE 61st Annual Technical Conference, New Orleans, LA, 5-8 October 1986.

8.2 In-situ Combustion

- Bailey, H.R., and B.K. Larkin: "Conduction-Convection in Underground Combustion," AIME Petroleum Transactions, Vol. 219, pp. 320-331, 1960.
- Buchanan, L. and M. Raicar: "Sensitivity Study of Field Scale Combustion Simulation for a Lloydminster-Type Heavy Oil Reservoir," Petroleum Society of CIM, paper No. 83-34-47.
- Coats, K.H.: "In-situ Combustion Model," Soc. Pet. Eng. J., Vol. 20(6), pp. 533-554, December 1980.
- Craig, F. F., Jr., and D.R. Parrish: "A Multipilot Evaluation of the COFCAW Process," J. Pet. Tech. pp. 659-666, June 1974.
- Crookston, R.B., W.E. Culham, and W.H. Chen: "A Numerical Simulation Model for Thermal Recovery Processes," SPE Paper 6724, 9-12 October 1977.
- Dingley, A.J.: "The Combustion Recovery Process -- Principles and Practice," J. Canadian Pet. Tech., pp. 196-205, October-December 1965.
- Farouq Ali, S.M.: "Multiphase, Multidimensional Simulation of In-Situ Combustion," SPE Paper 6896, presented at SPE 52nd Annual Technical Conference and Exhibition, Denver, 9-12 October 1977.
- Kumar, Mridul: "A Cross-Sectional Simulation of West Heidelberg In-Situ Combustion Project," SPE Reservoir Engineering, pp. 46-54, February 1991.
- Laureshen, C.J., S.A. Mehta, R.G. Moore, and M.G. Ursenbach: "Ramped Temperature Oxidation Characteristics of Alaska Crude Oil," report submitted by Dept. Chemical & Petroleum Eng., U. Calgary, 11 September 1998.
- Laureshen, C.J., S.A. Mehta, R.G. Moore, N.E. Okazawa, and M.G. Ursenbach: "BDM Petroleum Technologies Combustion Tube Test No. 1 (Test No. 287), Alaska Reservoir," report submitted by Dept. Chemical & Petroleum Eng., U. Calgary, 10 December 1998.
- Laureshen, C.J., S.A. Mehta, R.G. Moore, N.E. Okazawa, and M.G. Ursenbach: "BDM Petroleum Technologies Combustion Tube Test No. 2 (Test No. 287), Alaska Reservoir," report submitted by Dept. Chemical & Petroleum Eng., U. Calgary, 10 December 1998.
- Moore, R.G., M.G. Ursenbach, C.J. Laureshen, J.D.M. Belgrave, and R. Mehta: "Ramped Temperature Oxidation Analysis of Athabasca Oil Sands Bitumen," Petroleum Society of CIM paper 95-23, pres. 46th Annual Technical Meeting, Banff, Alberta Canada, 14-17 May 1995.
- Moore, R.G., C.J. Laureshen, M.G. Ursenbach, R. Mehta, and J.D.M. Belgrave: "Combustion/Oxidation Behavior of Athabasca Oil Sands Bitumen," SPE Paper 35392, pres. SPE/DOE Improved Oil Recovery Symposium, Tulsa, Oklahoma, 21-24 April 1996.
- Parrish, D.R., and Craig, F. F.: "Laboratory Study of a Combination of Forward Combustion and Waterflooding," the COFCAW Process, J. Pet. Tech. pp. 753-761, June 1969.

- Rubin, B. and W.L. Buchanan: "A General Purpose Thermal Model," SPE Paper 11713, presented at the 1983 California Regional Meeting, Ventura, California, 23-25 March 1983.
- Sarathi, P.S. and D.K. Olsen: DOE Cost-Shared In-situ Combustion Projects Revisited," Paper ISC-4 Pres. at 1994 DOE/NIPER Conference, Tulsa, Oklahoma, April 21-22, 1994; Proceedings publ. in U.S. DOE Report NIPER/BDM-OK-0086 (DE95000116),. January 1995.
- Sarathi, P.S. and D.K. Olsen (ed.): "Field Application of In Situ Combustion—Past Performance/Future Application, Symposium Proceedings," 1994 DOE/NIPER Conference, Tulsa, Oklahoma, April 21-22, 1994; Proceedings publ. in U.S. DOE Report NIPER/BDM-OK-0086 (DE95000116),. January 1995.
- Sarathi, P.S.: "In-Situ Combustion Handbook—Principles and Practices," U.S. DOE Report DOE/PC/91008-0374, 401 pp., January 1999.
- Strycker, A., P. Sarathi, and S. Wang: "Evaluation of In-situ Combustion for Schrader Bluff," U.S. DOE Report TRWPT/CRADA-002-1, 46 pp., March 1999.
- Todd, M.R., P.M. O'Dell, and G.J. Hiraski: "Methods for Increased Accuracy in Numerical Reservoir Simulators," Soc. Pet. Eng. J., pp. 515-530, December 1972; Trans. , AIME, p. 253.
- Wang, X., P.S. Sarathi, C.R. Bidinger: "Field Scale Combustion Simulation Studies—Investigation of Reservoir Fluid and Operational Parameters on Project Performance, Pres. Paper 1998.044 at the 7th UNITAR International Conference on Heavy Crude and Tar Sands, Beijing, China, 27-30 October 1998.
- Youngren, G.K.: "Development and Application of an In-Situ Combustion Reservoir Simulator," Soc. Pet. Eng. J., pp. 39-51, February 1980.